Space Science Reviews (2024) 220:19
https://doi.org/10.1007/s11214-024-01051-8

Strong Lensing by Galaxy Clusters

P. Natarajan[1,2,3] · L.L.R. Williams[4] · M. Bradač[5,6] · C. Grillo[7] · A. Ghosh[4] · K. Sharon[8] · J. Wagner[9]

Received: 18 April 2023 / Accepted: 23 January 2024 / Published online: 15 February 2024

Abstract
Galaxy clusters as gravitational lenses play a unique role in astrophysics and cosmology: they permit mapping the dark matter distribution on a range of scales; they reveal the properties of high and intermediate redshift background galaxies that would otherwise be unreachable with telescopes; they constrain the particle nature of dark matter and are a powerful probe of global cosmological parameters, like the Hubble constant. In this review we summarize the current status of cluster lensing observations and the insights they provide, and offer a glimpse into the capabilities that ongoing, and the upcoming next generation of telescopes and surveys will deliver. While many open questions remain, cluster lensing promises to remain at the forefront of discoveries in astrophysics and cosmology.

Keywords Gravitational lensing · Strong gravitational lensing · Galaxy clusters

1 Introduction

In hierarchical structure formation in the Universe, per the standard cold dark paradigm, galaxy clusters are now understood to be the most recently assembled and most massive

✉ P. Natarajan
priyamvada.natarajan@yale.edu

✉ M. Bradač
Marusa.Bradac@fmf.uni-lj.si

1 Department of Astronomy, Yale University, New Haven, CT, 06511, USA

2 Department of Physics, Yale University, New Haven, CT, 06511, USA

3 Yale Center for Astronomy & Astrophysics, Yale University, New Haven, CT, 06520, USA

4 Minnesota Institute for Astrophysics, School of Physics and Astronomy, University of Minnesota, Minneapolis, MN, 55455, USA

5 Department of Physics, University of California, Davis, CA, 95616, USA

6 University of Ljubljana, 1000, Ljubljana, Slovenia

7 Department of Physics, University of Milan, 20122, Milano, MI, Italy

8 Department of Astronomy, University of Michigan, Ann Arbor, MI, 48109, USA

9 Bahamas Advanced Study Institute and Conferences, 4A Ocean Heights, Hill View Circle, Stella Maris, Long Island, Bahamas

structures to form. Clusters are therefore also expected to be the largest repositories of dark matter. As a result, clusters are some of the most efficient gravitational lenses known to date. Zwicky (1937) was the first to point out that gravitational lensing by galaxy clusters might serve as a valuable tool to measure the amount of this unseen mass component and permit study of distant, magnified objects that lie behind clusters. Despite his bold prediction, the lack of appropriate resolution and imaging facilities at the time and the lack of theoretical understanding of how structure assembles deferred progress in gravitational lensing studies. Several decades later, the presence of a foreground cluster was proposed by Young et al. (1980) as the explanation for a larger-than-expected separation between the images of a double quasar in the first detected double quasar Q0957+561 (Walsh et al. 1979). With this observational impetus and hence renewed interest, the lensing properties of clusters were revisited and explored in detail by Narayan et al. (1984).

The first observational detection of strong lensing by a cluster—a giant arc in Abell 370—was reported in Lynds and Petrosian (1989) and independently by Soucail et al. (1987). These extremely elongated distorted shapes seen in the core of the massive cluster Abell 370 were recognized by Paczynski (1987) as merging images of a strongly lensed background galaxy, and were soon confirmed as such with the measurement of the redshift of the arc by Soucail et al. (1988). With this discovery of giant arcs, the strong lensing regime was established as a property of the deflection produced by dense cluster cores.

With the discovery of the weak, systematic alignment in the shapes of distant background galaxies produced in the outer regions of clusters as reported in Tyson et al. (1990), observational evidence for both strong and weak lensing were confirmed. Several significant early papers (Schneider 1984; Blandford and Narayan 1986; Blandford et al. 1989; Kochanek 1990; Miralda-Escude 1991; Kaiser 1992; Kaiser and Squires 1993) helped establish the formalism for "inverting" observed lensing effects into mapping the mass distributions of galaxy clusters. Subsequent technological advances in the CCD imaging that allowed deeper and sharper images as well as the development and availability of spectrographs drove the rapid discovery of cluster lenses.

The truly transformative revolution in lensing, and strong lensing studies in particular, came with imaging from space with the deployment of the *Hubble Space Telescope*. After correction of its initially blurry images with the repair mission that installed the WFPC-2 camera in 1993, Hubble recovered its image sharpness, and one of the first post-repair image releases was the now iconic image of the massive cluster lens Abell 2218 (Kneib et al. 1996), replete with strong lensing features that are discernible by eye. High resolution images combined with a large field of view have been a game changer for studies of cluster lenses (e.g., Smail and Dickinson 1995), for example, for tracing out the circularly averaged density profile of equilibrium clusters and comparing these to the predictions of cosmological models (Sect. 5.1), and for studying the most distant galaxies using the magnifying power of cluster lenses (Sect. 5.3). Strong lensing features in clusters are now detected in the inner one arc-minute central region and on arc-second scales (see left panel of Fig. 2 for a gallery of HST detected dramatic cluster arcs). On smaller scales, multiple images produced by individual cluster galaxies have also been detected in the deepest HST images (Natarajan et al. 1998, 2017; Meneghetti et al. 2020).

The *James Webb Space Telescope* (JWST), launched late 2021, looked at a galaxy cluster, SMACS J0723.3-7327, as one of its first targets, offering an unprecedented and detailed view of a massive lens in infra-red wavelengths. Figure 1 compares the HST images to the newly obtained JWST images (top two panels), and the bottom panel shows the X-ray image superimposed on the JWST image. The improvement in the quality of the JWST image, compared to an already spectacular HST image is visually apparent and striking.

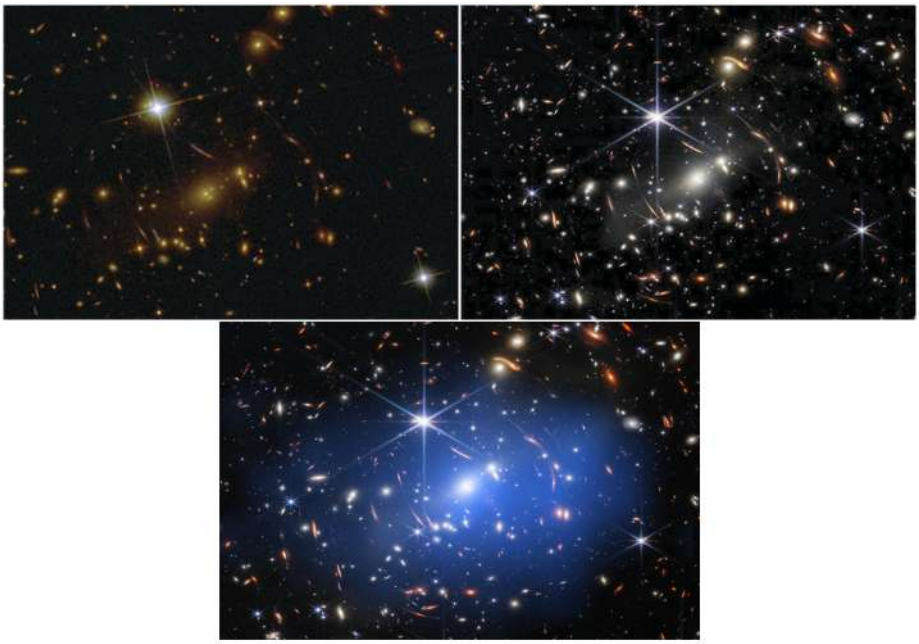

Fig. 1 The galaxy cluster lens SMACS J0723.3-7327 at $z = 0.39$. *Top left:* HST image of the cluster showing multiple strongly lensed features visible by eye. *Top right:* JWST image of the same cluster that in turn reveals a significantly larger number of strongly lensed features. The improvement in the quality of the image is evident upon visual inspection. *Bottom:* Chandra X-ray image showing the spatial distribution of the hot X-ray gas (blue) overlaid over the JWST image. The images span nearly the same field of view and scale. The top right and bottom panels are about 2.35 arcmin wide, or 750 kpc at the redshift of the cluster, $z = 0.388$

2 Strong Lensing as a Probe of Cluster Properties

Clusters are powerful astrophysical laboratories as they are objects where the interplay of dark matter and baryons can be effectively probed on multiple physical scales (see reviews by Kneib and Natarajan 2011; Umetsu 2020). On spatial scales greater than about 1-few kpc, clusters are dominated by dark matter, even at their centers. The baryonic component in clusters is mostly in the form of very hot plasma with $T \sim 10^7 K$, the Intra-Cluster Medium (ICM) detected through its bremsstrahlung, or free-free, emission observed in X-rays. The stellar component is mostly confined to cluster member galaxies, including, in many cases, a massive central dominant (cD) galaxy or the brightest cluster galaxy (BCG) that has been known to have an extended stellar distribution (Schombert 1986; Uson et al. 1991) and deeper recent observations have helped delineate this diffuse emission from a population of intra-cluster stars more clearly, referred to as the Intra-Cluster Light (ICL) component, in the form a diffuse cloud of light, which appears to trace the overall dark matter distribution with great fidelity (Gonzalez et al. 2005; Montes and Trujillo 2019). Notably, as discussed first by Uson et al. (1991), disentangling the BCG and the extended cD envelope is challenging even today. Even including all the baryonic components in the mass inventory in clusters, they still stand as dark matter dominated cosmic objects.

As noted in Sect. 1, the central $\lesssim 0.3$ Mpc of galaxy clusters are the regions that contain a high concentration of matter (dark + baryonic); these are the spatial scales on which the gravitational coupling between baryons and dark matter manifests. Currently the dark

matter component of the Universe is believed to be cold and collision-less, rendering it inert in terms of interactions aside from gravity with the baryonic components. Cosmological simulations of structure formation over cosmic time find that dark matter settles into a near universal density profile across several decades in mass—the Navarro, Frenk and White profile (NFW)—with an inner slope of $\rho \sim r^{-1}$, that is expected in clusters of galaxies as well. However, if for example, dark matter interacts weakly with itself, this unusual, additional self-interaction, would preferentially produce discernible effects in this central dense region (see Sect. 5.5). While the mass distribution in the innermost regions is typically dominated by baryons, fortunately, these regions are also the ones that are best probed by strong lensing observations.

One of the key measured properties for clusters is their mass and the detailed spatial distribution of the mass. The radial mass distribution in clusters can be probed and measured using 3 independent methods that all map the underlying gravitational potential: (i) the dynamics of cluster member galaxies assuming they are in equilibrium and robustly trace the gravitational potential, (ii) the X-ray emission from the hot plasma, also assuming it is in hydrostatic equilibrium with the cluster potential, and (iii) gravitational lensing, that makes no prior assumptions about the gravitational potential. The advantage of lensing as a technique is that light deflection is achromatic, and is also entirely independent of the dynamical state of the cluster. Lensing observations therefore permit study of merging and out-of-equilibrium clusters as well. Besides, lensing delivers not just the projected, *radially averaged* mass profiles for cluster, but also permits mapping of the *detailed* two-dimensional mass distribution.

The power of cluster lensing derives from the fact that deeper imaging data not only permit probing the detailed spatial distribution of dark matter in the cluster but that it also simultaneously acts as a cosmic telescope allowing us to probe faint sources in the background Universe. Strong lensing by galaxy clusters brings into view distant, faint background galaxies that would otherwise remain inaccessible to even the most powerful telescopes on the ground or in space; the high magnification of intermediate and high redshift star-forming galaxies allows us to study the building blocks of these galaxies at an unprecedented spatial scale and at a fraction of the observing time otherwise necessary. Modeling and characterizing the mass distribution of cluster lenses therefore stands to open a new window into the early Universe by magnifying the most distant first sources that assemble, a prospect keenly awaited for with JWST data. However, as massive clusters are rare objects, defining systematic criteria to characterize cluster lens samples has proved to be challenging. Furthermore, given the dependence of the strength of lensing on the underlying geometry of the Universe, lensing has also been established as a powerful method to constrain cosmological parameters that characterize the underlying world model (Gilmore and Natarajan 2009; Jullo et al. 2010, 2015; Magana et al. 2018; Caminha et al. 2022a). There are synergies in the general modeling approaches for characterizing the lensing properties of individual galaxies and those adopted for clusters. However, the existence of a richer phenomenology and more extensive data available in both the strong and weak lensing regimes, warrants more sophisticated models tailored for lensing clusters. We outline the range of mass modeling techniques that have been developed and applied to cluster lenses in Sect. 3.

The Hubble Frontier Fields program (HFF thereafter), a key Director's Discretionary large program (Lotz et al. 2017) dedicated 840 HST orbits to ultra-deep strong lensing imaging of six selected massive cluster lenses. These fields were also observed across several wavelengths, adding to wealth of information for modeling and deeper understanding of clusters and high redshift Universe. These coordinated multi-wavelength surveys include

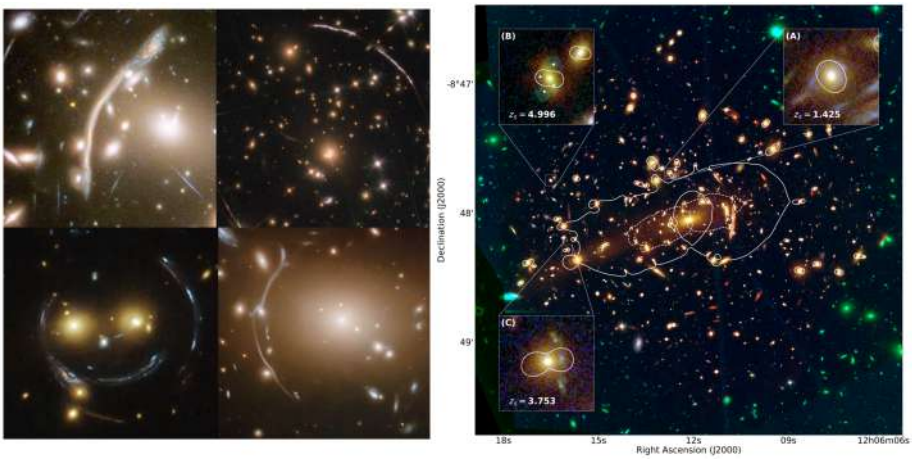

Fig. 2 Left Panel: Gallery of HST detected cluster arcs seen in the cluster Abell 370 (top-left); SDSS J1038+4849 (bottom-left); PSZ1 G311.65−18.48 (top-right) and Abell 611 (bottom-right). **Right Panel:** GGSL in the central region of the HFF galaxy cluster MACSJ1206: (Meneghetti et al. 2020). The image is a composite and combines HST observations in multiple bands: F105W, F110W, F125W, F140W, F160W (red channel), F606W, F625W, F775W, F814W, F850LP (green channel), F435W and F475W (blue channel). The dashed and solid lines in the right panel show the lens critical curves for potential sources at redshifts of 1 and 7, respectively. Panels A, B, C are zoom-ins of three individual GGSL events produced by sources measured to be at redshifts $z = 1.425$, $z = 4.996$, and $z = 3.753$. The GGSL sources in panel B were not visible in the HST image and were discovered in an observation with the Multi-Unit-Spectroscopic-Explorer (MUSE) spectrograph of the VLT

ALMA (González-López et al. 2017), the Spitzer Frontier Fields [1] and Chandra, and JVLA Frontier Fields Campaigns van Weeren et al. (2017). HFF has yet again transformed our understanding of the mass distribution and evolutionary states of clusters. Chosen as the most efficient lenses, these six massive cluster lenses permit probing high mass end of the cluster mass function. Intriguingly, with deeper HFF imaging, in addition to the giant arcs and multiple image families observed in cluster lenses, additional strong lensing features produced by individual cluster members, referred to as Galaxy-Galaxy Strong Lensing (GGSL), have also been detected (see the right panel of Fig. 2 for some notable GGSL examples).

3 Modeling the Mass Distribution in Cluster Lenses

The strong distortion of space-time by a massive cluster is so significant, that its effect on the shapes of background galaxies is unambiguously detectable, as evident in HST and even in ground-based images. Background sources, strongly lensed by foreground galaxy clusters result in the production of magnified, extremely distorted images referred to as giant arcs; and multiple images of the same source, that exhibit similar color and morphology, that albeit may have different levels of distortion and mirror symmetry. This wide range of phenomena—ranging from their geometry, brightness and observed spatial locations in the cluster—can and is used as input observational constraints to reconstruct the total mass of the cluster lens. Utilizing the observed distorted images to recover the original undistorted

[1] https://irsa.ipac.caltech.edu/data/SPITZER/Frontier/overview.html.

shapes enables constraining the mass distribution of the cluster lens, yielding "lens models". Lensing observations and the derived foreground cluster mass distributions have revealed that the bulk of the gravitational potential in clusters comprises the undetected "dark matter".

Several independent lens modeling algorithms to recover cluster mass distributions have been developed, widely tested and used by the strong lensing community. Regardless of the specific technique, all strong lensing modeling algorithms use as input constraints the positions of multiple images of the same background sources, sometimes referred to as "families", and ideally, when available the measured spectroscopic redshifts of the sources. Although the magnification in the strong lensing regime is conducive to follow-up spectroscopy to obtain redshifts, it is challenging, and often photometric redshifts are used instead.

The purpose of strong lens modeling algorithms is to find a representation of the projected mass distribution on the lens plane that offers the smallest scatter between the observed and model-predicted lensing observables. In the source plane (a.k.a. "source plane minimization"), this is accomplished by minimizing the scatter of the model-predicted (unobserved) source position: for a set of N images of the source, the source position β_i is calculated for each image i using the lens equation:

$$\beta_i = \theta_i - \alpha_i = \theta_i - \frac{D_{\rm ls}}{D_{\rm os}}\hat{\alpha}_i, \tag{1}$$

where α_i is the deflection angle at the observer, $\hat{\alpha}$ is the deflection angle at the lens plane, and $D's$ are angular diameter distances connecting lens, source and observer; and θ is observed source position (a schematic of the lensing geometry can be found in Fig. 3 of the review by Kneib and Natarajan 2011). In the image plane, the predicted positions of counter-images are calculated for each observed image, and compared to the observed ones. The latter, commonly referred to as "image plane minimization", is significantly more computationally intensive since the lensing equation cannot be inverted. The best-fit model is typically identified by maximizing a likelihood function, which usually means minimizing a χ^2 function. Finally, missing information can be dealt with in different ways, such as setting priors on the source redshifts based on photometric information using what are now standard methods, or allowing the model to predict the unknown redshifts of sources.

The different approaches to lens modeling are generally divided into two broad categories, referred to as "parametric" and "free-form" (the latter is also often referred to as "non parametric") methods. Parametric approaches involve representing the mass distribution of the cluster lens with a set of physically-motivated profiles for the surface mass density, which are well described by analytic functional forms, and profile specific properties such as the ellipticity, and positional angles. Parametric models are conceptually motivated by cosmological simulations of structure formation in which cluster scale masses are observed to comprise of large and small scale dark matter halos that are gravitationally bound. Cluster mass distributions are modeled as a superposition of one or more large scale components, corresponding to the smooth cluster and/or group scale dark matter halo seen in simulations and several small scale sub-halos that are associated with the positions of individual cluster member galaxies. The overall gravitational potential of a cluster is therefore modeled as a sum of contributions from large scale dark matter halos and smaller scale sub-halos:

$$\phi_{\rm cluster} = \phi_{\rm smooth} + \Sigma_i\, \phi_{\rm sub}. \tag{2}$$

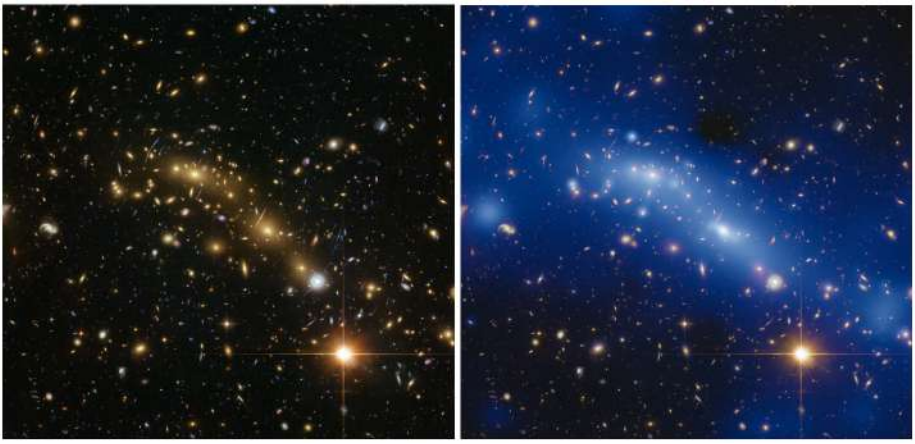

Fig. 3 Left: HST Frontier Fields image of the cluster MACS 0416 at $z = 0.397$. Right: Overlaid on HST image is reconstructed dark matter distribution of the cluster recovered using `Lenstool`shown as a blue haze. Image Credit: NASA/Hubble, ESA, HST Frontier Fields and J. Lotz, M. Mountain, A. Koekemoer, and the HFF Team (STScI). Acknowledgement for overlaid reconstructed dark matter map for Abell 2744: Mathilde Jauzac (Durham University, UK), Jean-Paul Kneib (Ecole Polytechnique Federale de Lausanne, Switzerland) & Priyamvada Natarajan (Yale University, USA). Image taken by the Advanced Camera for Surveys (ACS) and WFC3 including B, V, I, Y, J, H & W filters, with a FOV that is 2.08 x 2.32 arcminutes

As a result, at each position in the cluster, we can explicitly write the convergence, $\kappa(\mathbf{x})$, and the shear, $\gamma(\mathbf{x})$, as a sum over these components (Natarajan and Kneib 1997),

$$\kappa(\mathbf{x}) = \kappa_{\rm smooth}(\mathbf{x}) + \sum_i \kappa_{{\rm sub},i}(\mathbf{x}) \tag{3}$$

$$\gamma(\mathbf{x}) = \gamma_{\rm smooth}(\mathbf{x}) + \sum_i \gamma_{{\rm sub},i}(\mathbf{x}) \tag{4}$$

where $\kappa_{\rm smooth}$; $\gamma_{\rm smooth}$ and $\kappa_{{\rm sub},i}$; $\gamma_{{\rm sub},i}$ are the contributions to the convergence and shear from the smooth component and from the sub-halos respectively.

Examples of commonly used analytic density profiles used to model the gravitational potentials are: a generalized Navarro et al. (1997), and truncated pseudo isothermal models (PIEMDs) that permit the potential to have finite mass and non-zero ellipticity or cored isothermal models. Parametric models have therefore been particularly powerful for comparing properties of observed cluster lenses with theoretical predictions from cold dark matter simulations. An example of parametric reconstruction of the mass distribution of the HFF cluster MACS 0416 with the publicly available software `Lenstool` is shown in Fig. 3.

On the other hand, free-form approaches describe the gravitational lens without assuming a predetermined mass density profile. For example, the lens plane is divided into a fixed or adaptive grid. The lens plane is then populated with some basis functions set, each grid cell is assigned one member of that set. Depending on the method, the number of grid cells can range between a few dozen and many thousands. The amplitude, i.e., mass of each basis function is determined directly by image properties. The motivation for free-form methods is that the mass distribution need not follow simple parametric forms, especially on cluster-wide scales and in merging clusters.

Modeling approaches vary by the degree to which they assume that mass and light distribution in clusters are correlated. Most, if not all, of the parametric approaches assign

mass to observed individual cluster-member galaxies, motivated by empirical correlations like the Faber–Jackson relation derived from observations of early-type galaxies in clusters (Natarajan and Kneib 1997). Some algorithms make no such assumption, and rely only on the lensing evidence to reveal the presence of mass. Finally, several algorithms adopt a hybrid approach: some mass components are inserted as physically-motivated parametric halos, while other components within the same model are set as free-form functions (e.g., Niemiec et al. 2020).

As we note in the following section, when sufficient lensing constraints from rich observational data are available the different approaches outlined above perform equally well. However, they do vary in their strengths and weaknesses, and the decision of which approach to adopt depends primarily on the science goal and motivating question. The primary advantage of the parametric approach is that it can produce satisfactory results even with a small number of constraints that sparsely sample the image plane, as the assumed functional form that describes the lens plane fills in the gaps. And it is particularly well suited for comparison of the properties of observed cluster lenses with simulated clusters. Therefore, for tests of the CDM paradigm, where large cosmological simulations are the only available theoretical test-bed, parametric lensing models have been particularly useful and insightful (Natarajan et al. 2007, 2017; Meneghetti et al. 2020). The high flexibility[2] of free-form models, on the other hand, require rich data sets as a high density of lensing constraints in all regions of the lens plane. However, given sufficient constraints, free-form models can be used to compare properties like the radial slope of the projected mass density against theoretical predictions, and have the flexibility to uncover substructure that may be potentially not be associated with light (Ghosh et al. 2021). Models that do not include a prior assumption about the correlation between mass and light are particularly useful for investigating this exact question—to what extent does mass follow light in the Universe as a function of physical scale (Sebesta et al. 2016; Ghosh et al. 2023).

Development of the formalism and first cluster-scale lens modeling attempts appeared in the literature nearly 25 years ago (Narasimha and Chitre 1989; Kovner 1989; Kneib et al. 1993, 1996; Natarajan and Kneib 1997; Abdelsalam et al. 1998). As noted above, at present, with the availability of richer data from deeper HST imaging surveys over the past two decades, a number of reliable cluster lens mapping methods are available as tabulated below. While the most commonly used methods tend to be parametric, recent years have seen the introduction of several new free-form methods.

- `Lenstool` (parametric; Kneib et al. 1996; Jullo et al. 2007a; Jullo and Kneib 2009; Niemiec et al. 2020). An extension of `Lenstool` includes free-form B-splines in addition to parametric functions (Beauchesne et al. 2021; Limousin et al. 2022).
- Light-Traces-Mass (LTM, parametric; Broadhurst et al. 2005a; Zitrin et al. 2009a, 2015a), which closely ties the total mass to the observed light distribution.
- `GLAFIC` (parametric; Oguri 2010; Ishigaki et al. 2015; Kawamata et al. 2016).
- `GRAVLENS` (parametric; Keeton 2010; McCully et al. 2014).
- GLEE (parametric; Suyu and Halkola 2010; Suyu et al. 2012).
- Weak & Strong Lensing Analysis Package (WSLAP+, hybrid; Diego et al. 2005, 2007, 2016b), which combines parametrized galaxy-scale mass distributions with a free-form distribution on larger scales.
- Strong and Weak Lensing United (SWUnited, free-form; Bradač et al. 2006, 2009), which, unlike most other methods reconstructs lensing potential, not projected mass.

[2] It may be somewhat confusing that free-form models are also called "non-parametric", since they often have *more* free parameters than parametric models.

- PixeLens (free-form; Williams and Saha 2004; Saha et al. 2006; Köhlinger and Schmidt 2014), which is primarily designed for modeling systems with small number of images, but has been used for cluster reconstruction.
- `Grale` (free-form; Liesenborgs et al. 2006; Williams and Liesenborgs 2019; Liesenborgs et al. 2020; Ghosh et al. 2021), which uses an adaptive grid and a genetic algorithm to find solutions in a high dimensional parameter space.
- JPEG parametrization (free-form; Lam 2019), which takes inspiration from JPEG compression to do strong lensing inversion.
- `relensing` (free-form; Torres-Ballesteros and Castañeda 2023), which reconstructs gravitational deflection potential on an adaptive irregular grid.
- `MARS` (free-form; Cha and Jee 2022), which uses a MaxEnt-regularized strong lensing inversion.

3.1 Comparison of Mass Modeling Methods Using Synthetic and Real Clusters

The independent cluster lens modeling methodologies outlined above have been carefully compared and contrasted in order to better understand their relative advantages and limitations. Below, we describe significant community-wide comparison exercises conducted to date and their conclusions. The first (Sect. 3.1.1) involved invitation to multiple teams to reconstruct the mass distribution of two simulated lensing clusters from their produced images wherein all teams were provided with the same input constraints on the identified families of multiple images and their redshifts. By construction, the details of the true underlying mass distributions in this case were known. This exercise was in preparation for the production of publicly available magnification maps from multiple teams for the HFF sample.

For a second exercise (Sect. 3.1.2), since it involved deep HFF imaging data sets, the mapping teams first arrived at a consensus set of input constraints, i.e., mutually agreed upon the identification of multiple lensed image families and either their inferred or measured redshifts to use uniformly for lens mass modeling. And from this cooperative and collaborative effort, magnification maps generated from various independent codes and teams were then made publicly available for the larger astronomical community to use. These maps have been successfully deployed for studies beyond lensing since.

The third exercise (Sect. 3.1.3) was an unanticipated continuation of the previous one, with the serendipitous discovery of a lensed supernovae in the field of two HFF clusters MACS J1149.6+2223 and Abell 2744. Multiple independent teams with their respective methodologies predicted magnification (for the cluster Abell 2744), and the arrival time and magnification of the final image (in the case of MACS J1149) as its observation was awaited.

3.1.1 Comparison of Lens Modeling Methods: Reconstructing the Mass and Magnification of Simulated Cluster Lenses

In this detailed comparison exercise Meneghetti et al. (2017) compared mass distributions derived for the simulated clusters *"Ares"* and *"Hera"* from ten independent modeling groups. Simulated observations of these two simulated clusters that mocked the depth and resolution of HFF observations, were used as the reference sample. *Ares* was generated using the semi-analytical code MOKA, as a superposition of analytical elliptical profiles representing the main cluster and its member galaxies consistent with cosmological initial conditions. *Hera*, on the other hand was more realistic, as it was directly taken from the output of a large volume, high resolution cosmological N-body simulation of the cold dark matter Universe. A concise summary of the comparison results are presented in a figure in Meneghetti et al.

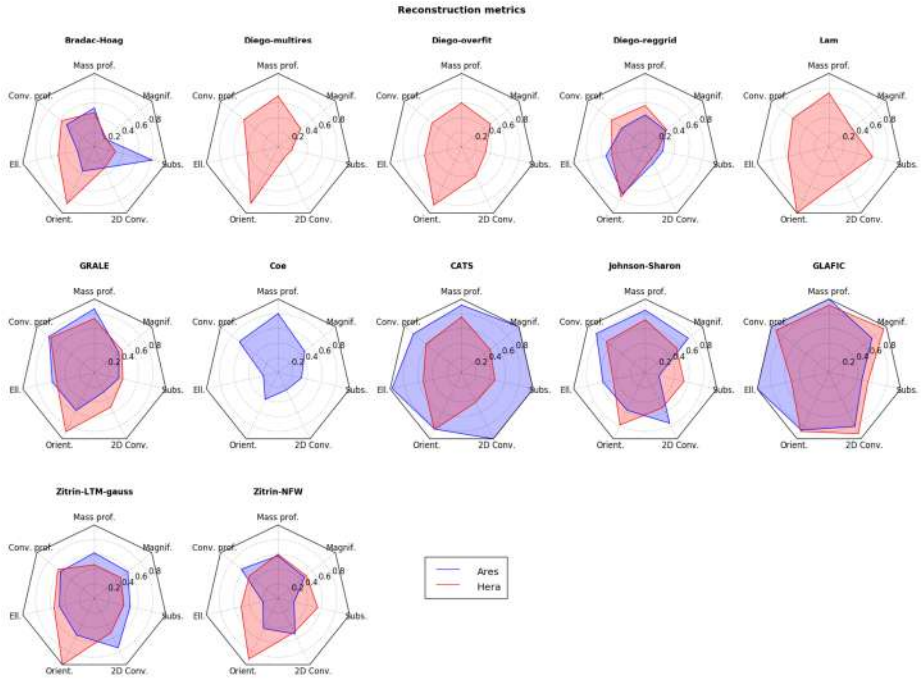

Fig. 4 Reproduced from Meneghetti et al. (2017), an HFF cluster lens mass model comparison project. Their caption reads: Radar plot showing the scores of each model for all metrics discussed in the paper. Larger polygons correspond to better overall performance. Each chart corresponds to a different lens model (see labels on the top) and shows results for both *Ares* (blue) and *Hera* (red), or whichever is available. The seven metrics are shown on the vertices of each chart. For each metric, the scores range from 0 (worst; plotted at the centre of the chart) to 1 (best; plotted at the vertex), normalized to the maximum value recorded by all models. A filled polygon is obtained by connecting the plotted scores of all metrics for each reconstruction

(2017), which we reproduce here as Fig. 4. It is a so-called radar plot; each of the 7 spokes represents a particular cluster property, such as mass profile slope, ellipticity, magnification, etc. If a property is reconstructed well (poorly) by a model the corresponding point is close to the vertex (center) of the black and white polygon. Reconstructed models of *Ares* and *Hera* are represented by blue and red colored polygons respectively. The larger the colored area the better that model reproduces the properties of the synthetic cluster. Upon detailed comparison it was found that several lensing properties that relied on integrated quantities were recovered equally well by the different lens modeling approaches using completely independent methodologies. For instance, the reconstructed mass profiles of the simulated clusters across methods matched at the level of $\sim 10\%$ for both parametric and free-form methods; and the agreement on the mass enclosed within the Einstein radius, was found to be extremely robust for all methods. The results also showed that the parametric modeling methods tend to be generally better at capturing two-dimensional properties of the lens core. This was true in particular for *Ares*, because its true mass distribution resembled assumptions made by parametric methods. In addition, parametric models that permit comparison of additional quantities derivable directly from simulations like the subhalo mass function, and the radial distribution of subhalos, fared well.

Predictably, the uncertainties in reconstructed magnification maps grew as a function of the magnification itself, resulting with largest uncertainties around the critical lines where

the magnification diverges. The accuracy in the magnification estimates dropped by a factor of three when the magnification increased from $\mu_{\rm true} = 3$ to $\mu_{\rm true} = 10$. Another interesting result from this work was that even groups that used the same mass reconstruction algorithms with slightly different priors (e.g., CATS and Johnson-Sharon teams that both used the code `Lenstool`) and very similar inputs, obtained somewhat different maps, revealing the impact of the choice of priors and enabling quantifying their downstream effect.

3.1.2 Comparison of Lens Modeling Methods: Magnification Maps for the HFF Sample

The six clusters of the HFF sample were selected to be amongst the most efficient lensing clusters on the sky and as they were legacy fields observed with Directors Discretionary time, the data was released immediately to the larger astronomical community. However, for exploitation of this unique data set, to interpret the properties of faint background lensed galaxies that these clusters bring into view for instance, reliable lensing maps for each cluster were required to be made available publicly as well. To do so, five independent lens modeling groups were selected to provide preliminary magnification maps for each of the HFF clusters prior to the observing campaign in order to facilitate rapid analysis of the HFF data by all members of the community. These models were initially based on a common set of input data, derived from shallower pre-HFF archival HST imaging, early spectroscopic campaigns, and a common shared catalog of lensed background galaxies. Once the data were taken, these models were continually collectively updated by each of the groups. As noted before the techniques adopted by groups spanned both parametric and free-form methods.

The public HFF lens models include maps of mass (κ) and shear (γ) from which magnifications can be derived for sources at any redshift using scripts provided on the HST site. The models cover regions constrained by strongly lensed, multiply-imaged galaxies, within the HST ACS fields of view of the cluster cores. Some models extend to larger areas, including the HFF parallel fields, and also incorporate ground-based weak lensing data. All data, models and detailed description of individual methods and maps are available at the following website: https://archive.stsci.edu/prepds/frontier/lensmodels/.

Since cluster magnification is of paramount importance for the HFF project, several papers compared magnification distributions as reconstructed by various independent groups. Figure 5 shows magnification maps of Abell 2744 from 6 HFF teams, analyzed in Priewe et al. (2017). It was found that in the broadest terms the reconstructed magnification maps more or less agreed with each other. However, differences are also seen, and often exceed their quoted statistical errors. The resulting dispersion ranged from 30% at low magnifications, $\mu \sim 2$, to 70% at high magnifications, $\mu \sim 40$. This implies that the true uncertainties are probably currently underestimated in most of the modeling methods. These differences are mainly attributed to lensing degeneracies, suggesting that a small lens plane rms value is not a sufficient condition for a model to robustly and reliably predict the true magnifications.

The more recent magnification comparison study by Raney et al. (2020b) also arrives at similar conclusions, finding $\sim 40\%$ dispersion at low magnifications ($\mu \sim 3$) that increases to $\sim 65\%$ dispersion at high magnifications ($\mu \sim 10$). In contrast, excellent agreement exists for the derived integrated quantities like the cumulative mass distribution and it is significantly well constrained within $1'$ radius from the cluster core, with $< 5\%$ dispersion. Additionally, Remolina González, Sharon and Mahler (2018) examined source plane scatter in 10 mass reconstruction models for the HFF cluster MACS J0416. Using source plane rms as a metric of diagnose lens model performance, they quantified the ability of different models to predict unknown multiple images. They found that while free-form reconstructions rely heavily on the quality and quantity of the lensing data, parametric models are not as

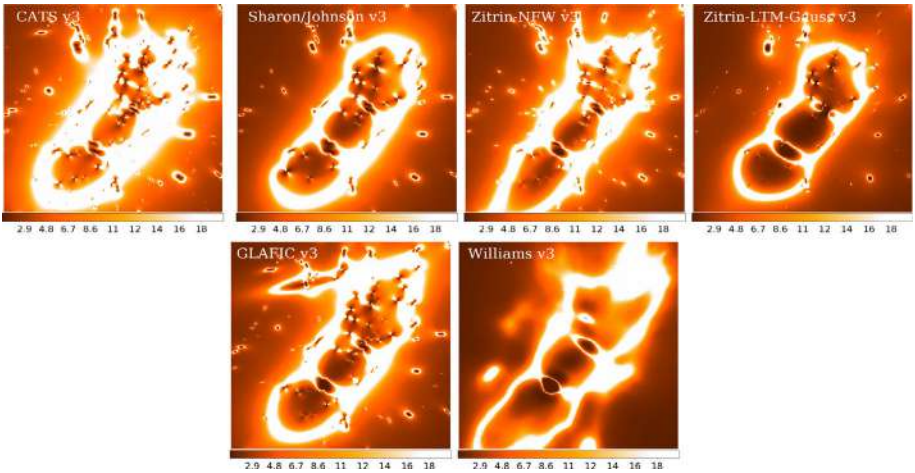

Fig. 5 Magnification maps of 6 different reconstructions of galaxy cluster Abell 2744. The reconstruction team names appear in the top left of each panel. Magnification scale is the same for all panels, and goes from $\mu = 1$ (darkest color) to $\mu = 20$ (white). Each panel is a square 100 arcsec on the side. Taken from Priewe et al. (2017)

susceptible to uncertainties in the data. However, parametric models do not necessarily benefit from adding more constraints with the inclusion of photometric redshift measurements when the existing amount of spectroscopic data available is large (of the order of measured redshifts for a hundred or so lensed images), as in the case of the HFF clusters.

3.1.3 Comparison of Lens Modeling Methods: Using Time Delays and Magnifications of Quasars and Supernovae

After the serendipitous discovery of the Supernova Refsdal in 2014, multiply imaged by a cluster member galaxy in the HFF cluster MACS J1149.6+2223 at $z = 0.544$, it was predicted that there would be the rare opportunity to see the supernova again in about one year, after the four images had faded away Kelly et al. (2015). This is because the initially observed four-image pattern was only one component of the lensing configuration. This supernova might have appeared as a single image some 10-20 years prior in the cluster field, and it reappeared at the predicted position between mid-November 2015 and December 11, 2015 (the approximately one month uncertainty is the interval between two consecutive Hubble observations). This was in good agreement with the blinded model predictions made by several independent groups deploying the range of lens reconstruction techniques prior to its observation Sharon and Johnson (2015), Oguri (2015), Diego et al. (2016a), Treu et al. (2016). The time delay between the original quadruplet observed in 2014 and the latest appearance of the supernova in 2015 was used to infer the value of the Hubble constant. This is the first time this technique, originally proposed by Refsdal, was successfully applied to supernovae Vega-Ferrero et al. (2018).

In the case of another supernova detected behind the HFF lensing cluster Abell 2744 at $z = 0.308$, once again, specific predictions for the magnification derived from different lensing models have been compared in detail. Rodney et al. (2015) computed the magnification predictions from various lens models for the location and redshift of the Type-Ia supernova HFF14Tom, leveraging the idea that the true luminosity of a SN-Ia can be inferred from

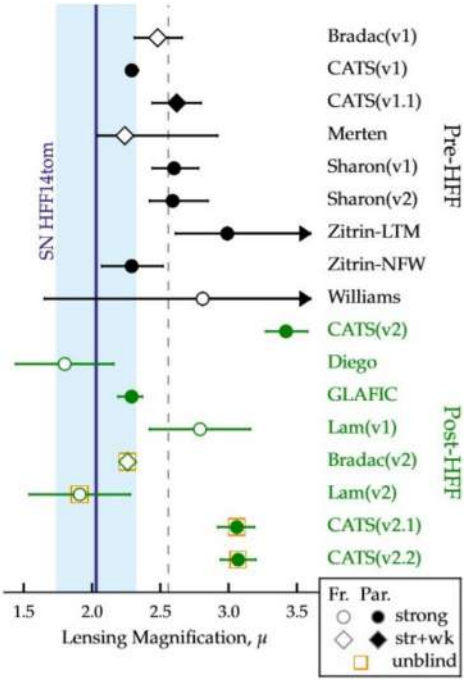

Fig. 6 The observed lensing magnification is compared to predictions from multiple independent lens models. The vertical blue line shows the constraints from SN HFF14Tom, with the shaded region marking the total uncertainty. Markers with horizontal error bars show the median magnification and 68% confidence region from each model. Circles indicate models that use only strong-lensing constraints, while diamonds denote those that also incorporate weak-lensing measurements. Free-form (parametric) models are shown as open (filled) markers. The top half, with points in black, shows the 9 models that were constructed using only data available before the start of the HFF observations. The lower 8 models in green use additional input constraints, including new multiply imaged systems and redshifts. The final four points, with square orange outlines, are the "unblind" models that were generated after the magnification of the SN was known. The black dashed line marks the unweighted mean for all 17 models, at $\mu = 2.6$. Image reproduced with permission from Rodney et al. (2015), copyright by AAS

its lightcurve (see Fig. 6). They report that the median of the lensing model magnification predictions is 25% higher than the magnifications deduced from the observed brightness of the supernova, and that many model predictions disagreed by more than their stated uncertainties. A possible reason for the discrepancy is that there are not enough spectroscopically confirmed multiple image systems to constrain the lens models: accurate and precise image redshifts are as important for lens reconstructions as image positions.

3.1.4 Comparison of Lens Modeling Methods: Detailed Comparison of Spatial Regions Within Clusters

In addition to the exercises described above, it is instructive to compare regions of special interest in the reconstructed mass maps generated by various lens modeling methods. These could include regions around main cluster galaxies, or those that have excess reconstructed mass but are deficient in light. Ghosh et al. (2021) show that reconstructions with distinct modelling philosophies – parametric vs. free-form – often lead to similar results regarding specific mass features, while at the same time, models using the same algorithm can draw

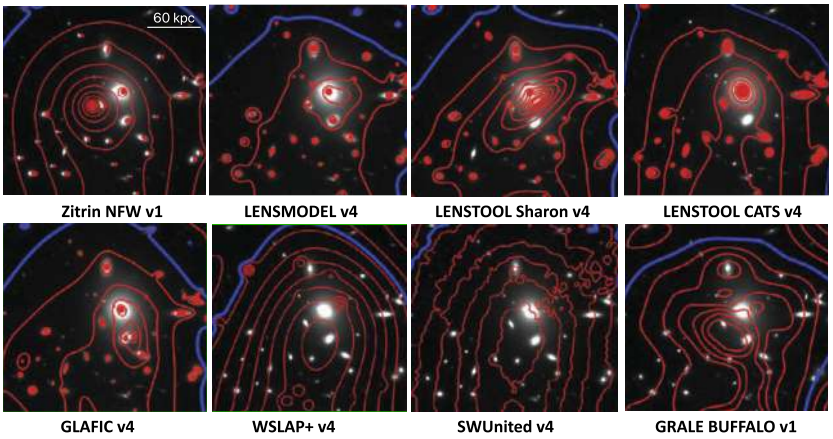

Fig. 7 Comparison between different lens inversion methods mass maps of the same region in the HFF cluster Abell 370, centered on the northern of the 2 brightest cluster galaxies. Each panel is a square of 45 arcseconds on the side, or ~ 250 kpc. The gray scale is the HST image in ACS/F814W filter. The panels show eight different reconstructions by various teams. The contours are those of equal projected dimensionless surface mass density, κ, with the blue contour corresponding to $\kappa = 1$. All but 3 (LENSMODEL HFFv4, LENSTOOL CATS HFFv4, Glafic HFFv4) show that the local center of mass and light do not coincide, with the center of mass offset the center of the BCG. For maps with offset centers, the offset is generally to the South of the BCG, though the morphology and the degree of displacement differs between models

contrasting conclusions, just by using somewhat different model priors and data constraints. Figure 7 presents a region in an HFF cluster Abell 370, centered on the northern BCG. The red contours show the projected surface mass density, κ, with the blue contour indicating $\kappa = 1$. Most models show that the center of mass appears to be displaced, generally towards the South, compared to the location of the center of light. This inferred feature of misalignment between mass and light is consistent with the merging, disturbed nature of this cluster. The fact that not all mass reconstructions agree on the detailed mass distribution in that region, including the misalignment between mass and light, is mostly due to lensing degeneracies, which are present not just on cluster scale, like the mass sheet degeneracy, but also on smaller scales (Lasko et al. 2023). A larger number of multiply imaged sources than currently available will help to map out that region more accurately (Lin et al. 2023) in the future. Other interesting examples are presented in Ghosh et al. (2021) and Ghosh et al. (2023). The high spatial resolution with which strong lensing can measure the mass distribution can test predictions of dark matter properties (e.g., Harvey et al. 2019). In summary, what these results imply is the importance of continued stress-testing of all lens mass modeling methods and continued comparison between them to delineate systematics that need to be understood in greater detail in cluster lensing studies.

3.2 Connecting the Strong and Weak Lensing Regimes

While strong-lensing driven mass modeling techniques have been used to obtain high signal-to-noise reconstructions in the central regions of clusters, the power of weak lensing is critical to extend the derived mass distributions out to the virial radius (e.g., Clowe et al. 2006b; Umetsu et al. 2014; Umetsu 2020). Connecting strong lensing and weak lensing regimes has therefore long been seen as a powerful way to recover the detailed and extended mass distribution of clusters from the central region to the outskirts. The method also has the advantage

of breaking the so-called mass-sheet degeneracy (MSD), which says that the surface mass density κ is invariant under the following global transformation $\kappa(\theta) \rightarrow \lambda\kappa(\theta) + (1 - \lambda)$, where λ is between 0 and 1. Non-zero λ rescales the original surface mass density, and adds a constant density sheet to the lens. As a result, the overall density slope becomes less steep (Schneider and Seitz 1995). Weak lensing helps break MSD because it is reasonable to assume that beyond the weak lensing regime, i.e., far from the cluster center, cluster density is negligible.

Many of the lens modeling methods described above leverage the potency of this combination and therefore include both weak and strong lensing data, and some methods also include higher order information from flexion as well. Flexion parameters are similar to shear, but instead of the second derivatives of the lensing potential, they encode the third derivatives (e.g., Goldberg and Natarajan 2002; Bacon et al. 2006; Lanusse et al. 2016). When both shear and flexion are important, image shapes deviate from purely elliptical distortion and can look 'banana'-shaped. Flexion has been used to reconstruct mass distribution in some clusters (e.g., Okura et al. 2008).

The simplest adopted approach is to combine strong and weak lensing in a parametric fashion (e.g., `Lenstool` has included strong and weak lensing out to large cluster radii; Natarajan et al. 2009; Niemiec et al. 2020; Schäfer et al. 2020). These and other methods that were used to model cluster cores previously have an advantage that they are numerically stable, they are, however, inherently limited to the fitting a set of parametrized models Natarajan et al. (1998). Recently, free-form methods have also been used for combined analysis (Diego et al. 2005; Bradač et al. 2006; Merten 2016; Liesenborgs et al. 2020). Modeling that include combining the two lensing regimes has been successful in predicting mass profiles on all scales and in determining other observables like the mass-concentration relation in clusters (Merten et al. 2015). They have also proven useful in reconstructing magnification fields for high-redshift galaxies beyond the regime where strongly lensed images at lower redshifts are typically found as this pertains to the regime and region where magnification is poorly constrained (Priewe et al. 2017). Inclusion of higher order constraints like flexion can also add useful information in this intermediate regime as demonstrated by Cain et al. (2016), Leonard et al. (2007).

Another successful example of combining strong and weak lensing mass reconstruction has been the case of the Bullet Cluster (Fig. 8, Clowe et al. 2006a; Bradač et al. 2006). The Bullet cluster comprises a pair of plane-of-the-sky merging sub-clusters, where the dominant baryonic mass in the form of X-ray emitting gas, and the total mass, dominated by dark matter are not aligned post collision on the sky, providing strong evidence that dark matter is collisionless. In particular strong lensing provides useful constraints – for instance, the offset between the peak of the baryonic mass, as traced by X-rays, and the peak of the total mass, as traced by strong and weak lensing, is over an arcminute, and was measured at $> 10\sigma$ (Bradač et al. 2006), while the limits with only weak lensing were 8σ (Clowe et al. 2006a). The Bullet Cluster configuration – the location of the mass peaks, the offset between baryonic and dark matter distributions and the inferred relative velocity of the colliding sub-clusters was a challenge to reproduce for cold dark matter simulations Springel and Farrar (2007). The strong constraints on the inferred positions of the peaks of mass distribution provides a challenge for simulations that assume non-negligible self-interaction cross sections for dark matter (Randall et al. 2008; Lage and Farrar 2015). In addition, results from combined analysis also provide useful and meaningful constraints on several alternative gravity models as they fail to predict large mass concentration needed to produce strong lensing constraints (e.g., Angus et al. 2006).

Many clusters now have successful measurements of mass and detailed mass distributions in combined regimes. HFF clusters have been reconstructed using combined strong

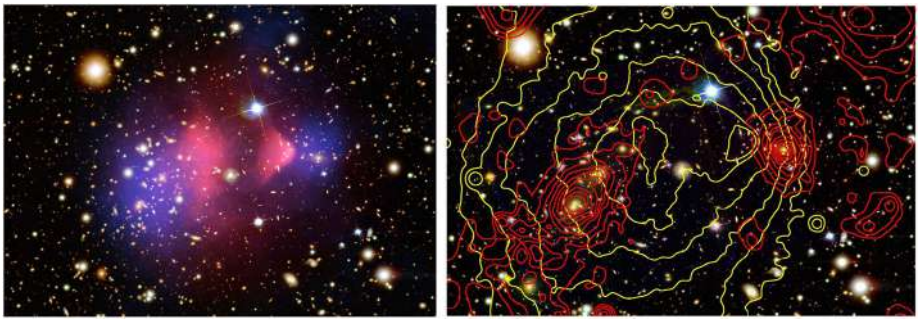

Fig. 8 Left: The color composite of the Bullet Cluster using only weak lensing measurement. Overlaid in *blue* shade is the surface mass density map from the weak lensing mass reconstruction. The X-ray emitting plasma is shown in *red*. Credit NASA/CXC/CfA/STScI/Magellan, Clowe et al. 2006a. Right: Strong and weak lensing reconstruction for the Bullet Cluster. Overlaid in red contours is the surface mass density κ from the combined weak and strong lensing mass reconstruction. The X-ray brightness contours from the 500 ks Chandra ACIS-I observations are overlaid in yellow. Bradač et al. 2006, 2009

and weak lensing analysis; see for example (Jauzac et al. 2016; Merten et al. 2011; Wang et al. 2015; Hoag et al. 2016; Finney et al. 2018; Strait et al. 2018). The scientific results from these studies are discussed in Sect. 5.

4 Surveys for Cluster Lenses

4.1 HST Cluster Lens Samples: CLASH, RELICS, HFF, BUFFALO Surveys

HST has devoted significant resources to cluster lensing observations via multiple programs including CLASH, RELICS, HFF and BUFFALO. Significant progress in the field of galaxy cluster physics has been made thanks to the data collected within the HST Multi-Cycle Treasury program Cluster Lensing And Supernova survey with Hubble (CLASH; Postman et al. 2012), complemented with a comprehensive and coordinated spectroscopic campaign carried out with the ground-based telescopes (e.g., the CLASH-VLT Large Programme; Rosati et al. 2014).

The CLASH survey was awarded 524 orbits of HST time (GO 12066; PI: M. Postman) to observe 25 massive (virial mass $M_{\rm vir} \approx 5\text{-}30 \times 10^{14}\, M_\odot$, and X-ray temperature $T_{\rm X} \geq 5$ keV) galaxy clusters in 16 broadband filters, ranging from approximately 2000 to 17000 Å, with the Wide Field Camera 3 (WFC3) and the Advanced Camera for Surveys (ACS). The sample, spanning a wide redshift range ($z = 0.18 - 0.90$), was carefully chosen to be largely free of lensing bias and representative of relaxed clusters, on the basis of their symmetric and smooth X-ray emission profiles. CLASH had four main scientific goals: 1) to measure the total mass profiles of cluster over a wide radial range by using strong and weak lensing observations; 2) to detect new Type Ia supernovae out to redshift $z \sim 2.5$ to improve the constraints on the dark energy equation of state; 3) to discover and study the highly magnified first galaxies that formed after the Big Bang ($z > 7$) and are brought into view by the cluster lens; and 4) to study galaxy evolution by comparing cluster member properties with those of and background galaxies (for a thorough overview, see Postman et al. 2012).

A Large Programme (186.A-0798, PI: P. Rosati; Rosati et al. 2014) of 225 hours with the VIMOS instrument at the VLT was also approved to perform a panoramic spectroscopic

survey of the 14 CLASH clusters that are visible from ESO-Paranal. This observational campaign was aimed at measuring in each cluster the redshifts of 1) approximately 500 cluster members within a radius of 3 Mpc; 2) determine spectroscopic redshifts for 10-30 lensed multiple images inside the HST field of view, including possible highly-magnified candidates out to $z \approx 7$ (e.g., Balestra et al. 2013); 3) possible supernova hosts. In the first CLASH cluster that was followed-up (i.e., MACS J1206.2−0847), the spectroscopic redshifts were exploited to build robust strong lensing models (Zitrin et al. 2012a, Umetsu et al. 2012, Eichner et al. 2013, Grillo et al. 2014); to obtain an independent total mass estimate from the spatial distribution and kinematics of the cluster members (Biviano et al. 2013, Sartoris et al. 2014); to study the properties of the intracluster light (Presotto et al. 2014), and to characterize the galaxy stellar masses as a function of environment and the stellar mass density profiles (Annunziatella et al. 2014).

Using the unprecedented data set—panchromatic HST imaging and VLT spectroscopic data, astronomers have measured the gravitational potential in the inner regions of the cluster (i.e., the total mass profile in the core) for some of the CLASH clusters, by modeling the multiple images of several newly discovered strong lensing systems (e.g., Zitrin et al. 2015b, Coe et al. 2012, Monna et al. 2014, Grillo et al. 2015). Moreover, the combination of the HST observations with deep, multi-band, wide-field imaging from Subaru has allowed the weak lensing detection and therefore extension of the mapping of the total mass profile of several clusters out to their virial radii (Medezinski et al. 2013, Umetsu et al. 2014, Merten et al. 2015).

The advent of the MUSE instrument at the VLT has revolutionized strong lensing studies in galaxy clusters. MUSE capabilities permit simultaneous identification and study of cluster members and multiply imaged background sources out to $z = 6.6$. The exceptional suitability of MUSE to reach these goals has been demonstrated by several successful programs (e.g., Karman et al. 2015, Richard et al. 2015, Grillo et al. 2016, Caminha et al. 2019, Bergamini et al. 2021), which have enabled the construction of detailed mass models of the cores of cluster lenses.

The results from systematic studies of lensing clusters with HST, including those from CLASH, led to the deeper Hubble Frontier Fields Initiative (HFF; Lotz et al. 2017) that targeted six massive galaxy clusters, for a total of 140 HST orbits per cluster in 7 broadband filters, achieving in all of them unprecedented depth of ∼29 mag (AB) using Director Discretionary Time. This program has detected some of the highest redshift galaxies and enabled the first characterization of this sample of star-forming galaxies in a statistically meaningful way (e.g., Bouwens et al. 2017a). The HFF data have also provided a great opportunity to study the structure of the dark matter halos hosting these clusters (e.g., Caminha et al. 2017, Natarajan et al. 2017, Bergamini et al. 2019, Meneghetti et al. 2020).

The Reionization Lensing Cluster Survey (RELICS; PI: D. Coe; Coe et al. 2019) consisted of 190 orbits of HST time to observe the cores of 41 galaxy clusters in 7 broadband filters, ranging from approximately 0.4 to 1.7 μm with the WFC3 and the ACS. This sample, spanning a wide redshift range (z = 0.18-0.97), was carefully chosen to be representative of the most massive clusters ($M_{500} \gtrsim 8 \times 10^{14}$ $M_{\odot}$; thus also many of the most efficient cluster lenses) discovered so far, on the basis of their Sunyaev-Zel'dovich (SZ) mass estimates released by the Planck collaboration, and other known strong lenses. These include ACT-CLJ0102−49151 (El Gordo) (Menanteau et al. 2012, Zitrin et al. 2013), PLCK G287.0+32.9 with arcs 80″ from the core (Gruen et al. 2014) and CL 0152−1357, a massive merging cluster at $z = 0.83$ (Acebron et al. 2019). The HST imaging of the HFF combined with Spitzer imaging (390 hours; PIs: M. Bradac & T. Soifer) yielded strongly lensed high-z candidates among the best and brightest known.

The latest contribution to the lensing data comes from The Beyond Ultra-deep Frontier Fields and Legacy Observations (BUFFALO) Program, with 101 orbits and 101 parallels as a part of Hubble Space Telescope's Treasury program, taking data from 2018-2020 (Steinhardt et al. 2020). BUFFALO expanded the existing coverage of the HFF fields in additonal filters: WFC3/IR F105W, F125W, and F160W and ACS/WFC F606W and F814W around each of the six HFF clusters and flanking fields. These fields are already covered by additional deep multi-wavelength datasets, including Spitzer and Chandra. Further important additions to the data are provided by the spectroscopic surveys, such as the Pilot-WINGS (Lagattuta et al. 2022).

4.2 X-ray and SZ Surveys for Cluster Lenses

X-ray selected clusters have been invaluable in identifying potential strong lensing clusters. Horesh et al. (2010) concluded that clusters from the MAssive Cluster Survey (MACS; Ebeling et al. 2001) are significantly more—by a factor of ~ 6—efficient as lenses than optically selected clusters. Many of the MACS clusters are now household names among those doing cluster lens modeling. X-ray clusters are also used in another capacity. Several efforts have been underway at X-ray wavelengths to obtain complementary information on the cluster hot gas component (e.g., Ogrean et al. 2015). Owing to the adopted selection criteria, in all the clusters of the CLASH sample, measurements of the X-ray emission of the hot intracluster medium, taken with the Chandra telescope (and in some cases also with the XMM-Newton telescope) were available. These observations are in most cases sufficiently deep to estimate the hot gas and total mass profiles, under the assumption of hydrostatic equilibrium (Donahue et al. 2014). In some clusters, a combined strong lensing, photometric and X-ray analysis has allowed a precise decomposition of the cluster total mass profiles into their stellar, hot-gas and dark-matter components (Annunziatella et al. 2017, Bonamigo et al. 2017, 2018, Granata et al. 2022). Systematic searches for clusters at high redshifts, $z \sim 1$, has become possible using their Sunyev-Zeldovich (SZ) emission. The important surveys were done by the Planck CMB satellite and the South Pole Telescope (SPT). The masses of these clusters can be calibrated through weak lensing (Sereno et al. 2017; Raghunathan et al. 2019; Schrabback et al. 2021).

4.3 Ground-Based Imaging Surveys for Cluster-Scale Strong Lenses

Wide optical and spectroscopic surveys such as the Sloan Digital Sky Survey (SDSS; Blanton et al. 2017) have been a fruitful hunting ground for several strong lensing surveys; from galaxy-lensed quasars, through galaxy-galaxy lenses, to the most massive cluster lenses. Teams have used different methods to identify candidate lenses in these public data. Some of the most well studied cluster lenses (e.g., the "poster child" cluster lens Abell 1689) are hardly unidentifiable as such in shallow SDSS imaging. The numerous multiple images in Abell 1689 are too faint to be robustly identified. Most shallow, ground-based surveys for cluster lenses aim to discover the lensing effect itself, i.e., an occurrence of highly distorted and magnified galaxy in the form of one of more giant arcs. The Sloan Giant Arcs Survey (SGAS; PI: M. Gladders; Bayliss et al. 2011; Sharon et al. 2020) yielded hundreds of cluster lenses by mining the SDSS DR7 imaging data. Starting with the SDSS public catalog, SGAS first identified clusters and groups using the red sequence technique (Gladders and Yee 2000). g, r, i, and z cutouts around these fields were then examined by eye to identify lines of sight with bright arcs, and given scores. Lens and arc candidates were confirmed through imaging and spectroscopy with larger telescopes, reaching close to 100% followup

completeness of high-scoring candidates. The selection process was designed such that purity and completeness could be quantified, making the results useful for statistical studies of lensing occurrence (a.k.a arcs statistics, see Sect. 5.4 and cluster studies. Due to its selection function, the SGAS sample provided a bountiful supply of highly magnified background sources at "cosmic noon" – those galaxies that reside in the epoch when the Universe formed most of its stars. The high magnification makes feasible detailed spectroscopic studies of the physical properties of these galaxies (see Sharon et al. 2020, and references therein), also leading to offshoot surveys such as MEGaSaURA (Rigby et al. 2018). Similar methods for discovery and confirmation of strong lensing clusters were employed in searching through the RCS-2 survey (Gilbank et al. 2011) for lenses, and most recently in the COOL-LAMPS (Khullar et al. 2021) survey.

4.4 Cosmological and Large Area Surveys

There are multiple on-going and planned surveys that will garner large samples of cluster lenses. While these are expected to be shallower than the HST cluster lens samples discussed above, the majority of them stand to detect and exploit weak lensing. One of recently concluded ground-based surveys is the Dark Energy Survey (DES).

DES is a large survey of distant galaxies including clusters that aims to uncover the nature of dark energy that drives cosmic acceleration using multiple techniques, that include its impact on the abundance of galaxy clusters; weak gravitational lensing signals; type Ia supernovae and the detection of large-scale correlations between galaxies. The survey uses a powerful wide-field imaging camera called the Dark Energy Camera, or DECam, installed on the 4-meter Blanco telescope in Chile. During its five-year campaign (2013-2018), the DECam imaged approximately 5000 square degrees of the sky using five broadband filters, taking advantage of the excellent viewing conditions available on Cerro Tololo. The final DES dataset will consist of precise photometric and morphological information for over 200 million galaxies out to redshifts of 2.0. The survey is also periodically revisiting smaller patches of sky to find and study over 2500 Type Ia supernovae. Forecasts for expected cluster weak lensing results from the DES and other ground based surveys with the Rubin Observatory as well as from the Nancy Grace Roman Space Telescope are promising for constraining cosmological parameters Wu et al. (2021).

The recently successfully launched and deployed Euclid mission consists of a 1.2 m space telescope that is dedicated to study the imprint of dark energy and gravity via two powerful, complementary cosmological probes: weak gravitational lensing and galaxy clustering (via baryonic acoustic oscillations and redshift space distortion). These two complementary probes will capture signatures of the expansion rate of the Universe and the assembly of cosmic structures (Amendola et al. 2013). The key instruments aboard the telescope are a high quality panoramic visible imager (VIS), a near infrared 3-filter (Y, J and H) photometer (NISP-P) and a slitless spectrograph (NISP-S). These instruments will permit accurate shape measurements and therefore quantify weak gravitational lensing effects of dark matter as well as three-dimensional mapping of structures with spectroscopic redshifts of galaxies and clusters of galaxies (Sartoris et al. 2016). Euclid will observe 15,000 deg^2 and is expected to find of the order of 60,000 galaxy clusters in the redshift range $z = 0.2 - 2$. It is forecast that $\sim$ 50,000 of them will have background galaxy densities > 15 galaxies per sq. arcmin allowing accurate determination of cluster masses from weak lensing studies out to the virial radius and beyond (Euclid Collaboration et al. 2019). The imaging and spectroscopic capabilities of Euclid will enable internal mass calibration from weak lensing and the study of the dynamics of cluster galaxies, in combination with ground based cluster

surveys like DES (Tutusaus et al. 2020). Euclid is also expected to detect several thousand lensed arcs, as predicted from the analysis with the Skylens simulation package, which has catalyzed the development of new automated arc-finder algorithms. Three "Euclid Deep Fields" covering around 40 $\deg^2$ in total will be also observed extending the scientific scope of the mission to access the very high-redshift universe.

5 Science Results from Modeling Observed Cluster Lenses

5.1 Insights on Larger-Scales

One of the first clusters to have the mass profile derived from observed lensing was Abell 1689 (Broadhurst et al. 2005a). Its profile is consistent with that expected in the LCDM universe, but with a somewhat larger concentration (Broadhurst et al. 2005b; Coe et al. 2010), which can be explained by the lensing selection bias because higher concentration makes a cluster a stronger lens. A number of studies over the next decade looked at the distribution of properties of large sets of clusters (Richard et al. 2010; Zitrin et al. 2011). More recently, Fox et al. (2022) analysed a large sample (74) of RELICS clusters using their strong lensing data. Not all of these were found to be in equilibrium and relaxed, and consequently they display a large diversity in their density profiles, especially in the radial range 50-200 kpc.

In order to test the standard LCDM cosmological model, one needs to select clusters that are in equilibrium, because simulations (Navarro et al. 1997, 2004), and theory (Hjorth and Williams 2010; Williams et al. 2010; Wagner 2020) make specific predictions for the spherically averaged density profiles of relaxed dark matter halos. To determine whether the cluster radial mass distribution is in good agreement with the predictions of, one needs a large radial range of the mass reconstructions. The strong lensing region of clusters, wherein the surface mass density exceeds the critical value, is relatively small, spanning at most one decade in radius. Therefore, it needs to be supplemented with weak lensing data. Umetsu et al. (2016) performed a joint analysis of 20 CLASH clusters using their strong, weak and magnification data, over two decades in radius, from $\sim 30 - 3000$ kpc, corresponding to approximately the virial radius of these clusters. They found that the stacked density profile in these clusters is well described by the fitting formulae from the cold dark matter simulations, i.e., NFW (Navarro et al. 1997) and Einasto (Navarro et al. 2004) profiles, as well theoretical DARKexp (Hjorth and Williams 2010) profiles for relaxed, collisionless, self-gravitating systems. We re-iterate that massive galaxy clusters are uniquely suited for this important test of dark matter properties because their mass is dominated by dark matter over a wide range of spatial scales. In addition to radially averaged density profile, one can also use the median ellipticity of a set of relaxed clusters as a test of standard cosmology and the nature of dark matter. Using the same set of 20 CLASH clusters, Umetsu et al. (2018) found that the median projected axis ratio of clusters' dark matter halos is in agreement with the predictions from recent numerical simulations of the standard collisionless cold dark matter model.

On much smaller scales than discussed above, the density profile in the very central regions of clusters, $\lesssim 50$ kpc, or a few percent of the virial radius, are often hard to estimate because the de-magnified central images (maxima in the Fermat potential) are usually not detected. A detection of two central images has been claimed in the cluster Abell 3827 by (Massey et al. 2018a). Yet, the question of the central profile—whether clusters have flat

density cores or cusps—is very important for constraining of the nature of dark matter (also see Sect. 5.5).

Limousin et al. (2022) modeled two unimodal clusters (i.e., with a single dominant center) AS 1063, and MACS J1206, and one bimodal cluster MACS J0416. While the last cluster is an ongoing merger, the dynamical status of the unimodal clusters is not clear; they show some evidence of disturbance, and so are probably not relaxed. A new metric utilizing the computation of the power spectrum of fluctuations in the mass and X-ray gas maps reveals that unimodal clusters that appear smooth may still be out of equilibrium Cerini et al. (2023). The authors conclude that cored profiles interior to ~ 50 kpc are favored over cusped ones in these 3 clusters. However, for the purposes of comparison with cosmological model predictions, and stress-testing the underlying structure formation model itself more clusters, and preferably relaxed ones, need to be analysed to make a conclusive statement about the mass distribution in the very central regions of clusters.

5.2 Mapping Dark Matter Substructure & Galaxy-Galaxy Lensing in Clusters

The standard paradigm that describes structure formation in the Universe is the concordance cold dark matter model with a non-zero cosmological constant (LCDM). In simulations of the LCDM model, where dark matter is collisionless, the internal density distribution in dark-matter halos, as noted previously, converges to a roughly "universal" and cuspy density profile, the NFW profile (Navarro et al. 1996, 1997) over several decades in mass. Moreover, the degree of central concentration of a halo in LCDM depends on its formation epoch, and hence on its total mass (Wechsler et al. 2002, Zhao et al. 2003). In this scenario, objects that virialize early are dense and compact if they get accreted and or bound into a larger halo during hierarchical assembly. These smaller scale collapsed structures are usually referred to as sub-halos that are held within the gravitational potential well of the more massive host halo. Spiraling in toward the center owing to dynamical friction, while they are truncated or disrupted by tidal forces, leads to changes in sub-halo masses, angular momentum and energy (Ghigna et al. 1998; De Lucia et al. 2004).

On cluster scales, observational tests of several concrete LCDM predictions using lensing mass models have been performed. The abundance of sub-halos in clusters, also referred to the mass function of substructure (or the sub-halo mass function) is predicted to be a power law of the form $dn/dm \propto m^{-1.8}$. This prediction has been robustly tested with increasingly higher resolution HST data of cluster lenses and generations of state-of-the-art cosmological simulations ranging from the Millenium simulation (Natarajan and Springel 2004; Natarajan et al. 2007) to the Illustris simulation suite (Natarajan et al. 2017). Predictions of tidal stripping of subhalos in LCDM have also been tested (Natarajan et al. 2002a; Sand et al. 2002, 2004; Natarajan et al. 2009) with tidal radii estimated from lensing mass models. Overall, properties of cluster lenses and their sub-halo mass functions were found to be in good agreement with LCDM predictions. Recently more sophisticated and detailed comparisons with high fidelity mass reconstructions for clusters have become possible, so much so that we are now in a position to stress-test the LCDM model (Grillo et al. 2015, Natarajan et al. 2017, Meneghetti et al. 2020). In fact, Natarajan et al. (2017) report tension between the observed radial distribution of subhalos in the massive HFF cluster lenses compared to simulated clusters in LCDM, an issue that is replicated on galaxy scales as well, wherein the radial distribution of observed satellites is discrepant with theoretical predictions Carlsten et al. (2020).

Meneghetti et al. (2020) reported that the observed number of Galaxy-Galaxy Strong Lensing (GGSL; see the right panels of Fig. 2) events, i.e., strong lensing events observed

on the scale of individual cluster galaxies on mass scales of $\sim 10^{11}\, M_{\odot}$ in cluster lenses, exceeds the expectations from LCDM simulations by more than one order of magnitude. These significant differences in the spatial and mass distributions of the cluster sub-halos do not seem to be fully fixed by the inclusion in cosmological simulations of baryonic physics, in the form of cooling, star formation, and feedback by active galactic nuclei. Robertson (2021) and Bahé (2021) argue that the reported under-abundance of GGSL events in simulations is due to their low resolution. These authors use considerably higher mass resolution runs, and also include several baryonic physical processes. They report that this results in a higher number density of substructures in lensing clusters, leading to comparable simulated and observed occurrence of GGSL events. GGSL is computed using the area enclosed within smaller scale secondary caustics. However, the majority of the contribution to the GGSL cross section computed from the simulations reported in Robertson (2021), Bahé (2021) arises from in-falling group-scale substructures that are more massive than those reported in Meneghetti et al. (2020). In addition, in recent work, Ragagnin et al. (2022) note that the stellar masses of cluster galaxies in the suite of simulations studied by Bahé (2021), Robertson (2021) vastly exceed that of observed cluster galaxies which in turn artificially enhances their computed GGSL cross section.

In continuing work pursuing the origin of this discrepancy Meneghetti et al. (2022) quantify the impact of the numerical resolution and AGN feedback scheme adopted on the predicted GGSL probability to alleviate the gap with observations. Improving the mass resolution by a factor of ten and twenty-five, while using the same galaxy formation model that includes AGN feedback does not affect the GGSL probability. Adopting an AGN feedback scheme that is less efficient at suppressing gas cooling and star formation leads to an increase in the GGSL probability by a factor between three and six, however, while such simulations form overly massive subhalos whose contribution to the GGSL would be higher, their Einstein radii are too large to be consistent with the observations. The primary contributors to the observed GGSL cross-sections are compact subhalos with lower masses (in the mass range of $\sim 10^{10-11.5}\, M_{\odot}$), which are not present in the appropriate abundance as inferred from observations even in the current highest resolution LCDM simulations. Meanwhile, Ragagnin et al. (2022) find that regardless of the resolution and galaxy formation model adopted, simulations are unable to simultaneously reproduce the observed stellar masses and compactness (or maximum circular velocities) of cluster galaxies and therefore account for GGSL as measured from observed lenses.

Substructure also exists further away from the centers of clusters and their distribution can also be compared to LCDM simulations. An excess of substructures in Abell 2744 as reconstructed from lensing effects compared to the galaxy clusters in the Millenium XXL N-body simulation, as discussed in Schwinn et al. (2017), suggested a mis-match. However, this disagremment can be brought into concordance by more carefully matching the definitions of substructure in simulations and observations. Applying the same definition, reconciles their abundances in Abell 2744 (Schwinn et al. 2018).

An alternative way to look at substructure within clusters is to analyse their projected mass power spectra. This recently proposed approach eliminates the need to identify individual substructures, and relies instead on characterizing the power spectrum of fluctuations as a function of scale to compare the lensing reconstructed mass maps with that of simulated clusters (Mohammed et al. 2016; Cerini et al. 2023).

Strong lensing when combined with kinematics has also made a significant impact on our understanding of the central galaxies in clusters, BCGs, and the dark matter profile slopes in these very central regions of clusters Natarajan and Kneib (1996). Sand et al. (2004, 2008), Newman et al. (2013) found that once the BCG stellar mass of the BCG is subtracted, the

dark matter slope is significantly shallower than NFW within $\sim$ 30kpc, comparable to the effective radius of BCGs. Newman et al. (2015a) placed these findings in a larger context of central profile slopes as a function of halo mass. For groups and individual galaxies the central slope get progressively steeper. They conclude that dissipation-less processes are more important in the assembly of BCGs in larger halos, like clusters, leading to shallower slopes. Baryons, through gas cooling, are more important in lower mass halos, like groups and individual galaxies, and lead to steeper central density profiles.

5.3 Cluster Lenses as Nature's Telescopes

One of the key benefits of gravitational lensing by clusters is the magnification they induce on the background galaxy population. Bringing into view faint background sources that would otherwise not be accessible even with the most powerful space-based telescopes, cluster lenses act as cosmic telescopes, that permit detailed studies of the magnified galaxies behind them. Lensing magnification stretches the area behind clusters by the magnification factor, thereby increasing the flux we receive from distant galaxies as lensing conserves surface brightness. Acting as nature's telescopes, clusters are expected to serendipitously reveal the earliest forming galaxies as magnification enhances their reach to probe the very early Universe.

At intermediate redshifts, the high lensing magnification by galaxy clusters allows us to peer *into* galaxies. A particularly valuable utility is in studying star forming galaxies at "Cosmic Noon", $z \sim 1-3$, a critical epoch for the assembly of the massive galaxy population in the Universe. Galaxies that would otherwise be too faint for detailed spectroscopy to be practical, even with the largest telescopes, are magnified by factors of tens to hundreds, making their detailed study feasible (Rigby et al. 2018). This is thanks to the overall magnification, which significantly reduces the required observing time for mid- and high-resolution spectroscopy. The high linear magnification, which is manifested as (usually tangential) distortion, resolves the internal structure of galaxies, allowing us to measure the sizes and physical properties of even individual star forming clumps within them (e.g., Johnson et al. 2017). Detailed lens models are then deployed to place the measurements in context of their intrinsic (source plane) values, reverse the magnification effect, and reconstruct the galaxy morphology (e.g., Sharon et al. 2022a).

A key output that lens mass modeling provides is the calculation of the area in the source plane that has been magnified by a given factor μ. The area in the source plane that has (unsigned) magnification greater than μ scales as μ^{-2}. As an example, we present in Fig. 9, taken from Johnson et al. (2014), the magnification power of the six HFF clusters modeled by `Lenstool`, plotted as the cumulative area (left axis) and volume (right axis) magnified above a certain value as a function of magnification. The source plane area in this illustrative case was computed by mapping background sources at $z = 9$, and summing the area that is magnified by more than a given magnification factor. To estimate the volume, the area is multiplied by the co-moving distance between $z = 8.5$ and $z = 9.5$. On average, the total $z = 9$ area that is observed through each cluster lens is about 20% of the WFC3/IR FOV. Approximately 10% of this area is magnified by more than a factor of six, which is equivalent to lowering the limiting magnitude by at least 2 magnitudes.

Cluster lenses have brought into view intrinsically faint and extremely high redshift sources, including a candidate Lyman-break galaxy MACS0647-JD at $z = 11$ in the CLASH survey Coe et al. (2013) and most recently galaxy candidates detected by JWST at $z \sim 9-13$ magnified by modest factors of 3–8 by the foreground cluster WHL0137 that was observed in 8 JWST filters spanning 0.8–5.0 microns and previously in 9 HST filters spanning 0.4–1.7

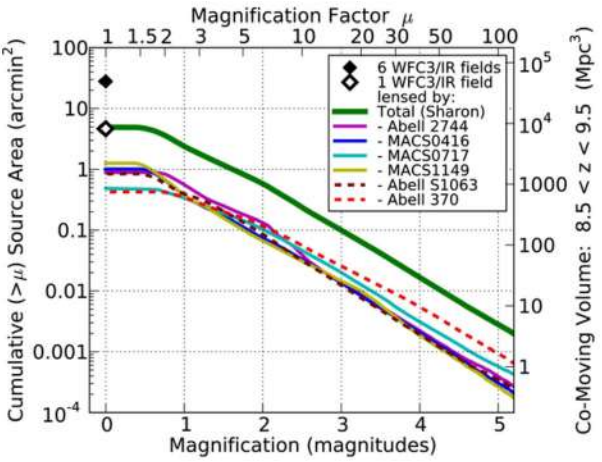

Fig. 9 The cumulative area (left axis) and co-moving volume (right axis) of background sources at $8.5 < z < 9.5$ lensed by each of the HFF clusters to magnification μ and higher. We show, for reference, the corresponding area and co-moving volume of one and six WFC3/IR field of view regions (diamonds). Image reproduced with permission from Johnson et al. (2014), copyright by AAS

microns. Recent data from the JWST UNCOVER & GLASS surveys have also revealed the presence of a high density of bright galaxies behind the cluster lens Abell 2744 (Castellano et al. 2023). Other cluster surveys like RELICS have uncovered several highly magnified sources at $z \sim 6-7$ (Acebron et al. 2018). In addition, the number counts of highly magnified sources obtained from cluster lenses permit constraining the faint end of the galaxy luminosity function from moderate to high redshifts (see for example results from the use of HFF cluster lenses: Alavi et al. 2016; Bouwens et al. 2017b; Livermore et al. 2017; Atek et al. 2018; Yue et al. 2018; Bouwens et al. 2022). The faint end slope encodes important information about the efficiency of star formation, a key unknown in our current understanding of galaxy formation. JWST with its access to the highest redshift, early forming galaxies is anticipated to transform these studies in the near future.

5.4 Statistics of Giant Arcs in Clusters

Bright, merging multiple images of extended background sources lensed by clusters often appear as curved, highly elongated arcs, called giant arcs. Originally, arc statistics were introduced in Grossman and Narayan (1988) to investigate the abundance of giant arcs as a test of the hypothesis that these features were actually produced by gravitationally lensing. The abundance and the observable properties of giant arcs depend on the total mass and density distribution of clusters, their redshift evolution, the properties and evolution of sources, the nature of dark matter, as well as global cosmology (e.g., Bartelmann et al. 1998; Williams et al. 1999; Wambsganss et al. 2004; D'Aloisio and Natarajan 2011; Mahdi et al. 2014). In recent years the global cosmological parameters are estimated from other observations, mostly the CMB and baryonic acoustic oscillations (BOA), however giant arcs can be potentially used as a probe of redshift evolution of non-linear structure in the Universe, and the nature of dark matter.

The impact of the evolution of structure formation, in particular for different types of dark matter, on strong gravitational lensing observables is detailed in Mahdi et al. (2014) and Elahi et al. (2014) in which warm and cold dark matter structure growth is compared with respect to their giant arc statistics. Both works conclude that warm dark matter (WDM) clusters show more extended and massive substructures than those of their cold dark matter (CDM) counterparts, thus enhancing the shear and convergence. In addition, these WDM

substructures reach farther out into the cluster halo than the CDM ones. These effects lead to WDM clusters having enhanced giant arc production and not a reduced one as one would naively expect, if one considers only that small-scale structures are smoothed out in WDM cosmologies. Beyond the single lens plane, the impact of deflecting structures along the line of sight which are uncorrelated with the main lens are analysed in, e.g., Puchwein and Hilbert (2009), Bayliss et al. (2014), Li et al. (2019). They conclude that such structures need to be taken into account in order not to underestimate the abundance of giant arcs, because line-of-sight structures can boost the lensing cross-section for individual clusters by up to 50%.

Complementary to using giant arcs, highly magnified but undistorted images (e.g., Zitrin and Broadhurst 2009) can also be used to probe the structure of clusters (Williams and Lewis 1998; Morioka and Futamase 2015). Another approach to arc statistics is to search for observations of uncommon and irregular multiple image configurations deviating from the theoretically predicted ones (usually fold and cusp configurations) (Orban de Xivry and Marshall 2009; Meena and Bagla 2021). Finding extremely rare image properties can refute the underlying assumptions, e.g., about the statistical distribution of dark matter in a given background cosmology. Though a potentially powerful diagnostic, statistics of giant arcs still needs further improvement in order to be turned into a reliable probe. The main difficulties—accounting for selection effects in sufficiently realistic lensing mass models (e.g., Li et al. 2016; Plazas Malagón 2020)—will need to be tackled to make use the upcoming data: a 30-fold increase in the number of giant arcs from the full sky surveys like *Euclid* (Meneghetti et al. 2013). Extensive reviews of the development of arc statistics are given in the introduction of Caminha et al. (2013), and in the overview paper by Meneghetti et al. (2013).

5.5 Constraints on the Nature of Dark Matter

Though in the standard cosmological model dark matter particles are cold and collisionless, and none of the existing observations rule that out, the possibility remains that dark matter, or some fraction thereof, is either warm (WDM) or self-interacting (SIDM). Cluster strong lensing can be used to test the properties of dark matter particles and constrain the level of self-interaction.

WDM: predicts the existence of numerous sub-galactic scale dark matter halos, which would be largely invisible through in electromagnetic emission (Diemand et al. 2007; Springel et al. 2008). In WDM cosmologies, these low mass subhalos would be erased by the large streaming length of relativistic particles (Bose et al. 2017; Rossi 2020). Specifically, and WDM predict very different abundances of subhalos with masses $\lesssim 10^8 - 10^9 \mathrm{M}_\odot$. Therefore, measuring subhalo abundances and properties down to this mass range will help indicate what cosmological model we live in. Isolated subhalos are very hard to detect gravitationally, however, in galaxies and clusters of galaxies their small individual lensing effects can be detected because they are superimposed and are amplified by the magnification effect of the underlying larger scale lens Şengül et al. (2023). In clusters, their presence will be especially easy to detect near the critical curves created by the cluster as whole, where magnifications are very high over ∼arcsec scales. These probes hold great promise (Kaurov et al. 2019; Dai et al. 2020; Griffiths et al. 2021; Diego et al. 2022), and as suggested in recent work, new lens modeling methodologies like the use of the curved arc bases might permit future detection Şengül et al. (2023).

SIDM: The recent interest in self-interacting dark matter was spurred by apparent discrepancies with the predictions of on galaxy scales (Spergel and Steinhardt 2000) – the so-called cusp-core problem. And even though most of these observations can now probably

be accounted for with collisionless dark matter, the interest in dark matter self-interactions persists. There are a few cluster-scale measurements that can be performed using strong lensing to place constraints on dark matter particle self-interaction cross-section per unit mass, σ/m. Some of the earliest proposed tests were cluster ellipticity (Miralda-Escudé 2002): SIDM should result in rounder cluster cores and the sizes of tidal truncation radii for subhalos, that provide an estimate on the interaction cross-section (Natarajan et al. 2002b). However, it was later shown (Peter et al. 2013) that ellipticity is likely subject to other dynamical effects, and cluster core sizes may likely provide a better diagnostic. The size of constant density cores in clusters can also place constraints on SIDM; a recent core estimate of $\lesssim$ 4kpc in Abell 611 implies $\sigma/m \lesssim 0.1\mathrm{g/cm}^2$ (Andrade et al. 2019). Using results of BAHAMAS-SIDM hydrodynamic simulations Robertson et al. (2019) discuss lensing-based test of SIDM for future cluster surveys. For the current CLASH survey they conclude that cross-section $\sigma/m \gtrsim 1\mathrm{g/cm}^2$ (for systems with velocity dispersions of $1000\,\mathrm{km\,s}^{-1}$) can be ruled out. Baryons play an important role in determining the properties of clusters' central regions. Taking their distribution into account, Despali et al. (2019) conclude that future wide-field surveys might be able to distinguish between CDM and SIDM models based on the distribution of the Einstein radii of cluster lenses. Because SIDM leads to flat density cores in clusters, the central bright galaxies are expected to wobble (i.e., wander away from the cluster center) and result in larger cluster-mass dependent offsets in SIDM cosmologies, compared to LCDM. Based on BAHAMAS-SIDM simulations, Harvey et al. (2019) conclude that their sample of 10 observed clusters is consistent with CDM at 1.5σ level. One of the additional predictions of SIDM is that dark matter halos can undergo gravothermal collapse late in their evolution, similar to that of Globular Clusters, thereby increasing the central halo densities by a factor of several (Yang and Yu 2021). In that case one could expect individual galaxies in galaxy clusters to act as exceptionally strong lenses, producing $\sim$ arcsecond scale multiple images. As noted previously many such GGSLs have recently been observed in galaxy clusters (Meneghetti et al. 2020), and though their high abundance still remains an open question within collisionless, SIDM accompanied by gravothermal collapse may offer an alternative if warranted.

Clusters offer yet another powerful test of the nature of dark matter. Similar to gas ram pressure stripping, self-interactions between dark matter particles would tend to transfer momentum between two cluster-scale halos in merging clusters, or between cluster-scale halo and embedded galaxy-scale halo, resulting in offsets between baryonic and dark matter peaks. These effects have been investigated in simulations (Kahlhoefer et al. 2015), and signatures of these interactions were searched for in galaxy clusters. After initial reports about finding offsets (Massey et al. 2015), better data acquired later showed that the offsets were consistent with zero interaction cross-section (Massey et al. 2018b). Robertson et al. (2017) use the Bullet Cluster and estimated that even an interaction cross-section as large as $\sigma/m = 2\ \mathrm{cm}^2\mathrm{g}^{-1}$ is not ruled out by this cluster. However, they also caution that measuring offsets between baryonic and dark matter peaks must be done consistently in simulations and observations and this remains a challenge.

5.6 Cosmography with Cluster Lenses

If a source is strongly lensed into two images, the difference in time that light takes to reach the observer from the two different directions, i.e., the time delay (Δt) between the two images due to the difference in path length, is related to the gravitational potential of the lens ($\phi[\theta]$) and the so-called time-delay distance ($D_{\Delta t}$). The latter scales with the three angular-diameter distances, observer-deflector (D_d), observer-source (D_s), and deflector-source (D_ds): $D_{\Delta t} \propto D_\mathrm{d} \times D_\mathrm{s}/D_\mathrm{ds}$. Since each of the distances is proportional to c/H_0,

it implies that $D_{\Delta t} \propto 1/H_0$. The uncertainty in $D_{\Delta t}$ (and thus on H_0) is approximately the sum in quadrature of the uncertainty in time-delay ($\delta\Delta t$) and the uncertainty in differences in gravitational potential ($\delta\phi$). The time delays observed in the multiple images of time-varying sources strongly lensed by galaxy clusters have typical values of several months/years, so they can be measured with an approximate 1-3% precision (e.g., Fohlmeister et al. 2013, Dahle et al. 2015, Kelly et al. 2016). Most recently, Muñoz et al. (2022) report $< 0.05\%$ precision on the 3 time delays of the quasar in cluster SDSS J1004+4114, which has been monitored for 14.5 years. Supernova, with their known lightcurves can provide precise estimates with considerably shorter monitoring. The main remaining uncertainty lies in the potential of the cluster lens. With sufficient photometric and spectroscopic observational data, it may be possible that $\delta\phi \lesssim 5\%$ can be reached in lens galaxy clusters (e.g., Grillo et al. 2015, 2016). This corresponds to a remarkable precision of $\sim$6% on the value of H_0 from a single lens cluster with measured time delays (e.g., Grillo et al. 2018, 2020).

Time-delay distances are primarily sensitive to the value of H_0, and more mildly on those of other cosmological parameters. If a lens produces multiple images of two sources (1 and 2), located at different redshifts, the observed positions of the multiple images provide information about ϕ and the so-called family ratio $(D_{\rm ds1} \times D_{\rm s2})/(D_{\rm s1} \times D_{\rm ds2})$. In galaxy clusters, usually showing several multiple images, different values of this ratio can be used at the same time to estimate the values of the cosmological matter ($\Omega_{\rm m}$) and dark-energy (Ω_Λ) density parameters, and the dark-energy equation-of state (w) parameter (e.g. Soucail et al. 2004; Gilmore and Natarajan 2009), defining the global geometry of the Universe. Using observed cluster lenses Jullo et al. (2010), Caminha et al. (2016), Magana et al. (2018) have demonstrated that cluster strong lensing cosmography could be competitive with other cosmological probes once systematics are better quantified and controlled.

Multiple images of supernova Refsdal in HFF cluster MACS J1149 was recently used to constraint H_0 (Kelly et al. 2023). In addition to supernova, variable quasars can also be used as sources behind clusters. One of these is SDSS J1004+4112. The time delay of the fourth arriving image was predicted by different groups some years ago. After a nearly 15 year observing campaign that delay was finally measured to be 6.73 ± 0.003 years (Muñoz et al. 2022), and agrees well with some of the predictions (Liesenborgs et al. 2009; Mohammed et al. 2015). Using the measured time delays in three clusters with background quasars and archival HST imaging, Napier et al. (2023) measured the value of H_0 which agrees with the one from Refsdal within 1σ, but has somewhat larger modeling uncertainties, because the 3 clusters have fewer lensed images than HFF clusters. They estimate that of order of 50 cluster-lensed quasar systems would help reduce the uncertainties on H_0 to below the 1% level, which is expected to be detected in the next decade (Robertson et al. 2020). These results show that galaxy clusters are competitive in the measurement of the Hubble constant, once sufficient systems are discovered and analyzed.

Most of the baryons in galaxy clusters are in the form of hot, X-ray emitting gas. Massive galaxy clusters can be assumed to have formed from representative regions of the Universe, and hence the ratio of the mass in baryons they contain to that of dark matter (i.e., the gas mass fraction) should be a constant, not evolving with redshift. This assumption can be used to constrain global cosmological parameters, like $h^2\Omega_b$, and Ω_m (Applegate et al. 2016; Allen et al. 2011; Mantz et al. 2014). Lensing plays a key role in this determination as it measures the cluster masses. One can also turn the argument around: assume cosmological parameters and determine if the baryon fraction in clusters evolves with redshift. Holanda et al. (2017) estimate that there is no statistically significant evolution of the baryon mass fraction with z.

5.7 Impact of Line-of-Sight Structures and Multiple-Lens Planes

Traditional single-plane lensing analyses assume that the mass of the deflector is concentrated in a single plane, at the redshift of a cluster. More advanced multi-plane lensing studies, taking into account the observed mass distributions at redshifts different from that of the cluster, are becoming possible, thanks to some recent software developments. In the former case, the light rays emitted from a distant source and received by an observer are deflected only once (i.e., when crossing the galaxy cluster); in the latter, multiple deflections have to be added properly (see Blandford and Narayan 1986; Schneider 2014). The observed positions and fluxes of each galaxy contributing to the total deflection has to be re-scaled iteratively in the modeling process, according to the deflection and magnification values associated with the mass of the objects in the foreground.

Studies by Bayliss et al. (2014), D'Aloisio et al. (2014), Chirivì et al. (2018), Williams et al. (2018), McCully et al. (2017) found that line-of-sight (LOS) galaxies can have a significant impact on the reconstruction of some multiple image positions, but the inclusion of LOS mass distributions in the strong lensing models of galaxy clusters can reduce only modestly the rms offset between the observed and model-predicted positions of all multiple images. These studies also noted that the perturbing contribution of foreground galaxies is more important than that of the background ones and that accounting for LOS mass structures, as if they were at the cluster redshift, can partially lower this offset. Recently, Raney et al. (2020a) confirmed that LOS galaxies can account for a significant fraction of the typical image position residuals of current state-of-the-art strong lensing models of galaxy clusters and that the values of the image magnifications can be affected by a few percent.

5.8 Local Properties of Clusters Around Extended Images

Most of the work on cluster lensing presented in the literature involves reconstruction of the mass distribution over the whole lens plane region of the cluster. As described in earlier sections, this reconstruction can use simply parametrized models, free-form models, or hybrid ones. However, a very different type of analysis is also possible, one that does not involve modeling the whole contiguous central region of the cluster, and recovers cluster properties only *at* the locations of extended images.

The strong gravitational lensing formalism provides only *local* information about the deflecting mass distribution in the lens plane at the positions of the multiple images. Assuming that the surface mass density and shear are constant over the area considered for evaluation around the multiple image locations, we can use the image morphology to retrieve ratios of convergences, $f^{(ij)}$ between multiple images i and j arising from the same individual source, $i, j = 1, \ldots, n_{\rm i}$ (with $n_{\rm i}$ being the total number of images from the same source), and the reduced shear components at the positions of all $n_{\rm i}$ images

$$f^{(ij)} \equiv \frac{1-\kappa(\boldsymbol{\theta}^{(i)})}{1-\kappa(\boldsymbol{\theta}^{(j)})}\,, \quad g_1^{(i)} = \frac{\gamma_1(\boldsymbol{\theta}^{(i)})}{1-\kappa(\boldsymbol{\theta}^{(i)})}\,, \quad g_2^{(i)} = \frac{\gamma_2(\boldsymbol{\theta}^{(i)})}{1-\kappa(\boldsymbol{\theta}^{(i)})}\,. \tag{5}$$

These convergence ratios and reduced shear components can be determined by features in the brightness distributions of the multiple images, most often star forming regions. At least three multiple images with three features that are not aligned in each image are required. Wagner (2019) details how to uniquely determine the $f^{(ij)}$ and $g^{(i)}$ from these feature vectors, Lin et al. (2022) and Lin et al. (2023) show the impact of non-unique feature matching when one image contains multiple candidate features that can be matched with one single

feature showing in other images. Lin et al. (2022) also set up an algorithm to identify the positions of these features in the presence of noise. Alternatively, the quadrupole moment of a featureless brightness profile around its centre of light can be employed.[3]

Inserting Eq. (5) into the distortion matrix for each multiple image

$$\mathrm{A} = \begin{pmatrix} 1-\kappa-\gamma_1 & \gamma_2 \\ \gamma_2 & 1-\kappa+\gamma_1 \end{pmatrix}, \tag{6}$$

ratios of magnifications can also be determined based on these local lens properties. If flux measurements covering the same area of the multiple images are available, a comparison between the flux ratios and the magnification ratios yields a consistency check for the local lens properties in Eq. (5). Deviations may hint at dust extinction, additional micro-lensing, or lensing effects beyond convergence and shear.

To investigate the impact of higher-order lensing effects in galaxy clusters, gradients of reduced shear and convergence maps in simulated clusters, like *Ares* and *Hera* (Meneghetti et al. 2017), are analysed, as further detailed in Wagner (2022). On the resolution scale of the pixels used in these simulations, the results reveal that, in more than 90% of all pixels covering the lensing area, the gradients in θ_1- and θ_2-directions are less than 10% of the convergence and reduced shear values at these pixels. More than 67% of all pixels in the *Ares* and *Hera* lensing area have gradients of less than 2% of their respective distortion matrix entries. Hence, at current observational precision, neglecting higher-order lensing effects on galaxy-cluster scales is valid to a good approximation.

In addition, assuming a smooth deflecting mass density in the vicinity of the multiple images that straddle a critical curve, we can use the observables in the multiple images to constrain the position of the critical curve between these images. To leading order, points on the critical curve between two images in a fold-configuration can be determined as the mid-point dividing the connection line of corresponding features in the two multiple images. Retrieving local lens properties is very useful in newly detected galaxy clusters in which only few spectroscopically confirmed multiple images have been identified. Using a synthetic cluster *Ares*, Johnson and Sharon (2016) estimate that one needs > 10 spectroscopically confirmed image sets to precisely determine the mass enclosed within the Einstein radius of a cluster-lens. Thus, the lens modelling algorithms introduced in Sect. 3 cannot be applied to galaxy clusters like RM J223013.1-080853.1 (Rykoff et al. 2016), which was identified after a serendipitous discovery of a multiple-image system. So far, it only shows three spectroscopically confirmed multiple images for a common background galaxy at $z_\mathrm{s} = 0.8200$. Nevertheless, Griffiths et al. (2021) succeeded in constraining the smoothness scale of dark matter by applying the approach outlined above to the three highly resolved images. Figure 10 shows the galaxy cluster at $z_\mathrm{d} = 0.526$, determined by its $\sim$60 cluster member galaxies, and details of the confirmed multiple images.

Using the `ptmatch`-program[4] Wagner and Tessore (2018), Wagner et al. (2018) determine the properties in Eq. (5). The fact that the algorithm obtains a solution supports the assumption of constant entries in the distortion matrix in the areas spanned by the brightness features shown in Fig. 10 (left). The observed flux ratios in all five available *HST* filters (F110W, F140W, F160W, F606W, F814W) also show a high degree of agreement with the magnification ratios of `ptmatch`, which is a second consistency check corroborating the assumption. Each lens model has its underlying assumptions, for instance that light traces mass

[3] An example for the usage of the quadrupole ellipticity and direction is given in Wagner and Williams (2020) albeit for a galaxy-scale lens.

[4] available at https://github.com/ntessore/imagemap.

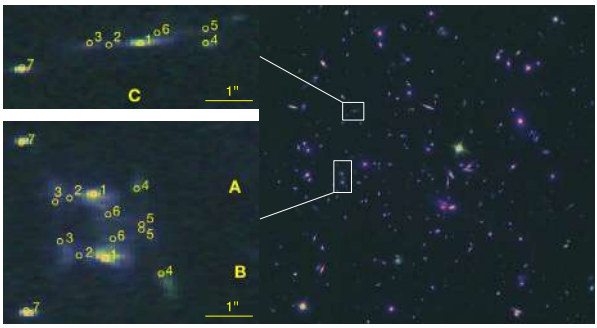

Fig. 10 Galaxy cluster RM J223013.1-080853.1 at $z_d = 0.526 \pm 0.018$ with a cusp configuration of highly resolved images from a clumpy disk galaxy at $z_s = 0.8200 \pm 0.0005$ (right). The features in the brightness profiles (numbered yellow circles in the details on the left) are used to reconstruct the local lens properties in Eq. (5)

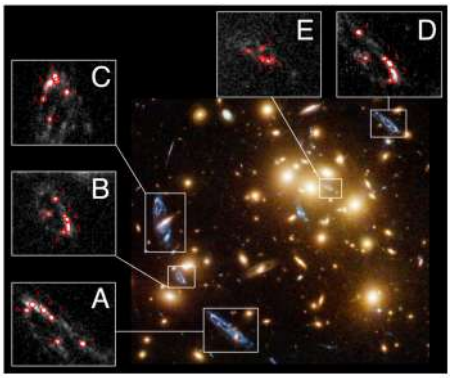

Fig. 11 The galaxy cluster strong gravitational lens CL0024+1654 at $z_d = 0.39$ (background) and the five multiple images of a blue spiral background galaxy at $z_s = 0.1675$ (details around CL0024) with their six brightness features, star-forming regions, that can be used to extract the local lens properties in Eq. (5). (See Lin et al. 2022, for details.)

(see Jullo et al. 2007b; Zitrin et al. 2009b), or regularisation constraints on the smoothness of the mass density. Such assumptions are not employed in the observation-based approach outlined in Sect. 5.8. A comparison between the local lens properties (Eq. (5)) extracted from the lens-model reconstructions at the multiple image positions and the same properties directly obtained from the multiple-image observables (according to the procedure described in Sect. 5.8) allows us to corroborate or refute lens model assumptions.

As an example, Wagner et al. (2018) use the strongly-lensing galaxy cluster CL0024+1654 at $z_d = 0.39$ to investigate the differences between the lens-model-independent local lens properties, those obtained in a `Lenstool` and a `Grale` reconstruction. The local lens properties are extracted at the positions of five highly resolved images of a blue spiral background galaxy at $z_s = 1.675$. In addition to these images, the `Lenstool` and `Grale` reconstructions employ the same set of 14 multiple image positions of 5 other background sources. Images' extended nature is not taken into account, only their centres of light are used as image positions.

The six brightness features in the five resolved multiple images shown in Fig. 11 constrain the local lens properties of Eq. (5) at the five positions in the cluster area for several filter bands, which shows overall consistency of these local lens properties (Lin et al. 2022). Extracting the same local lens properties determined by the `Lenstool` and `Grale` reconstructions, the authors find a high degree of agreement between the $f^{(ij)}$- and $g^{(j)}$-values of all three approaches. This implies that in the vicinity of the highly resolved multiple images, (i) the light-traces-mass assumption and the hypothesis of a constant mass-to-light-ratio for the brightest cluster member galaxies as used in `Lenstool` can both be corroborated for CL0024+1654; (ii) `Grale` arrives at similar conclusions via a completely different route.

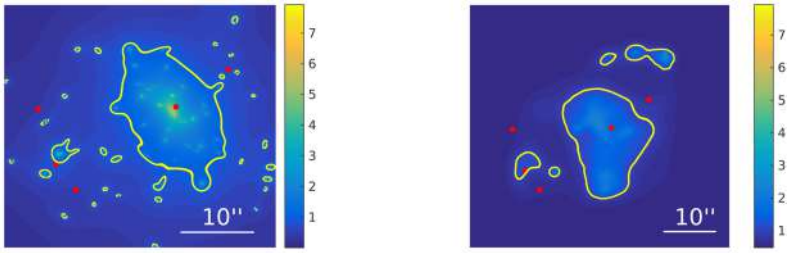

Fig. 12 Convergence maps for CL0024+1654 obtained from `Lenstool` (left) and `Grale` (right) using the five images of the highly resolved spiral galaxy (red dots) and 14 additional images from five other source. The yellow curves mark the isocontour $\kappa = 1$. Image reproduced with permission from Wagner et al. (2018), copyright by ESO

Despite the fact that `Lenstool` and `Grale` generate the same *local* lens properties at the five image positions, their *global* convergence maps greatly differ, as shown in Fig. 12. This is to be expected because the lens models are dominated by the multiple image observables only at their positions. Farther away from the data points, lens-model specific additional assumptions determine the global morphology of the reconstruction, causing the differences in the resulting convergence maps.

In the regime of several tens of multiple-image systems, the differences in the convergence maps between model-based lens reconstructions, as described above, occur because the sparse multiple-image constraints are not sufficient, and need to be complemented by additional assumptions to obtain a global lens morphology. The observation-based, model-free method discussed in this Section can be used to compare and cross-check additional modeling assumptions. In the future, observations with JWST will increase the number of multiple images per cluster by an order of magnitude from about 100 to 1000 (Ghosh et al. 2020). Accordingly, the impact of model assumptions will decrease and the area covered by multiple images which is reconstructed with an accuracy above 90% will increase from about 40-50% to about 65%. The use of model-free methods can also be extended to more images, further confirming the recovered mass distribution in clusters.

6 Lensing by Galaxy Groups

Galaxy groups are similar to clusters, but have lower masses, $\sim 10^{13} - 10^{15} M_{\odot}$, and so 'fill' the mass gap between individual galaxies and clusters. Given that they are more numerous, galaxy groups can be important contributors to the study of background sources, the mass distribution in lenses, or cosmological parameters. For that reason, Fox and Pen (2001) suggested that groups can be used to test for the NFW profile. They analytically compared the lensing efficiency of NFW vs. singular isothermal sphere (SIS) profiles, and concluded that NFW dark matter halos are ~ 200 less efficient than SIS, therefore strong lensing statistics by groups could provide a sensitive test of the inner density region of virialized structures. Their finding of low group cross-section to strong lensing is consistent with there being no instances of strong lensing by groups in the Hubble Deep Field. Newman et al. (2015b) addressed the same question of group's density profile. They used a sample of 10 strong lensing groups and found that the central regions are consistent with NFW, but are possibly somewhat steeper, which they ascribed to the contribution from the central elliptical galaxy. Verdugo et al. (2014) analyzed how the Einstein radius of galaxy groups

in the Strong Lensing Legacy Survey (Limousin et al. 2009; More et al. 2012) relates to the group's properties, like velocity dispersion. They showed that all correlations between group properties have a considerable amount of scatter, but there is some evidence that the Einstein radius is decreasing with increasing redshift. Foëx et al. (2014) used weak lensing data for 80 strong lensing galaxy groups to estimate the groups' mass vs. concentration relation. The relation they found is steeper than that seen in simulations. They attribute this to the fact that strong lensing selected groups are preferentially aligned along our line of sight because that way they present a larger strong lensing cross-section, and are more easily detected. Detailed study of one group, SL2S J02140-0535 by Verdugo et al. (2011), whose measured concentration parameter is somewhat larger than predicted by simulations, is in agreement with this. Therefore galaxy groups selected by their strong lensing features may constitute a biased sample of groups in general.

In the recent years there have been a few dedicated searches for strong lensing in galaxy groups that aim to find and analyze or order 100 or more groups, instead of 10 or so used in earlier works. Jaelani et al. (2020) carried out a Survey of Gravitationally-lensed Objects in HSC Imaging using Hyper Suprime-Cam Subaru Strategic Program (HSC-SSP) Survey (Aihara et al. 2018), covering $\sim 1114\text{deg}^2$. They discovered 641 candidate lens systems, of which 47 are almost certainly bonafide lenses; see Fig. 13 for some examples. The future of group-scale lensing will definitely make use of such large surveys where the observational selection effects are well quantified, and resulting catalogues of groups can be used for statistical studies. But the other aspect of groups, detailed study of individual groups that have abundant data on both lensing and kinematics also promises to yield interesting results. For example, Wang et al. (2022) studies the mass distribution in CASSOWARY 31, using strong lensing data from HST imaging and kinematics from MUSE integral-field spectroscopy. They identified 5 sets of multiple images, on par with some clusters, and obtained detailed mass maps of the system, concluding that it is peculiar fossil group, strongly dominated by dark matter in its central regions. Systems like this can finally realize the prediction from 20 years ago (Fox and Pen 2001) that groups are excellent systems to probe the structure of dark matter halos.

7 Prospects for Cluster Lensing from Upcoming Instruments and Surveys

JWST observations are expected to revolutionize the study of cluster lensing. The early results are very promising and exciting. Caminha et al. (2022b), Golubchik et al. (2022), Mahler et al. (2023), Sharon et al. (2022b) all present mass models of the first strong gravitational lens observed by the JWST, SMACS J0723.3-7327. In Fig. 1 we show the lens model presented in Mahler et al. (2023). The first deep-field observations of the JWST have yielded a surprisingly large number of very high redshift galaxy candidates, $z = 10 - 16$ (Furtak et al. 2023). The JWST Prime Extragalactic Areas for Reionization and Lensing Science (PEARLS) project will look for high redshift galaxies behind 7 lensing clusters (Windhorst et al. 2023). Meanwhile Laporte et al. (2022) report finding a lensed protocluster candidate at $z = 7.66$ behind a lensing galaxy cluster SMACS0723-7327. JWST data will allow testing our current cosmological paradigm via the detailed studies of substructure that it will provide for direct comparison with LCDM simulations and predictions.

The upcoming Euclid space mission with the expectation of detecting upto 60,000 galaxy clusters from $z \sim 0.2 - 2$, and of the order of several thousand strongly lensed arcs stands to transform our understanding of the assembly history of clusters. With accurate weak lensing

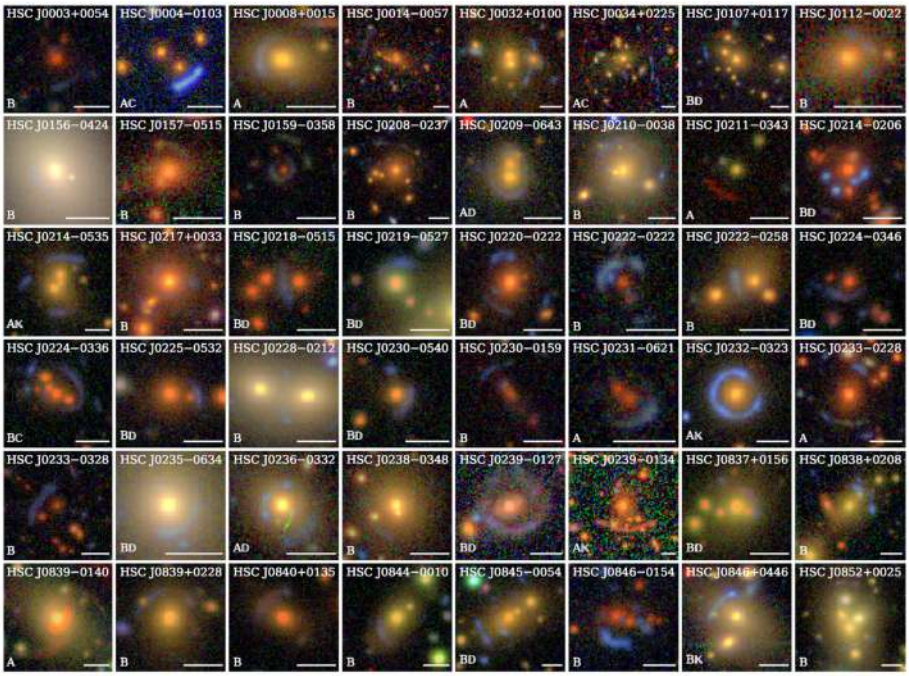

Fig. 13 Examples of group-scale lensing candidates from the Hyper Supreme Cam on the *Subaru Telescope* (Jaelani et al. 2020). The letters A or B at the bottom of each panel indicate the confidence grade of this being a lens. The white horizontal bar at the bottom of each panel is 5 arcseconds long. North is up, East is to the left

mass estimates out to the virial radius, Euclid will enable tracing the mass build-up and growth of structure in the Universe. Euclid is expected to provide a stringent test of the cold dark matter paradigm as data from the mission will permit probing the radial density profile and the ellipticity of clusters, both of which are predicted by LCDM. The anticipated data deluge has catalyzed the development of many new automatic lensing detection algorithms. In combination with DES, Euclid data will provide tighter cosmological constraints from clusters. On the modeling side, improved existing lens inversion methods, as well as new reconstruction methodologies under development currently will rise to meet the challenge of JWST data and data from other planned surveys are expected to improve our understanding of the clusters and the high redshift Universe.

Acknowledgements We thank the International Space Science Institute in Bern (ISSI) for their hospitality for organizing the stimulating workshop on "Strong Gravitational Lensing". We thank Masamune Oguri and Anupreeta More for helpful comments and discussions.

Declarations

Competing Interests The authors declare no competing interests.

References

Abdelsalam HM, Saha P, Williams LLR (1998) Nonparametric reconstruction of Abell 2218 from combined weak and strong lensing. Astron J 116(4):1541–1552. https://doi.org/10.1086/300546. arXiv:astro-ph/9806244 [astro-ph]

Acebron A, Cibirka N, Zitrin A, Coe D, Agulli I, Sharon K, Bradač M, Frye B, Livermore RC, Mahler G, Salmon B, Umetsu K, Bradley L, Andrade-Santos F, Avila R, Carrasco D, Cerny C, Czakon NG, Dawson WA, Hoag AT, Huang KH, Johnson TL, Jones C, Kikuchihara S, Lam D, Lovisari L, Mainali R, Oesch PA, Ogaz S, Ouchi M, Past M, Paterno-Mahler R, Peterson A, Ryan RE, Sendra-Server I, Stark DP, Strait V, Toft S, Trenti M, Vulcani B (2018) RELICS: strong-lensing analysis of the massive clusters MACS J0308.9+2645 and PLCK G171.9-40.7. Astrophys J 858(1):42. https://doi.org/10.3847/1538-4357/aabe29. arXiv:1803.00560 [astro-ph.CO]

Acebron A, Alon M, Zitrin A, Mahler G, Coe D, Sharon K, Cibirka N, Bradač M, Trenti M, Umetsu K, Andrade-Santos F, Avila RJ, Bradley L, Carrasco D, Cerny C, Czakon NG, Dawson WA, Frye B, Hoag AT, Huang KH, Johnson TL, Jones C, Kikuchihara S, Lam D, Livermore RC, Lovisari L, Mainali R, Oesch PA, Ogaz S, Ouchi M, Past M, Paterno-Mahler R, Peterson A, Ryan RE, Salmon B, Sendra-Server I, Stark DP, Strait V, Toft S, Vulcani B (2019) RELICS: high-resolution constraints on the inner mass distribution of the z = 0.83 merging cluster RXJ0152.7-1357 from strong lensing. Astrophys J 874(2):132. https://doi.org/10.3847/1538-4357/ab0adf. arXiv:1810.08122 [astro-ph.CO]

Aihara H, Arimoto N, Armstrong R et al (2018) The hyper suprime-cam SSP survey: overview and survey design. Publ Astron Soc Jpn 70:S4. https://doi.org/10.1093/pasj/psx066. arXiv:1704.05858 [astro-ph.IM]

Alavi A, Siana B, Richard J, Rafelski M, Jauzac M, Limousin M, Freeman WR, Scarlata C, Robertson B, Stark DP, Teplitz HI, Desai V (2016) The evolution of the faint end of the UV luminosity function during the peak epoch of star formation ($1 < z < 3$). Astrophys J 832(1):56. https://doi.org/10.3847/0004-637X/832/1/56. arXiv:1606.00469 [astro-ph.GA]

Allen SW, Evrard AE, Mantz AB (2011) Cosmological parameters from observations of galaxy clusters. Annu Rev Astron Astrophys 49(1):409–470. https://doi.org/10.1146/annurev-astro-081710-102514. arXiv:1103.4829 [astro-ph.CO]

Amendola L, Appleby S, Bacon D, Baker T, Baldi M, Bartolo N, Blanchard A, Bonvin C, Borgani S, Branchini E, Burrage C, Camera S, Carbone C, Casarini L, Cropper M, de Rham C, Di Porto C, Ealet A, Ferreira PG, Finelli F, García-Bellido J, Giannantonio T, Guzzo L, Heavens A, Heisenberg L, Heymans C, Hoekstra H, Hollenstein L, Holmes R, Horst O, Jahnke K, Kitching TD, Koivisto T, Kunz M, La Vacca G, March M, Majerotto E, Markovic K, Marsh D, Marulli F, Massey R, Mellier Y, Mota DF, Nunes NJ, Percival W, Pettorino V, Porciani C, Quercellini C, Read J, Rinaldi M, Sapone D, Scaramella R, Skordis C, Simpson F, Taylor A, Thomas S, Trotta R, Verde L, Vernizzi F, Vollmer A, Wang Y, Weller J, Zlosnik T (2013) Cosmology and fundamental physics with the Euclid satellite. Living Rev Relativ 16(1):6. https://doi.org/10.12942/lrr-2013-6. arXiv:1206.1225 [astro-ph.CO]

Andrade KE, Minor Q, Nierenberg A, Kaplinghat M (2019) Detecting dark matter cores in galaxy clusters with strong lensing. Mon Not R Astron Soc 487(2):1905–1926. https://doi.org/10.1093/mnras/stz1360. arXiv:1901.00507 [astro-ph.GA]

Angus GW, Famaey B, Zhao HS (2006) Can MOND take a bullet? Analytical comparisons of three versions of MOND beyond spherical symmetry. Mon Not R Astron Soc 371(1):138–146. https://doi.org/10.1111/j.1365-2966.2006.10668.x. arXiv:astro-ph/0606216 [astro-ph]

Annunziatella M, Biviano A, Mercurio A, Nonino M, Rosati P, Balestra I, Presotto V, Girardi M, Gobat R, Grillo C, Kelson D, Medezinski E, Postman M, Scodeggio M, Brescia M, Demarco R, Fritz A, Koekemoer A, Lemze D, Lombardi M, Sartoris B, Umetsu K, Vanzella E, Bradley L, Coe D, Donahue M, Infante L, Kuchner U, Maier C, Regős E, Verdugo M, Ziegler B (2014) CLASH-VLT: the stellar mass function and stellar mass density profile of the z = 0.44 cluster of galaxies MACS J1206.2-0847. Astron Astrophys 571:A80. https://doi.org/10.1051/0004-6361/201424102. arXiv:1408.6356 [astro-ph.GA]

Annunziatella M, Bonamigo M, Grillo C, Mercurio A, Rosati P, Caminha G, Biviano A, Girardi M, Gobat R, Lombardi M, Munari E (2017) Mass profile decomposition of the frontier fields cluster MACS J0416-2403: insights on the dark-matter inner profile. Astrophys J 851(2):81. https://doi.org/10.3847/1538-4357/aa9845. arXiv:1711.02109 [astro-ph.CO]

Applegate DE, Mantz A, von Allen SW, der Linden A, Morris RG, Hilbert S, Kelly PL, Burke DL, Ebeling H, Rapetti DA, Schmidt RW (2016) Cosmology and astrophysics from relaxed galaxy clusters - IV. Robustly calibrating hydrostatic masses with weak lensing. Mon Not R Astron Soc 457(2):1522–1534. https://doi.org/10.1093/mnras/stw005. arXiv:1509.02162 [astro-ph.CO]

Atek H, Richard J, Kneib JP, Schaerer D (2018) The extreme faint end of the UV luminosity function at z $\sim$ 6 through gravitational telescopes: a comprehensive assessment of strong lensing uncertainties. Mon Not R Astron Soc 479(4):5184–5195. https://doi.org/10.1093/mnras/sty1820. arXiv:1803.09747 [astro-ph.GA]

Bacon DJ, Goldberg DM, Rowe BTP, Taylor AN (2006) Weak gravitational flexion. Mon Not R Astron Soc 365(2):414–428. https://doi.org/10.1111/j.1365-2966.2005.09624.x. arXiv:astro-ph/0504478 [astro-ph]

Bahé YM (2021) Strongly lensed cluster substructures are not in tension with ΛCDM. Mon Not R Astron Soc. https://doi.org/10.1093/mnras/stab1392. arXiv:2101.12112 [astro-ph.GA]

Balestra I, Vanzella E, Rosati P, Monna A, Grillo C, Nonino M, Mercurio A, Biviano A, Bradley L, Coe D, Fritz A, Postman M, Seitz S, Scodeggio M, Tozzi P, Zheng W, Ziegler B, Zitrin A, Annunziatella M, Bartelmann M, Benitez N, Broadhurst T, Bouwens R, Czoske O, Donahue M, Ford H, Girardi M, Infante L, Jouvel S, Kelson D, Koekemoer A, Kuchner U, Lemze D, Lombardi M, Maier C, Medezinski E, Melchior P, Meneghetti M, Merten J, Molino A, Moustakas L, Presotto V, Smit R, Umetsu K (2013) CLASH-VLT: spectroscopic confirmation of a z = 6.11 quintuply lensed galaxy in the frontier fields cluster RXC J2248.7-4431. Astron Astrophys 559:L9. https://doi.org/10.1051/0004-6361/201322620. arXiv:1309.1593 [astro-ph.CO]

Bartelmann M, Huss A, Colberg JM, Jenkins A, Pearce FR (1998) Arc statistics with realistic cluster potentials. IV. Clusters in different cosmologies. Astron Astrophys 330:1–9. arXiv:astro-ph/9707167 [astro-ph]

Bayliss MB, Hennawi JF, Gladders MD, Koester BP, Sharon K, Dahle H, Oguri M (2011) Gemini/GMOS spectroscopy of 26 strong-lensing-selected galaxy cluster cores. Astrophys J Suppl Ser 193(1):8. https://doi.org/10.1088/0067-0049/193/1/8. arXiv:1010.2714 [astro-ph.CO]

Bayliss MB, Johnson T, Gladders MD, Sharon K, Oguri M (2014) Line-of-sight structure toward strong lensing galaxy clusters. Astrophys J 783(1):41. https://doi.org/10.1088/0004-637X/783/1/41. arXiv:1312.3637 [astro-ph.CO]

Beauchesne B, Clément B, Richard J, Kneib JP (2021) Improving parametric mass modelling of lensing clusters through a perturbative approach. Mon Not R Astron Soc. https://doi.org/10.1093/mnras/stab1684. arXiv:2106.05029 [astro-ph.CO]

Bergamini P, Rosati P, Mercurio A, Grillo C, Caminha GB, Meneghetti M, Agnello A, Biviano A, Calura F, Giocoli C, Lombardi M, Rodighiero G, Vanzella E (2019) Enhanced cluster lensing models with measured galaxy kinematics. Astron Astrophys 631:A130. https://doi.org/10.1051/0004-6361/201935974. arXiv:1905.13236 [astro-ph.GA]

Bergamini P, Rosati P, Vanzella E, Caminha GB, Grillo C, Mercurio A, Meneghetti M, Angora G, Calura F, Nonino M, Tozzi P (2021) A new high-precision strong lensing model of the galaxy cluster MACS J0416.1-2403. Robust characterization of the cluster mass distribution from VLT/MUSE deep observations. Astron Astrophys 645:A140. https://doi.org/10.1051/0004-6361/202039564. arXiv:2010.00027 [astro-ph.GA]

Biviano A, Rosati P, Balestra I, Mercurio A, Girardi M, Nonino M, Grillo C, Scodeggio M, Lemze D, Kelson D, Umetsu K, Postman M, Zitrin A, Czoske O, Ettori S, Fritz A, Lombardi M, Maier C, Medezinski E, Mei S, Presotto V, Strazzullo V, Tozzi P, Ziegler B, Annunziatella M, Bartelmann M, Benitez N, Bradley L, Brescia M, Broadhurst T, Coe D, Demarco R, Donahue M, Ford H, Gobat R, Graves G, Koekemoer A, Kuchner U, Melchior P, Meneghetti M, Merten J, Moustakas L, Munari E, Regős E, Sartoris B, Seitz S, Zheng W (2013) CLASH-VLT: the mass, velocity-anisotropy, and pseudo-phase-space density profiles of the z = 0.44 galaxy cluster MACS J1206.2-0847. Astron Astrophys 558:A1. https://doi.org/10.1051/0004-6361/201321955. arXiv:1307.5867 [astro-ph.CO]

Blandford R, Narayan R (1986) Fermat's principle, caustics, and the classification of gravitational lens images. Astrophys J 310:568. https://doi.org/10.1086/164709

Blandford RD, Kochanek CS, Kovner I, Narayan R (1989) Gravitational lens optics. Science 245(4920):824–830. https://doi.org/10.1126/science.245.4920.824

Blanton MR, Bershady MA, Abolfathi B et al (2017) Sloan digital sky survey IV: mapping the Milky Way, nearby galaxies, and the distant universe. Astron J 154(1):28. https://doi.org/10.3847/1538-3881/aa7567. arXiv:1703.00052 [astro-ph.GA]

Bonamigo M, Grillo C, Ettori S, Caminha GB, Rosati P, Mercurio A, Annunziatella M, Balestra I, Lombardi M (2017) Joining X-ray to lensing: an accurate combined analysis of MACS J0416.1-2403. Astrophys J 842(2):132. https://doi.org/10.3847/1538-4357/aa75cc. arXiv:1705.10322 [astro-ph.GA]

Bonamigo M, Grillo C, Ettori S, Caminha GB, Rosati P, Mercurio A, Munari E, Annunziatella M, Balestra I, Lombardi M (2018) Dissection of the collisional and collisionless mass components in a mini sample of CLASH and HFF massive galaxy clusters at z ≈ 0.4. Astrophys J 864(1):98. https://doi.org/10.3847/1538-4357/aad4a7. arXiv:1807.10286 [astro-ph.GA]

Bose S, Hellwing WA, Frenk CS, Jenkins A, Lovell MR, Helly JC, Li B, Gonzalez-Perez V, Gao L (2017) Substructure and galaxy formation in the Copernicus Complexio warm dark matter simulations. Mon Not R Astron Soc 464(4):4520–4533. https://doi.org/10.1093/mnras/stw2686. arXiv:1604.07409 [astro-ph.CO]

Bouwens RJ, Illingworth GD, Oesch PA, Atek H, Lam D, Stefanon M (2017a) Extremely small sizes for faint z ∼ 2-8 galaxies in the Hubble frontier fields: a key input for establishing their volume density and UV emissivity. Astrophys J 843(1):41. https://doi.org/10.3847/1538-4357/aa74e4. arXiv:1608.00966 [astro-ph.GA]

Bouwens RJ, Oesch PA, Illingworth GD, Ellis RS, Stefanon M (2017b) The z ∼ 6 luminosity function fainter than -15 mag from the Hubble frontier fields: the impact of magnification uncertainties. Astrophys J 843(2):129. https://doi.org/10.3847/1538-4357/aa70a4. arXiv:1610.00283 [astro-ph.GA]

Bouwens RJ, Illingworth G, Ellis RS, Oesch P, Stefanon M (2022) z 2-9 galaxies magnified by the Hubble frontier field clusters. II. Luminosity functions and constraints on a faint-end turnover. Astrophys J 940(1):55. https://doi.org/10.3847/1538-4357/ac86d1. arXiv:2205.11526 [astro-ph.GA]

Bradač M, Clowe D, Gonzalez AH, Marshall P, Forman W, Jones C, Markevitch M, Randall S, Schrabback T, Zaritsky D (2006) Strong and weak lensing united. III. Measuring the mass distribution of the merging galaxy cluster 1ES 0657-558. Astrophys J 652:937–947. https://doi.org/10.1086/508601. arXiv:astro-ph/0608408 [astro-ph]

Bradač M, Treu T, Applegate D, Gonzalez AH, Clowe D, Forman W, Jones C, Marshall P, Schneider P, Zaritsky D (2009) Focusing cosmic telescopes: exploring redshift $z \sim 5$–6 galaxies with the bullet cluster 1E0657 - 56. Astrophys J 706(2):1201–1212. https://doi.org/10.1088/0004-637X/706/2/1201. arXiv:0910.2708 [astro-ph.CO]

Broadhurst T, Benítez N, Coe D, Sharon K, Zekser K, White R, Ford H, Bouwens R, Blakeslee J, Clampin M, Cross N, Franx M, Frye B, Hartig G, Illingworth G, Infante L, Menanteau F, Meurer G, Postman M, Ardila DR, Bartko F, Brown RA, Burrows CJ, Cheng ES, Feldman PD, Golimowski DA, Goto T, Gronwall C, Herranz D, Holden B, Homeier N, Krist JE, Lesser MP, Martel AR, Miley GK, Rosati P, Sirianni M, Sparks WB, Steindling S, Tran HD, Tsvetanov ZI, Zheng W (2005a) Strong-lensing analysis of A1689 from deep advanced camera images. Astrophys J 621(1):53–88. https://doi.org/10.1086/426494. arXiv:astro-ph/0409132 [astro-ph]

Broadhurst T, Takada M, Umetsu K, Kong X, Arimoto N, Chiba M, Futamase T (2005b) The surprisingly steep mass profile of A1689, from a lensing analysis of subaru images. Astrophys J Lett 619(2):L143–L146. https://doi.org/10.1086/428122. arXiv:astro-ph/0412192 [astro-ph]

Cain B, Bradač M, Levinson R (2016) Reconstruction of small-scale galaxy cluster substructure with lensing flexion. Mon Not R Astron Soc 463(4):4287–4300. https://doi.org/10.1093/mnras/stw2270. arXiv:1503.08218 [astro-ph.CO]

Caminha GB, Estrada J, Makler M (2013) Magnification Bias in Gravitational Arc Statistics. ArXiv e-prints arXiv:1308.6569 [astro-ph.CO]

Caminha GB, Grillo C, Rosati P, Balestra I, Karman W, Lombardi M, Mercurio A, Nonino M, Tozzi P, Zitrin A, Biviano A, Girardi M, Koekemoer AM, Melchior P, Meneghetti M, Munari E, Suyu SH, Umetsu K, Annunziatella M, Borgani S, Broadhurst T, Caputi KI, Coe D, Delgado-Correal C, Ettori S, Fritz A, Frye B, Gobat R, Maier C, Monna A, Postman M, Sartoris B, Seitz S, Vanzella E, Ziegler B (2016) CLASH-VLT: a highly precise strong lensing model of the galaxy cluster RXC J2248.7-4431 (Abell S1063) and prospects for cosmography. Astron Astrophys 587:A80. https://doi.org/10.1051/0004-6361/201527670. arXiv:1512.04555 [astro-ph.CO]

Caminha GB, Grillo C, Rosati P, Balestra I, Mercurio A, Vanzella E, Biviano A, Caputi KI, Delgado-Correal C, Karman W, Lombardi M, Meneghetti M, Sartoris B, Tozzi P (2017) A refined mass distribution of the cluster MACS J0416.1-2403 from a new large set of spectroscopic multiply lensed sources. Astron Astrophys 600:A90. https://doi.org/10.1051/0004-6361/201629297. arXiv:1607.03462 [astro-ph.GA]

Caminha GB, Rosati P, Grillo C, Rosani G, Caputi KI, Meneghetti M, Mercurio A, Balestra I, Bergamini P, Biviano A, Nonino M, Umetsu K, Vanzella E, Annunziatella M, Broadhurst T, Delgado-Correal C, Demarco R, Koekemoer AM, Lombardi M, Maier C, Verdugo M, Zitrin A (2019) Strong lensing models of eight CLASH clusters from extensive spectroscopy: accurate total mass reconstructions in the cores. Astron Astrophys 632:A36. https://doi.org/10.1051/0004-6361/201935454. arXiv:1903.05103 [astro-ph.GA]

Caminha GB, Suyu SH, Grillo C, Rosati P (2022a) Galaxy cluster strong lensing cosmography. Cosmological constraints from a sample of regular galaxy clusters. Astron Astrophys 657:A83. https://doi.org/10.1051/0004-6361/202141994. arXiv:2110.06232 [astro-ph.CO]

Caminha GB, Suyu SH, Mercurio A, Brammer G, Bergamini P, Acebron A, Vanzella E (2022b) First JWST observations of a gravitational lens. Mass model from new multiple images with near-infrared observations of SMACS J0723.3−7327. Astron Astrophys 666:L9. https://doi.org/10.1051/0004-6361/202244517. arXiv:2207.07567 [astro-ph.GA]

Carlsten SG, Greene JE, Peter AHG, Greco JP, Beaton RL (2020) Radial distributions of dwarf satellite systems in the local volume. Astrophys J 902(2):124. https://doi.org/10.3847/1538-4357/abb60b. arXiv:2006.02444 [astro-ph.GA]

Castellano M, Fontana A, Treu T, Merlin E, Santini P, Bergamini P, Grillo C, Rosati P, Acebron A, Leethochawalit N, Paris D, Bonchi A, Belfiori D, Calabrò A, Correnti M, Nonino M, Polenta G, Trenti M, Boyett K, Brammer G, Broadhurst T, Caminha GB, Chen W, Filippenko AV, Fortuni F, Glazebrook K, Mascia S, Mason CA, Menci N, Meneghetti M, Mercurio A, Metha B, Morishita T, Nanayakkara T, Pentericci L, Roberts-Borsani G, Roy N, Vanzella E, Vulcani B, Yang L, Wang X (2023) Early results from GLASS-JWST. XIX. A high density of bright galaxies at z ≈ 10 in the A2744 region. Astrophys J Lett 948(2):L14. https://doi.org/10.3847/2041-8213/accea5. arXiv:2212.06666 [astro-ph.GA]

Cerini G, Cappelluti N, Natarajan P (2023) New metrics to probe the dynamical state of galaxy clusters. Astrophys J 945(2):152. https://doi.org/10.3847/1538-4357/acbccb. arXiv:2209.06831 [astro-ph.CO]

Cha S, Jee MJ (2022) MARS: a new maximum-entropy-regularized strong lensing mass reconstruction method. Astrophys J 931(2):127. https://doi.org/10.3847/1538-4357/ac69df. arXiv:2202.10489 [astro-ph.CO]

Chirivì G, Suyu SH, Grillo C, Halkola A, Balestra I, Caminha GB, Mercurio A, Rosati P (2018) MACS J0416.1-2403: impact of line-of-sight structures on strong gravitational lensing modelling of galaxy clusters. Astron Astrophys 614:A8. https://doi.org/10.1051/0004-6361/201731433. arXiv:1706.07815 [astro-ph.CO]

Clowe D, Bradač M, Gonzalez AH, Markevitch M, Randall SW, Jones C, Zaritsky D (2006a) A direct empirical proof of the existence of dark matter. Astrophys J Lett 648(2):L109–L113. https://doi.org/10.1086/508162. arXiv:astro-ph/0608407 [astro-ph]

Clowe D, Schneider P, Aragón-Salamanca A, Bremer M, De Lucia G, Halliday C, Jablonka P, Milvang-Jensen B, Pelló R, Poggianti B, Rudnick G, Saglia R, Simard L, White S, Zaritsky D (2006b) Weak lensing mass reconstructions of the ESO distant cluster survey. Astron Astrophys 451(2):395–408. https://doi.org/10.1051/0004-6361:20041787. arXiv:astro-ph/0511746 [astro-ph]

Coe D, Benítez N, Broadhurst T, Moustakas LA (2010) A high-resolution mass map of galaxy cluster substructure: LensPerfect analysis of A1689. Astrophys J 723(2):1678–1702. https://doi.org/10.1088/0004-637X/723/2/1678. arXiv:1005.0398 [astro-ph.CO]

Coe D, Umetsu K, Zitrin A, Donahue M, Medezinski E, Postman M, Carrasco M, Anguita T, Geller MJ, Rines KJ, Diaferio A, Kurtz MJ, Bradley L, Koekemoer A, Zheng W, Nonino M, Molino A, Mahdavi A, Lemze D, Infante L, Ogaz S, Melchior P, Host O, Ford H, Grillo C, Rosati P, Jiménez-Teja Y, Moustakas J, Broadhurst T, Ascaso B, Lahav O, Bartelmann M, Benítez N, Bouwens R, Graur O, Graves G, Jha S, Jouvel S, Kelson D, Moustakas L, Maoz D, Meneghetti M, Merten J, Riess A, Rodney S, Seitz S (2012) CLASH: precise new constraints on the mass profile of the galaxy cluster A2261. Astrophys J 757(1):22. https://doi.org/10.1088/0004-637X/757/1/22. arXiv:1201.1616 [astro-ph.CO]

Coe D, Zitrin A, Carrasco M, Shu X, Zheng W, Postman M, Bradley L, Koekemoer A, Bouwens R, Broadhurst T, Monna A, Host O, Moustakas LA, Ford H, Moustakas J, van der Wel A, Donahue M, Rodney SA, Benítez N, Jouvel S, Seitz S, Kelson DD, Rosati P (2013) CLASH: three strongly lensed images of a candidate z ≈ 11 galaxy. Astrophys J 762(1):32. https://doi.org/10.1088/0004-637X/762/1/32. arXiv:1211.3663 [astro-ph.CO]

Coe D, Salmon B, Bradač M et al (2019) RELICS: reionization lensing cluster survey. Astrophys J 884(1):85. https://doi.org/10.3847/1538-4357/ab412b. arXiv:1903.02002 [astro-ph.GA]

Dahle H, Gladders MD, Sharon K, Bayliss MB, Rigby JR (2015) Time delay measurements for the cluster-lensed sextuple quasar SDSS J2222+2745. Astrophys J 813(1):67. https://doi.org/10.1088/0004-637X/813/1/67. arXiv:1505.06187 [astro-ph.CO]

Dai L, Kaurov AA, Sharon K, Florian M, Miralda-Escudé J, Venumadhav T, Frye B, Rigby JR, Bayliss M (2020) Asymmetric surface brightness structure of caustic crossing arc in SDSS J1226+2152: a case for dark matter substructure. Mon Not R Astron Soc 495(3):3192–3208. https://doi.org/10.1093/mnras/staa1355. arXiv:2001.00261 [astro-ph.GA]

D'Aloisio A, Natarajan P (2011) The effects of primordial non-Gaussianity on giant-arc statistics. Mon Not R Astron Soc 415(2):1913–1927. https://doi.org/10.1111/j.1365-2966.2011.18837.x. arXiv:1102.5097 [astro-ph.CO]

D'Aloisio A, Natarajan P, Shapiro PR (2014) The effect of large-scale structure on the magnification of high-redshift sources by cluster lenses. Mon Not R Astron Soc 445(4):3581–3591. https://doi.org/10.1093/mnras/stu1931. arXiv:1311.1614 [astro-ph.CO]

De Lucia G, Kauffmann G, Springel V, White SDM, Lanzoni B, Stoehr F, Tormen G, Yoshida N (2004) Substructures in cold dark matter haloes. Mon Not R Astron Soc 348(1):333–344. https://doi.org/10.1111/j.1365-2966.2004.07372.x. arXiv:astro-ph/0306205 [astro-ph]

Despali G, Sparre M, Vegetti S, Vogelsberger M, Zavala J, Marinacci F (2019) The interplay of self-interacting dark matter and baryons in shaping the halo evolution. Mon Not R Astron Soc 484(4):4563–4573. https://doi.org/10.1093/mnras/stz273. arXiv:1811.02569 [astro-ph.GA]

Diego JM, Protopapas P, Sandvik HB, Tegmark M (2005) Non-parametric inversion of strong lensing systems. Mon Not R Astron Soc 360(2):477–491. https://doi.org/10.1111/j.1365-2966.2005.09021.x. arXiv:astro-ph/0408418 [astro-ph]

Diego JM, Tegmark M, Protopapas P, Sandvik HB (2007) Combined reconstruction of weak and strong lensing data with WSLAP. Mon Not R Astron Soc 375(3):958–970. https://doi.org/10.1111/j.1365-2966.2007.11380.x. arXiv:astro-ph/0509103 [astro-ph]

Diego JM, Broadhurst T, Chen C, Lim J, Zitrin A, Chan B, Coe D, Ford HC, Lam D, Zheng W (2016a) A free-form prediction for the reappearance of supernova Refsdal in the Hubble Frontier Fields cluster MACSJ1149.5+2223. Mon Not R Astron Soc 456(1):356–365. https://doi.org/10.1093/mnras/stv2638. arXiv:1504.05953 [astro-ph.CO]

Diego JM, Broadhurst T, Wong J, Silk J, Lim J, Zheng W, Lam D, Ford H (2016b) A free-form mass model of the Hubble Frontier Fields cluster AS1063 (RXC J2248.7-4431) with over one hundred constraints. Mon Not R Astron Soc 459(4):3447–3459. https://doi.org/10.1093/mnras/stw865. arXiv:1512.07916 [astro-ph.CO]

Diego JM, Pascale M, Kavanagh BJ, Kelly P, Dai L, Frye B, Broadhurst T (2022) Godzilla, a monster lurks in the Sunburst galaxy. Astron Astrophys 665:A134. https://doi.org/10.1051/0004-6361/202243605. arXiv:2203.08158 [astro-ph.GA]

Diemand J, Kuhlen M, Madau P (2007) Formation and evolution of galaxy dark matter halos and their substructure. Astrophys J 667(2):859–877. https://doi.org/10.1086/520573. arXiv:astro-ph/0703337 [astro-ph]

Donahue M, Voit GM, Mahdavi A, Umetsu K, Ettori S, Merten J, Postman M, Hoffer A, Baldi A, Coe D, Czakon N, Bartelmann M, Benitez N, Bouwens R, Bradley L, Broadhurst T, Ford H, Gastaldello F, Grillo C, Infante L, Jouvel S, Koekemoer A, Kelson D, Lahav O, Lemze D, Medezinski E, Melchior P, Meneghetti M, Molino A, Moustakas J, Moustakas LA, Nonino M, Rosati P, Sayers J, Seitz S, Van der Wel A, Zheng W, Zitrin A (2014) CLASH-X: a comparison of lensing and X-ray techniques for measuring the mass profiles of galaxy clusters. Astrophys J 794(2):136. https://doi.org/10.1088/0004-637X/794/2/136. arXiv:1405.7876 [astro-ph.CO]

Ebeling H, Edge AC, Henry JP (2001) MACS: a quest for the most massive galaxy clusters in the universe. Astrophys J 553(2):668–676. https://doi.org/10.1086/320958. arXiv:astro-ph/0009101 [astro-ph]

Eichner T, Seitz S, Suyu SH, Halkola A, Umetsu K, Zitrin A, Coe D, Monna A, Rosati P, Grillo C, Balestra I, Postman M, Koekemoer A, Zheng W, Høst O, Lemze D, Broadhurst T, Moustakas L, Bradley L, Molino A, Nonino M, Mercurio A, Scodeggio M, Bartelmann M, Benitez N, Bouwens R, Donahue M, Infante L, Jouvel S, Kelson D, Lahav O, Medezinski E, Melchior P, Merten J, Riess A (2013) Galaxy halo truncation and giant arc surface brightness reconstruction in the cluster MACSJ1206.2-0847. Astrophys J 774(2):124. https://doi.org/10.1088/0004-637X/774/2/124. arXiv:1306.5240 [astro-ph.CO]

Elahi PJ, Mahdi HS, Power C, Lewis GF (2014) Warm dark haloes accretion histories and their gravitational signatures. Mon Not R Astron Soc 444(3):2333–2345. https://doi.org/10.1093/mnras/stu1614. arXiv:1406.3413 [astro-ph.CO]

Euclid Collaboration, Adam R, Vannier M, Maurogordato S, Biviano A, Adami C, Ascaso B, Bellagamba F, Benoist C, Cappi A, Díaz-Sánchez A, Durret F, Farrens S, Gonzalez AH, Iovino A, Licitra R, Maturi M, Mei S, Merson A, Munari E, Pelló R, Ricci M, Rocci PF, Roncarelli M, Sarron F, Amoura Y, Andreon S, Apostolakos N, Arnaud M, Bardelli S, Bartlett J, Baugh CM, Borgani S, Brodwin M, Castander F, Castignani G, Cucciati O, De Lucia G, Dubath P, Fosalba P, Giocoli C, Hoekstra H, Mamon GA, Melin JB, Moscardini L, Paltani S, Radovich M, Sartoris B, Schultheis M, Sereno M, Weller J, Burigana C, Carvalho CS, Corcione L, Kurki-Suonio H, Lilje PB, Sirri G, Toledo-Moreo R, Zamorani G (2019) Euclid preparation. III. Galaxy cluster detection in the wide photometric survey, performance and algorithm selection. Astron Astrophys 627:A23. https://doi.org/10.1051/0004-6361/201935088. arXiv:1906.04707 [astro-ph.CO]

Finney EQ, Bradač M, Huang KH, Hoag A, Morishita T, Schrabback T, Treu T, Borello Schmidt K, Lemaux BC, Wang X, Mason C (2018) Mass modeling of frontier fields cluster MACS J1149.5+2223 using strong and weak lensing. Astrophys J 859:58. https://doi.org/10.3847/1538-4357/aabf97

Foëx G, Motta V, Jullo E, Limousin M, Verdugo T (2014) SARCS strong-lensing galaxy groups. II. Mass-concentration relation and strong-lensing bias. Astron Astrophys 572:A19. https://doi.org/10.1051/0004-6361/201424706. arXiv:1409.5905 [astro-ph.CO]

Fohlmeister J, Kochanek CS, Falco EE, Wambsganss J, Oguri M, Dai X (2013) A two-year time delay for the lensed quasar SDSS J1029+2623. Astrophys J 764(2):186. https://doi.org/10.1088/0004-637X/764/2/186. arXiv:1207.5776 [astro-ph.CO]

Fox DC, Pen UL (2001) Gravitational lensing by galaxy groups in the Hubble deep field. Astrophys J 546(1):35–46. https://doi.org/10.1086/318242. arXiv:astro-ph/0009068 [astro-ph]

Fox C, Mahler G, Sharon K, Remolina González JD (2022) The strongest cluster lenses: an analysis of the relation between strong gravitational lensing strength and the physical properties of galaxy clusters. Astrophys J 928(1):87. https://doi.org/10.3847/1538-4357/ac5024. arXiv:2104.05585 [astro-ph.CO]

Furtak LJ, Shuntov M, Atek H, Zitrin A, Richard J, Lehnert MD, Chevallard J (2023) Constraining the physical properties of the first lensed $z \sim 9$–16 galaxy candidates with JWST. Mon Not R Astron Soc 519(2):3064–3075. https://doi.org/10.1093/mnras/stac3717. arXiv:2208.05473 [astro-ph.GA]

Ghigna S, Moore B, Governato F, Lake G, Quinn T, Stadel J (1998) Dark matter haloes within clusters. Mon Not R Astron Soc 300(1):146–162. https://doi.org/10.1046/j.1365-8711.1998.01918.x. arXiv:astro-ph/9801192 [astro-ph]

Ghosh A, Williams LLR, Liesenborgs J (2020) Free-form grale lens inversion of galaxy clusters with up to 1000 multiple images. Mon Not R Astron Soc 494(3):3998–4014. https://doi.org/10.1093/mnras/staa962. arXiv:2004.01724 [astro-ph.CO]

Ghosh A, Williams LLR, Liesenborgs J, Acebron A, Jauzac M, Koekemoer AM, Mahler G, Niemiec A, Steinhardt C, Faisst AL, Lagattuta D, Natarajan P (2021) Further support for a trio of mass-to-light deviations in Abell 370: free-form grale lens inversion using BUFFALO strong lensing data. Mon Not R Astron Soc 506(4):6144–6158. https://doi.org/10.1093/mnras/stab1196. arXiv:2104.11781 [astro-ph.CO]

Ghosh A, Adams D, Williams LLR, Liesenborgs J, Alavi A, Scarlata C (2023) An excursion into the core of the cluster lens Abell 1689. Mon Not R Astron Soc 525(2):2519–2534. https://doi.org/10.1093/mnras/stad2418. arXiv:2206.08584 [astro-ph.CO]

Gilbank DG, Gladders MD, Yee HKC, Hsieh BC (2011) The red-sequence cluster survey-2 (RCS-2): survey details and photometric catalog construction. Astron J 141(3):94. https://doi.org/10.1088/0004-6256/141/3/94. arXiv:1012.3470 [astro-ph.CO]

Gilmore J, Natarajan P (2009) Cosmography with cluster strong lensing. Mon Not R Astron Soc 396(1):354–364. https://doi.org/10.1111/j.1365-2966.2009.14612.x. arXiv:astro-ph/0605245 [astro-ph]

Gladders MD, Yee HKC (2000) A new method for galaxy cluster detection. I. The algorithm. Astron J 120(4):2148–2162. https://doi.org/10.1086/301557. arXiv:astro-ph/0004092 [astro-ph]

Goldberg DM, Natarajan P (2002) The galaxy octopole moment as a probe of weak-lensing shear fields. Astrophys J 564(1):65–72. https://doi.org/10.1086/324202. arXiv:astro-ph/0107187 [astro-ph]

Golubchik M, Furtak LJ, Meena AK, Zitrin A (2022) HST strong-lensing model for the first JWST galaxy cluster SMACS J0723.3-7327. Astrophys J 938(1):14. https://doi.org/10.3847/1538-4357/ac8ff1. arXiv:2207.05007 [astro-ph.CO]

Gonzalez AH, Zabludoff AI, Zaritsky D (2005) Intracluster light in nearby galaxy clusters: relationship to the halos of brightest cluster galaxies. Astrophys J 618(1):195–213. https://doi.org/10.1086/425896. arXiv:astro-ph/0406244 [astro-ph]

González-López J, Bauer FE, Romero-Cañizales C, Kneissl R, Villard E, Carvajal R, Kim S, Laporte N, Anguita T, Aravena M, Bouwens RJ, Bradley L, Carrasco M, Demarco R, Ford H, Ibar E, Infante L, Messias H, Muñoz Arancibia AM, Nagar N, Padilla N, Treister E, Troncoso P, Zitrin A (2017) The ALMA frontier fields survey. I. 1.1 mm continuum detections in Abell 2744, MACS J0416.1-2403 and MACS J1149.5+2223. Astron Astrophys 597:A41. https://doi.org/10.1051/0004-6361/201628806. arXiv:1607.03808 [astro-ph.GA]

Granata G, Mercurio A, Grillo C, Tortorelli L, Bergamini P, Meneghetti M, Rosati P, Caminha GB, Nonino M (2022) Improved strong lensing modelling of galaxy clusters using the fundamental plane: detailed mapping of the baryonic and dark matter mass distribution of Abell S1063. Astron Astrophys 659:A24. https://doi.org/10.1051/0004-6361/202141817. arXiv:2107.09079 [astro-ph.GA]

Griffiths RE, Rudisel M, Wagner J, Hamilton T, Huang PC, Villforth C (2021) Hamilton's object – a clumpy galaxy straddling the gravitational caustic of a galaxy cluster: constraints on dark matter clumping. Mon Not R Astron Soc 506(2):1595–1608. https://doi.org/10.1093/mnras/stab1375. arXiv:2105.04562 [astro-ph.CO]

Grillo C, Gobat R, Presotto V, Balestra I, Mercurio A, Rosati P, Nonino M, Vanzella E, Christensen L, Graves G, Biviano A, Lemze D, Bartelmann M, Benitez N, Bouwens R, Bradley L, Broadhurst T, Coe D, Donahue M, Ford H, Infante L, Jouvel S, Kelson D, Koekemoer A, Lahav O, Medezinski E, Melchior P, Meneghetti M, Merten J, Molino A, Monna A, Moustakas J, Moustakas LA, Postman M, Seitz S, Umetsu K, Zheng W, Zitrin A (2014) CLASH: extending galaxy strong lensing to small physical scales with distant sources highly magnified by galaxy cluster members. Astrophys J 786(1):11. https://doi.org/10.1088/0004-637X/786/1/11. arXiv:1403.0573 [astro-ph.CO]

Grillo C, Suyu SH, Rosati P, Mercurio A, Balestra I, Munari E, Nonino M, Caminha GB, Lombardi M, De Lucia G, Borgani S, Gobat R, Biviano A, Girardi M, Umetsu K, Coe D, Koekemoer AM, Postman M, Zitrin A, Halkola A, Broadhurst T, Sartoris B, Presotto V, Annunziatella M, Maier C, Fritz A, Vanzella E, Frye B (2015) CLASH-VLT: insights on the mass substructures in the frontier fields cluster MACS J0416.1-2403 through accurate strong lens modeling. Astrophys J 800(1):38. https://doi.org/10.1088/0004-637X/800/1/38. arXiv:1407.7866 [astro-ph.CO]

Grillo C, Karman W, Suyu SH, Rosati P, Balestra I, Mercurio A, Lombardi M, Treu T, Caminha GB, Halkola A, Rodney SA, Gavazzi R, Caputi KI (2016) The story of supernova "Refsdal" told by MUSE. Astrophys J 822(2):78. https://doi.org/10.3847/0004-637X/822/2/78. arXiv:1511.04093 [astro-ph.GA]

Grillo C, Rosati P, Suyu SH, Balestra I, Caminha GB, Halkola A, Kelly PL, Lombardi M, Mercurio A, Rodney SA, Treu T (2018) Measuring the value of the Hubble constant "à la refsdal". Astrophys J 860(2):94. https://doi.org/10.3847/1538-4357/aac2c9. arXiv:1802.01584 [astro-ph.CO]

Grillo C, Rosati P, Suyu SH, Caminha GB, Mercurio A, Halkola A (2020) On the accuracy of time-delay cosmography in the frontier fields cluster MACS J1149.5+2223 with supernova refsdal. Astrophys J 898(1):87. https://doi.org/10.3847/1538-4357/ab9a4c. arXiv:2001.02232 [astro-ph.CO]

Grossman SA, Narayan R (1988) Arcs from gravitational lensing. Astrophys J Lett 324:L37. https://doi.org/10.1086/185086

Gruen D, Seitz S, Brimioulle F, Kosyra R, Koppenhoefer J, Lee CH, Bender R, Riffeser A, Eichner T, Weidinger T, Bierschenk M (2014) Weak lensing analysis of SZ-selected clusters of galaxies from the SPT and Planck surveys. Mon Not R Astron Soc 442(2):1507–1544. https://doi.org/10.1093/mnras/stu949. arXiv:1310.6744 [astro-ph.CO]

Harvey D, Robertson A, Massey R, McCarthy IG (2019) Observable tests of self-interacting dark matter in galaxy clusters: BCG wobbles in a constant density core. Mon Not R Astron Soc 488(2):1572–1579. https://doi.org/10.1093/mnras/stz1816. arXiv:1812.06981 [astro-ph.CO]

Hjorth J, Williams LLR (2010) Statistical mechanics of collisionless orbits. I. Origin of central cusps in dark-matter halos. Astrophys J 722(1):851–855. https://doi.org/10.1088/0004-637X/722/1/851. arXiv:1010.0265 [astro-ph.CO]

Hoag A, Huang KH, Treu T, Bradač M, Schmidt KB, Wang X, Brammer GB, Broussard A, Amorin R, Castellano M, Fontana A, Merlin E, Schrabback T, Trenti M, Vulcani B (2016) The grism lens-amplified survey from space (GLASS). VI. Comparing the mass and light in MACS J0416.1-2403 using frontier field imaging and GLASS spectroscopy. Astrophys J 831:182. https://doi.org/10.3847/0004-637X/831/2/182. arXiv:1603.00505

Holanda RFL, Busti VC, Gonzalez JE, Andrade-Santos F, Alcaniz JS (2017) Cosmological constraints on the gas depletion factor in galaxy clusters. J Cosmol Astropart Phys 2017(12):016. https://doi.org/10.1088/1475-7516/2017/12/016. arXiv:1706.07321 [astro-ph.CO]

Horesh A, Maoz D, Ebeling H, Seidel G, Bartelmann M (2010) The lensing efficiencies of MACS X-ray-selected versus RCS optically selected galaxy clusters. Mon Not R Astron Soc 406(2):1318–1336. https://doi.org/10.1111/j.1365-2966.2010.16763.x. arXiv:1004.2048 [astro-ph.CO]

Ishigaki M, Kawamata R, Ouchi M, Oguri M, Shimasaku K, Ono Y (2015) Hubble frontier fields first complete cluster data: faint galaxies at $z \sim 5$–10 for UV luminosity functions and cosmic reionization. Astrophys J 799(1):12. https://doi.org/10.1088/0004-637X/799/1/12. arXiv:1408.6903 [astro-ph.GA]

Jaelani AT, More A, Oguri M, Sonnenfeld A, Suyu SH, Rusu CE, Wong KC, Chan JHH, Kayo I, Lee CH, Chao DCY, Coupon J, Inoue KT, Futamase T (2020) Survey of Gravitationally lensed Objects in HSC Imaging (SuGOHI) - V. Group-to-cluster scale lens search from the HSC-SSP survey. Mon Not R Astron Soc 495(1):1291–1310. https://doi.org/10.1093/mnras/staa1062. arXiv:2002.01611 [astro-ph.GA]

Jauzac M, Eckert D, Schwinn J, Harvey D, Baugh CM, Robertson A, Bose S, Massey R, Owers M, Ebeling H, Shan HY, Jullo E, Kneib JP, Richard J, Atek H, Clément B, Egami E, Israel H, Knowles K, Limousin M, Natarajan P, Rexroth M, Taylor P, Tchernin C (2016) The extraordinary amount of substructure in the Hubble Frontier Fields cluster Abell 2744. Mon Not R Astron Soc 463(4):3876–3893. https://doi.org/10.1093/mnras/stw2251. arXiv:1606.04527 [astro-ph.CO]

Johnson TL, Sharon K (2016) The systematics of strong lens modeling quantified: the effects of constraint selection and redshift information on magnification, mass, and multiple image predictability. Astrophys J 832(1):82. https://doi.org/10.3847/0004-637X/832/1/82. arXiv:1608.08713 [astro-ph.CO]

Johnson TL, Sharon K, Bayliss MB, Gladders MD, Coe D, Ebeling H (2014) Lens models and magnification maps of the six Hubble frontier fields clusters. Astrophys J 797(1):48. https://doi.org/10.1088/0004-637X/797/1/48. arXiv:1405.0222 [astro-ph.CO]

Johnson TL, Rigby JR, Sharon K, Gladders MD, Florian M, Bayliss MB, Wuyts E, Whitaker KE, Livermore R, Murray KT (2017) Star formation at z = 2.481 in the lensed galaxy SDSS J1110+6459: star formation down to 30 pc scales. Astrophys J Lett 843(2):L21. https://doi.org/10.3847/2041-8213/aa7516. arXiv:1707.00706 [astro-ph.GA]

Jullo E, Kneib JP (2009) Multiscale cluster lens mass mapping - I. Strong lensing modelling. Mon Not R Astron Soc 395(3):1319–1332. https://doi.org/10.1111/j.1365-2966.2009.14654.x. arXiv:0901.3792 [astro-ph.CO]

Jullo E, Kneib JP, Limousin M, Elíasdóttir Á., Marshall PJ, Verdugo T (2007a) A Bayesian approach to strong lensing modelling of galaxy clusters. New J Phys 9(12):447. https://doi.org/10.1088/1367-2630/9/12/447. arXiv:0706.0048 [astro-ph]

Jullo E, Kneib JP, Limousin M, Elíasdóttir Á., Marshall PJ, Verdugo T (2007b) A Bayesian approach to strong lensing modelling of galaxy clusters. New J Phys 9(12):447. https://doi.org/10.1088/1367-2630/9/12/447. arXiv:0706.0048 [astro-ph]

Jullo E, Natarajan P, Kneib JP, D'Aloisio A, Limousin M, Richard J, Schimd C (2010) Cosmological constraints from strong gravitational lensing in clusters of galaxies. Science 329:924–927. https://doi.org/10.1126/science.1185759. arXiv:1008.4802 [astro-ph.CO]

Jullo E, Acebron A, Limousin M, Giocoli C, Despali G, Bonamigo M (2015) Strong lensing cosmography in the frontier fields. Proc Int Astron Union 11(A29B):801–803. https://doi.org/10.1017/S1743921316006888

Kahlhoefer F, Schmidt-Hoberg K, Kummer J, Sarkar S (2015) On the interpretation of dark matter self-interactions in Abell 3827. Mon Not R Astron Soc 452(1):L54–L58. https://doi.org/10.1093/mnrasl/slv088. arXiv:1504.06576 [astro-ph.CO]

Kaiser N (1992) Weak gravitational lensing of distant galaxies. Astrophys J 388:272. https://doi.org/10.1086/171151

Kaiser N, Squires G (1993) Mapping the dark matter with weak gravitational lensing. Astrophys J 404:441. https://doi.org/10.1086/172297

Karman W, Caputi KI, Grillo C, Balestra I, Rosati P, Vanzella E, Coe D, Christensen L, Koekemoer AM, Krühler T, Lombardi M, Mercurio A, Nonino M, van der Wel A (2015) MUSE integral-field spectroscopy towards the frontier fields cluster Abell S1063. I. Data products and redshift identifications. Astron Astrophys 574:A11. https://doi.org/10.1051/0004-6361/201424962. arXiv:1409.3507 [astro-ph.GA]

Kaurov AA, Dai L, Venumadhav T, Miralda-Escudé J, Frye B (2019) Highly magnified stars in lensing clusters: new evidence in a galaxy lensed by MACS J0416.1-2403. Astrophys J 880(1):58. https://doi.org/10.3847/1538-4357/ab2888. arXiv:1902.10090 [astro-ph.GA]

Kawamata R, Oguri M, Ishigaki M, Shimasaku K, Ouchi M (2016) Precise strong lensing mass modeling of four Hubble frontier field clusters and a sample of magnified high-redshift galaxies. Astrophys J 819(2):114. https://doi.org/10.3847/0004-637X/819/2/114. arXiv:1510.06400 [astro-ph.GA]

Keeton CR (2010) On modeling galaxy-scale strong lens systems. Gen Relativ Gravit 42(9):2151–2176. https://doi.org/10.1007/s10714-010-1041-1

Kelly PL, Rodney SA, Treu T, Foley RJ, Brammer G, Schmidt KB, Zitrin A, Sonnenfeld A, Strolger LG, Graur O, Filippenko AV, Jha SW, Riess AG, Bradac M, Weiner BJ, Scolnic D, von Malkan MA, der Linden A, Trenti M, Hjorth J, Gavazzi R, Fontana A, Merten JC, McCully C, Jones T, Postman M, Dressler A, Patel B, Cenko SB, Graham ML, Tucker BE (2015) Multiple images of a highly magnified supernova formed by an early-type cluster galaxy lens. Science 347(6226):1123–1126. https://doi.org/10.1126/science.aaa3350. arXiv:1411.6009 [astro-ph.CO]

Kelly PL, Rodney SA, Treu T, Strolger LG, Foley RJ, Jha SW, Selsing J, Brammer G, Bradač M, Cenko SB, Graur O, Filippenko AV, Hjorth J, McCully C, Molino A, Nonino M, Riess AG, Schmidt KB, Tucker B, von der Linden A, Weiner BJ, Zitrin A (2016) Deja vu all over again: the reappearance of supernova refsdal. Astrophys J Lett 819(1):L8. https://doi.org/10.3847/2041-8205/819/1/L8. arXiv:1512.04654 [astro-ph.CO]

Kelly PL, Rodney S, Treu T, Oguri M, Chen W, Zitrin A, Birrer S, Bonvin V, Dessart L, Diego JM, Filippenko AV, Foley RJ, Gilman D, Hjorth J, Jauzac M, Mandel K, Millon M, Pierel J, Sharon K, Thorp S, Williams L, Broadhurst T, Dressler A, Graur O, Jha S, McCully C, Postman M, Schmidt KB, Tucker BE, von der Linden A (2023) Constraints on the Hubble constant from supernova Refsdal's reappearance Science 380:6649:abh1322. https://doi.org/10.1126/science.abh1322

Khullar G, Gozman K, Lin JJ, Martinez MN, Matthews Acuña OS, Medina E, Merz K, Sanchez JA, Sisco EE, Kavin Stein DJ, Sukay EO, Tavangar K, Bayliss MB, Bleem LE, Brownsberger S, Dahle H, Florian MK, Gladders MD, Mahler G, Rigby JR, Sharon K, Stark AA (2021) COOL-LAMPS. I. An extraordinarily bright lensed galaxy at redshift 5.04. Astrophys J 906(2):107. https://doi.org/10.3847/1538-4357/abcb86. arXiv:2011.06601 [astro-ph.GA]

Kneib JP, Natarajan P (2011) Cluster lenses. Astron Astrophys Rev 19:47. https://doi.org/10.1007/s00159-011-0047-3. arXiv:1202.0185 [astro-ph.CO]

Kneib JP, Mellier Y, Fort B, Mathez G (1993) The distribution of dark matter in distant cluster-lenses: modelling A 370. Astron Astrophys 273:367.

Kneib JP, Ellis RS, Smail I, Couch WJ, Sharples RM (1996) Hubble space telescope observations of the lensing cluster Abell 2218. Astrophys J 471:643. https://doi.org/10.1086/177995. arXiv:astro-ph/9511015 [astro-ph]

Kochanek CS (1990) Inverting cluster gravitational lenses. Mon Not R Astron Soc 247:135.

Köhlinger F, Schmidt RW (2014) Strong lensing in RX J1347.5-1145 revisited. Mon Not R Astron Soc 437(2):1858–1871. https://doi.org/10.1093/mnras/stt2017. arXiv:1310.0021 [astro-ph.CO]

Kovner I (1989) Diagnostics of compact clusters of galaxies by giant luminous arcs. Astrophys J 337:621. https://doi.org/10.1086/167133

Lagattuta DJ, Richard J, Bauer FE, Cerny C, Claeyssens A, Guaita L, Jauzac M, Jeanneau A, Koekemoer AM, Mahler G, Prieto Lyon G, Acebron A, Meneghetti M, Niemiec A, Zitrin A, Bianconi M, Connor T, Cen R, Edge A, Faisst AL, Limousin M, Massey R, Sereno M, Sharon K, Weaver JR (2022) Pilot-WINGS: an extended MUSE view of the structure of Abell 370. Mon Not R Astron Soc 514(1):497–517. https://doi.org/10.1093/mnras/stac418. arXiv:2202.04663 [astro-ph.GA]

Lage C, Farrar GR (2015) The bullet cluster is not a cosmological anomaly. J Cosmol Astropart Phys 2015(2):038. https://doi.org/10.1088/1475-7516/2015/02/038. arXiv:1406.6703 [astro-ph.GA]

Lam D (2019) A new approach to free-form cluster lens modeling inspired by the JPEG image compression method. Publ Astron Soc Pac 131(1005):114505. https://doi.org/10.1088/1538-3873/ab35c0. arXiv:1906.00006 [astro-ph.CO]

Lanusse F, Starck JL, Leonard A, Pires S (2016) High resolution weak lensing mass mapping combining shear and flexion. Astron Astrophys 591:A2. https://doi.org/10.1051/0004-6361/201628278. arXiv:1603.01599 [astro-ph.CO]

Laporte N, Zitrin A, Dole H, Roberts-Borsani G, Furtak LJ, Witten C (2022) A lensed protocluster candidate at z = 7.66 identified in JWST observations of the galaxy cluster SMACS0723−7327. Astron Astrophys 667:L3. https://doi.org/10.1051/0004-6361/202244719. arXiv:2208.04930 [astro-ph.GA]

Lasko K, Williams LLR, Ghosh A (2023) What multiple images say about the large-scale mass maps of galaxy clusters. Mon Not R Astron Soc 525(4):5423–5436. https://doi.org/10.1093/mnras/stad2622. arXiv:2309.05730

Leonard A, Goldberg DM, Haaga JL, Massey R (2007) Gravitational shear, flexion, and strong lensing in Abell 1689. Astrophys J 666(1):51–63. https://doi.org/10.1086/520109. arXiv:astro-ph/0702242 [astro-ph]

Li N, Gladders MD, Rangel EM, Florian MK, Bleem LE, Heitmann K, Habib S, Fasel P (2016) PICS: simulations of strong gravitational lensing in galaxy clusters. Astrophys J 828(1):54. https://doi.org/10.3847/0004-637X/828/1/54. arXiv:1511.03673 [astro-ph.CO]

Li N, Gladders MD, Heitmann K, Rangel EM, Child HL, Florian MK, Bleem LE, Habib S, Finkel HJ (2019) The importance of secondary halos for strong lensing in massive galaxy clusters across redshift. Astrophys J 878(2):122. https://doi.org/10.3847/1538-4357/ab1f74. arXiv:1810.13330 [astro-ph.CO]

Liesenborgs J, De Rijcke S, Dejonghe H (2006) A genetic algorithm for the non-parametric inversion of strong lensing systems. Mon Not R Astron Soc 367(3):1209–1216. https://doi.org/10.1111/j.1365-2966.2006.10040.x. arXiv:astro-ph/0601124 [astro-ph]

Liesenborgs J, de Rijcke S, Dejonghe H, Bekaert P (2009) Non-parametric strong lens inversion of SDSS J1004+4112. Mon Not R Astron Soc 397(1):341–349. https://doi.org/10.1111/j.1365-2966.2009.14912.x. arXiv:0904.2382 [astro-ph.CO]

Liesenborgs J, Williams LLR, Wagner J, De Rijcke S (2020) Extended lens reconstructions with grale: exploiting time-domain, substructural, and weak lensing information. Mon Not R Astron Soc 494(3):3253–3274. https://doi.org/10.1093/mnras/staa842. arXiv:2003.10377 [astro-ph.CO]

Limousin M, Cabanac R, Gavazzi R, Kneib JP, Motta V, Richard J, Thanjavur K, Foex G, Pello R, Crampton D, Faure C, Fort B, Jullo E, Marshall P, Mellier Y, More A, Soucail G, Suyu S, Swinbank M, Sygnet JF, Tu H, Valls-Gabaud D, Verdugo T, Willis J (2009) A new window of exploration in the mass spectrum: strong lensing by galaxy groups in the SL2S. Astron Astrophys 502(2):445–456. https://doi.org/10.1051/0004-6361/200811473. arXiv:0812.1033 [astro-ph]

Limousin M, Beauchesne B, Jullo E (2022) Dark matter in galaxy clusters: parametric strong-lensing approach. Astron Astrophys 664:A90. https://doi.org/10.1051/0004-6361/202243278. arXiv:2202.02992 [astro-ph.CO]

Lin J, Wagner J, Griffiths RE (2022) Generalised model-independent characterisation of strong gravitational lenses VIII. Automated multi-band feature detection to constrain local lens properties. Mon Not R Astron Soc. https://doi.org/10.1093/mnras/stac2576

Lin J, Wagner J, Griffiths RE (2023) Much ado about no offset – characterizing the anomalous multiple-image configuration and the model-driven displacement between light and mass in the multiplane strong lens Abell 3827. Mon Not R Astron Soc 526(2):2776–2794. https://doi.org/10.1093/mnras/stad2800

Livermore RC, Finkelstein SL, Lotz JM (2017) Directly observing the galaxies likely responsible for reionization. Astrophys J 835(2):113. https://doi.org/10.3847/1538-4357/835/2/113. arXiv:1604.06799 [astro-ph.GA]

Lotz JM, Koekemoer A, Coe D, Grogin N, Capak P, Mack J, Anderson J, Avila R, Barker EA, Borncamp D, Brammer G, Durbin M, Gunning H, Hilbert B, Jenkner H, Khandrika H, Levay Z, Lucas RA, MacKenty J, Ogaz S, Porterfield B, Reid N, Robberto M, Royle P, Smith LJ, Storrie-Lombardi LJ, Sunnquist B, Surace J, Taylor DC, Williams R, Bullock J, Dickinson M, Finkelstein S, Natarajan P, Richard J, Robertson B, Tumlinson J, Zitrin A, Flanagan K, Sembach K, Soifer BT, Mountain M (2017) The frontier fields: survey design and initial results. Astrophys J 837(1):97. https://doi.org/10.3847/1538-4357/837/1/97. arXiv:1605.06567 [astro-ph.GA]

Lynds R, Petrosian V (1989) Luminous arcs in clusters of galaxies. Astrophys J 336:1. https://doi.org/10.1086/166989

Magana J, Acebron A, Motta V, Verdugo T, Jullo E, Limousin M (2018) Strong lensing modeling in galaxy clusters as a promising method to test cosmography. I. Parametric dark energy models. Astrophys J 865(2):122. https://doi.org/10.3847/1538-4357/aada7d

Mahdi HS, van Beek M, Elahi PJ, Lewis GF, Power C, Killedar M (2014) Gravitational lensing in WDM cosmologies: the cross-section for giant arcs. Mon Not R Astron Soc 441(3):1954–1963. https://doi.org/10.1093/mnras/stu705. arXiv:1404.1644 [astro-ph.CO]

Mahler G, Jauzac M, Richard J, Beauchesne B, Ebeling H, Lagattuta D, Natarajan P, Sharon K, Atek H, Claeyssens A, Clément B, Eckert D, Edge A, Kneib JP, Niemiec A (2023) Precision modeling of JWST's first cluster lens SMACS J0723.3-7327. Astrophys J 945(1):49. https://doi.org/10.3847/1538-4357/acaea9. arXiv:2207.07101 [astro-ph.GA]

Mantz AB, Allen SW, Morris RG, Rapetti DA, Applegate DE, von Kelly PL, der Linden A, Schmidt RW (2014) Cosmology and astrophysics from relaxed galaxy clusters - II. Cosmological constraints. Mon Not R Astron Soc 440(3):2077–2098. https://doi.org/10.1093/mnras/stu368. arXiv:1402.6212 [astro-ph.CO]

Massey R, Williams L, Smit R, Swinbank M, Kitching TD, Harvey D, Jauzac M, Israel H, Clowe D, Edge A, Hilton M, Jullo E, Leonard A, Liesenborgs J, Merten J, Mohammed I, Nagai D, Richard J, Robertson A, Saha P, Santana R, Stott J, Tittley E (2015) The behaviour of dark matter associated with four bright cluster galaxies in the 10 kpc core of Abell 3827. Mon Not R Astron Soc 449(4):3393–3406https://doi.org/10.1093/mnras/stv467. arXiv:1504.03388 [astro-ph.CO]

Massey R, Harvey D, Liesenborgs J, Richard J, Stach S, Swinbank M, Taylor P, Williams L, Clowe D, Courbin F, Edge A, Israel H, Jauzac M, Joseph R, Jullo E, Kitching TD, Leonard A, Merten J, Nagai D, Nightingale J, Robertson A, Romualdez LJ, Saha P, Nagai T, Smit R, Tam SI Tittley E (2018b) Dark matter dynamics in Abell 3827: new data consistent with standard cold dark matter. Mon Not R Astron Soc 477(1):669–677, https://doi.org/10.1093/mnras/sty630. arXiv:1708.04245 [astro-ph.CO]

Massey R, Harvey D, Liesenborgs J, Richard J, Stach S, Swinbank M, Taylor P, Williams L, Clowe D, Courbin F, Edge A, Israel H, Jauzac M, Joseph R, Jullo E, Kitching TD, Leonard A, Merten J, Nagai D, Nightingale J, Robertson A, Romualdez LJ, Saha P, Smit R, Tam SI, Tittley E (2018a) Dark matter dynamics in Abell 3827: new data consistent with standard cold dark matter. Mon Not R Astron Soc 477(1):669–677. https://doi.org/10.1093/mnras/sty630. arXiv:1708.04245 [astro-ph.CO]

McCully C, Keeton CR, Wong KC, Zabludoff AI (2014) A new hybrid framework to efficiently model lines of sight to gravitational lenses. Mon Not R Astron Soc 443(4):3631–3642. https://doi.org/10.1093/mnras/stu1316. arXiv:1401.0197 [astro-ph.CO]

McCully C, Keeton CR, Wong KC, Zabludoff AI (2017) Quantifying environmental and line-of-sight effects in models of strong gravitational lens systems. Astrophys J 836(1):141. https://doi.org/10.3847/1538-4357/836/1/141. arXiv:1601.05417 [astro-ph.CO]

Medezinski E, Umetsu K, Nonino M, Merten J, Zitrin A, Broadhurst T, Donahue M, Sayers J, Waizmann JC, Koekemoer A, Coe D, Molino A, Melchior P, Mroczkowski T, Czakon N, Postman M, Meneghetti M, Lemze D, Ford H, Grillo C, Kelson D, Bradley L, Moustakas J, Bartelmann M, Benítez N, Biviano A, Bouwens R, Golwala S, Graves G, Infante L, Jiménez-Teja Y, Jouvel S, Lahav O, Moustakas L, Ogaz S, Rosati P, Seitz S, Zheng W (2013) CLASH: complete lensing analysis of the largest cosmic lens MACS J0717.5+3745 and surrounding structures. Astrophys J 777(1):43. https://doi.org/10.1088/0004-637X/777/1/43. arXiv:1304.1223 [astro-ph.CO]

Meena AK, Bagla JS (2021) Exotic image formation in strong gravitational lensing by clusters of galaxies - I. Cross-section. Mon Not R Astron Soc 503(2):2097–2107. https://doi.org/10.1093/mnras/stab577. arXiv:2009.13418 [astro-ph.CO]

Menanteau F, Hughes JP, Sifón C, Hilton M, González J, Infante L, Barrientos LF, Baker AJ, Bond JR, Das S, Devlin MJ, Dunkley J, Hajian A, Hincks AD, Kosowsky A, Marsden D, Marriage TA, Moodley K, Niemack MD, Nolta MR, Page LA, Reese ED, Sehgal N, Sievers J, Spergel DN, Staggs ST, Wollack E (2012) The Atacama cosmology telescope: ACT-CL J0102-4915 "el gordo," a massive merging cluster at redshift 0.87. Astrophys J 748(1):7. https://doi.org/10.1088/0004-637X/748/1/7. arXiv:1109.0953 [astro-ph.CO]

Meneghetti M, Bartelmann M, Dahle H, Limousin M (2013) Arc statistics. Space Sci Rev 177(1–4):31–74. https://doi.org/10.1007/s11214-013-9981-x. arXiv:1303.3363 [astro-ph.CO]

Meneghetti M, Natarajan P, Coe D, Contini E, De Lucia G, Giocoli C, Acebron A, Borgani S, Bradac M, Diego JM, Hoag A, Ishigaki M, Johnson TL, Jullo E, Kawamata R, Lam D, Limousin M, Liesenborgs J, Oguri M, Sebesta K, Sharon K, Williams LLR, Zitrin A (2017) The Frontier Fields lens modelling comparison project. Mon Not R Astron Soc 472(3):3177–3216. https://doi.org/10.1093/mnras/stx2064. arXiv:1606.04548 [astro-ph.CO]

Meneghetti M, Davoli G, Bergamini P, Rosati P, Natarajan P, Giocoli C, Caminha GB, Metcalf RB, Rasia E, Borgani S, Calura F, Grillo C, Mercurio A, Vanzella E (2020) An excess of small-scale gravitational lenses observed in galaxy clusters. Science 369(6509):1347–1351. https://doi.org/10.1126/science.aax5164. arXiv:2009.04471 [astro-ph.GA]

Meneghetti M, Ragagnin A, Borgani S, Calura F, Despali G, Giocoli C, Granato GL, Grillo C, Moscardini L, Rasia E, Rosati P, Angora G, Bassini L, Bergamini P, Caminha GB, Granata G, Mercurio A, Metcalf RB, Natarajan P, Nonino M, Pignataro GV, Ragone-Figueroa C, Vanzella E, Acebron A, Dolag K, Murante G, Taffoni G, Tornatore L, Tortorelli L, Valentini M (2022) The probability of galaxy-galaxy strong lensing events in hydrodynamical simulations of galaxy clusters. Astron Astrophys 668:A188. https://doi.org/10.1051/0004-6361/202243779. arXiv:2204.09065 [astro-ph.CO]

Merten J (2016) Mesh-free free-form lensing - I. Methodology and application to mass reconstruction. Mon Not R Astron Soc 461(3):2328–2345. https://doi.org/10.1093/mnras/stw1413. arXiv:1412.5186 [astro-ph.CO]

Merten J, Coe D, Dupke R, Massey R, Zitrin A, Cypriano ES, Okabe N, Frye B, Braglia FG, Jiménez-Teja Y, Benítez N, Broadhurst T, Rhodes J, Meneghetti M, Moustakas LA, Sodré LJ, Krick J, Bregman JN (2011) Creation of cosmic structure in the complex galaxy cluster merger Abell 2744. Mon Not R Astron Soc 417(1):333–347. https://doi.org/10.1111/j.1365-2966.2011.19266.x. arXiv:1103.2772 [astro-ph.CO]

Merten J, Meneghetti M, Postman M, Umetsu K, Zitrin A, Medezinski E, Nonino M, Koekemoer A, Melchior P, Gruen D, Moustakas LA, Bartelmann M, Host O, Donahue M, Coe D, Molino A, Jouvel S, Monna A, Seitz S, Czakon N, Lemze D, Sayers J, Balestra I, Rosati P, Benítez N, Biviano A, Bouwens R, Bradley L, Broadhurst T, Carrasco M, Ford H, Grillo C, Infante L, Kelson D, Lahav O, Massey R, Moustakas J, Rasia E, Rhodes J, Vega J, Zheng W (2015) CLASH: the concentration-mass relation of galaxy clusters. Astrophys J 806(1):4. https://doi.org/10.1088/0004-637X/806/1/4. arXiv:1404.1376 [astro-ph.CO]

Miralda-Escude J (1991) Gravitational lensing by clusters of galaxies: constraining the mass distribution. Astrophys J 370:1. https://doi.org/10.1086/169789

Miralda-Escudé J (2002) A test of the collisional dark matter hypothesis from cluster lensing. Astrophys J 564(1):60–64. https://doi.org/10.1086/324138. arXiv:astro-ph/0002050 [astro-ph]

Mohammed I, Saha P, Liesenborgs J (2015) Lensing time delays as a substructure constraint: a case study with the cluster SDSS J1004+4112. Publ Astron Soc Jpn 67(2):21. https://doi.org/10.1093/pasj/psu155. arXiv:1412.3464 [astro-ph.CO]

Mohammed I, Saha P, Williams LLR, Liesenborgs J, Sebesta K (2016) Quantifying substructures in Hubble Frontier Field clusters: comparison with ΛCDM simulations. Mon Not R Astron Soc 459(2):1698–1709. https://doi.org/10.1093/mnras/stw727. arXiv:1507.01532 [astro-ph.CO]

Monna A, Seitz S, Greisel N, Eichner T, Drory N, Postman M, Zitrin A, Coe D, Halkola A, Suyu SH, Grillo C, Rosati P, Lemze D, Balestra I, Snigula J, Bradley L, Umetsu K, Koekemoer A, Kuchner U, Moustakas L, Bartelmann M, Benítez N, Bouwens R, Broadhurst T, Donahue M, Ford H, Host O, Infante L, Jimenez-Teja Y, Jouvel S, Kelson D, Lahav O, Medezinski E, Melchior P, Meneghetti M, Merten J, Molino A, Moustakas J, Nonino M, Zheng W (2014) CLASH: $z \sim 6$ young galaxy candidate quintuply lensed by the frontier field cluster RXC J2248.7-4431. Mon Not R Astron Soc 438(2):1417–1434. https://doi.org/10.1093/mnras/stt2284. arXiv:1308.6280 [astro-ph.CO]

Montes M, Trujillo I (2019) Intracluster light: a luminous tracer for dark matter in clusters of galaxies. Mon Not R Astron Soc 482(2):2838–2851. https://doi.org/10.1093/mnras/sty2858. arXiv:1807.11488 [astro-ph.GA]

More A, Cabanac R, More S, Alard C, Limousin M, Kneib JP, Gavazzi R, Motta V (2012) The CFHTLS-Strong Lensing Legacy Survey (SL2S): Investigating the group-scale lenses with the SARCS sample. Astrophys J 749(1):38. https://doi.org/10.1088/0004-637x/749/1/38

Morioka M, Futamase T (2015) Lens statistics with gravitationally lensed yet morphologically regular images. Astrophys J 805(2):184. https://doi.org/10.1088/0004-637X/805/2/184

Muñoz JA, Kochanek CS, Fohlmeister J, Wambsganss J, Falco E, Forés-Toribio R (2022) The longest delay: a 14.5 yr campaign to determine the third time delay in the lensing cluster SDSS J1004+4112. Astrophys J 937(1):34. https://doi.org/10.3847/1538-4357/ac8877. arXiv:2206.08597 [astro-ph.GA]

Napier K, Sharon K, Dahle H, Bayliss M, Gladders MD, Mahler G, Rigby JR, Florian M (2023) Hubble constant measurement from three large-separation quasars strongly lensed by galaxy clusters. Astrophys J 959(2):134. https://doi.org/10.3847/1538-4357/ad045a. arXiv:2301.11240 [astro-ph.CO]

Narasimha D, Chitre SM (1989) Lensing of extended sources by dark galactic halos. Astron J 97:327. https://doi.org/10.1086/114983
Narayan R, Blandford R, Nityananda R (1984) Multiple imaging of quasars by galaxies and clusters. Nature 310(5973):112–115. https://doi.org/10.1038/310112a0
Natarajan P, Kneib JP (1996) Probing the dynamics of cluster-lenses. Mon Not R Astron Soc 283(3):1031–1046. https://doi.org/10.1093/mnras/283.3.1031. arXiv:astro-ph/9602035 [astro-ph]
Natarajan P, Kneib JP (1997) Lensing by galaxy haloes in clusters of galaxies. Mon Not R Astron Soc 287(4):833–847. https://doi.org/10.1093/mnras/287.4.833. arXiv:astro-ph/9609008 [astro-ph]
Natarajan P, Springel V (2004) Abundance of substructure in clusters of galaxies. Astrophys J Lett 617(1):L13–L16. https://doi.org/10.1086/427079. arXiv:astro-ph/0411515 [astro-ph]
Natarajan P, Kneib JP, Smail I, Ellis RS (1998) The mass-to-light ratio of early-type galaxies: constraints from gravitational lensing in the rich cluster AC 114. Astrophys J 499(2):600–607. https://doi.org/10.1086/305660. arXiv:astro-ph/9706129 [astro-ph]
Natarajan P, Kneib JP, Smail I (2002a) Evidence for tidal stripping of dark matter halos in massive cluster lenses. Astrophys J Lett 580(1):L11–L15. https://doi.org/10.1086/345399. arXiv:astro-ph/0207049 [astro-ph]
Natarajan P, Loeb A, Kneib JP, Smail I (2002b) Constraints on the collisional nature of the dark matter from gravitational lensing in the cluster A2218. Astrophys J 580(1):L17. https://doi.org/10.1086/345547
Natarajan P, De Lucia G, Springel V (2007) Substructure in lensing clusters and simulations. Mon Not R Astron Soc 376(17):180–192. https://doi.org/10.1111/j.1365-2966.2007.11399.x. arXiv:astro-ph/0604414 [astro-ph]
Natarajan P, Kneib JP, Smail I, Treu T, Ellis R, Moran S, Limousin M, Czoske O (2009) The survival of dark matter halos in the cluster cl 0024+16. Astrophys J 693(1):970–983. https://doi.org/10.1088/0004-637X/693/1/970. arXiv:0711.4587 [astro-ph]
Natarajan P, Chadayammuri U, Jauzac M, Richard J, Kneib JP, Ebeling H, Jiang F, van den Bosch F, Limousin M, Jullo E, Atek H, Pillepich A, Popa C, Marinacci F, Hernquist L, Meneghetti M, Vogelsberger M (2017) Mapping substructure in the HST Frontier Fields cluster lenses and in cosmological simulations. Mon Not R Astron Soc 468(2):1962–1980. https://doi.org/10.1093/mnras/stw3385. arXiv:1702.04348 [astro-ph.GA]
Navarro JF, Frenk CS, White SDM (1996) The structure of cold dark matter halos. Astrophys J 462:563. https://doi.org/10.1086/177173. arXiv:astro-ph/9508025 [astro-ph]
Navarro JF, Frenk CS, White SDM (1997) A universal density profile from hierarchical clustering. Astrophys J 490(2):493–508. https://doi.org/10.1086/304888. arXiv:astro-ph/9611107 [astro-ph]
Navarro JF, Hayashi E, Power C, Jenkins AR, Frenk CS, White SDM, Springel V, Stadel J, Quinn TR (2004) The inner structure of ΛCDM haloes – III. Universality and asymptotic slopes. Mon Not R Astron Soc 349(3):1039–1051. https://doi.org/10.1111/j.1365-2966.2004.07586.x. arXiv:astro-ph/0311231 [astro-ph]
Newman AB, Treu T, Ellis RS, Sand DJ (2013) The density profiles of massive, relaxed galaxy clusters. II. Separating luminous and dark matter in cluster cores. Astrophys J 765(1):25. https://doi.org/10.1088/0004-637X/765/1/25. arXiv:1209.1392 [astro-ph.CO]
Newman AB, Ellis RS, Treu T (2015a) Luminous and dark matter profiles from galaxies to clusters: bridging the gap with group-scale lenses. Astrophys J 814(1):26. https://doi.org/10.1088/0004-637X/814/1/26. arXiv:1503.05282 [astro-ph.GA]
Newman AB, Ellis RS, Treu T (2015b) Luminous and dark matter profiles from galaxies to clusters: bridging the gap with group-scale lenses. Astrophys J 814(1):26. https://doi.org/10.1088/0004-637X/814/1/26. arXiv:1503.05282 [astro-ph.GA]
Niemiec A, Jauzac M, Jullo E, Limousin M, Sharon K, Kneib JP, Natarajan P, Richard J (2020) Hybrid-LENSTOOL: a self-consistent algorithm to model galaxy clusters with strong- and weak-lensing simultaneously. Mon Not R Astron Soc 493(3):3331–3340. https://doi.org/10.1093/mnras/staa473. arXiv:2002.04635 [astro-ph.CO]
Ogrean GA, van Weeren RJ, Jones C, Clarke TE, Sayers J, Mroczkowski T, Nulsen PEJ, Forman W, Murray SS, Pandey-Pommier M, Randall S, Churazov E, Bonafede A, Kraft R, David L, Andrade-Santos F, Merten J, Zitrin A, Umetsu K, Goulding A, Roediger E, Bagchi J, Bulbul E, Donahue M, Ebeling H, Johnston-Hollitt M, Mason B, Rosati P, Vikhlinin A (2015) Frontier Fields clusters: Chandra and JVLA view of the pre-merging cluster MACS J0416.1-2403. Astrophys J 812(2):153. https://doi.org/10.1088/0004-637X/812/2/153. arXiv:1505.05560 [astro-ph.CO]
Oguri M (2010) The mass distribution of SDSS J1004+4112 revisited. Publ Astron Soc Jpn 62:1017. https://doi.org/10.1093/pasj/62.4.1017. arXiv:1005.3103 [astro-ph.CO]
Oguri M (2015) Predicted properties of multiple images of the strongly lensed supernova SN Refsdal. Mon Not R Astron Soc 449:L86–L89. https://doi.org/10.1093/mnrasl/slv025. arXiv:1411.6443 [astro-ph.CO]

Okura Y, Umetsu K, Futamase T (2008) A method for weak-lensing flexion analysis by the HOLICs moment approach. Astrophys J 680(1):1–16. https://doi.org/10.1086/587676. arXiv:0710.2262 [astro-ph]

Orban de Xivry G, Marshall P (2009) An atlas of predicted exotic gravitational lenses. Mon Not R Astron Soc 399(1):2–20. https://doi.org/10.1111/j.1365-2966.2009.14925.x. arXiv:0904.1454 [astro-ph.CO]

Paczynski B (1987) Giant luminous arcs discovered in two clusters of galaxies. Nature 325(6105):572–573. https://doi.org/10.1038/325572a0

Peter AHG, Rocha M, Bullock JS, Kaplinghat M (2013) Cosmological simulations with self-interacting dark matter - II. Halo shapes versus observations. Mon Not R Astron Soc 430(1):105–120. https://doi.org/10.1093/mnras/sts535. arXiv:1208.3026 [astro-ph.CO]

Plazas Malagón AA (2020) Image simulations for strong and weak gravitational lensing. Symmetry 12(4):494. https://doi.org/10.3390/sym12040494. arXiv:2003.06090 [astro-ph.CO]

Postman M, Coe D, Benítez N et al (2012) The cluster lensing and supernova survey with Hubble: an overview. Astrophys J Suppl Ser 199(2):25. https://doi.org/10.1088/0067-0049/199/2/25. arXiv:1106.3328 [astro-ph.CO]

Presotto V, Girardi M, Nonino M, Mercurio A, Grillo C, Rosati P, Biviano A, Annunziatella M, Balestra I, Cui W, Sartoris B, Lemze D, Ascaso B, Moustakas J, Ford H, Fritz A, Czoske O, Ettori S, Kuchner U, Lombardi M, Maier C, Medezinski E, Molino A, Scodeggio M, Strazzullo V, Tozzi P, Ziegler B, Bartelmann M, Benitez N, Bradley L, Brescia M, Broadhurst T, Coe D, Donahue M, Gobat R, Graves G, Kelson D, Koekemoer A, Melchior P, Meneghetti M, Merten J, Moustakas LA, Munari E, Postman M, Regős E, Seitz S, Umetsu K, Zheng W, Zitrin A (2014) Intracluster light properties in the CLASH-VLT cluster MACS J1206.2-0847. Astron Astrophys 565:A126. https://doi.org/10.1051/0004-6361/201323251. arXiv:1403.4979 [astro-ph.CO]

Priewe J, Williams LLR, Liesenborgs J, Coe D, Rodney SA (2017) Lens models under the microscope: comparison of Hubble Frontier Field cluster magnification maps. Mon Not R Astron Soc 465(1):1030–1045. https://doi.org/10.1093/mnras/stw2785. arXiv:1605.07621 [astro-ph.CO]

Puchwein E, Hilbert S (2009) Cluster strong lensing in the Millennium simulation: the effect of galaxies and structures along the line-of-sight. Mon Not R Astron Soc 398(3):1298–1308. https://doi.org/10.1111/j.1365-2966.2009.15227.x. arXiv:0904.0253 [astro-ph.CO]

Ragagnin A, Meneghetti M, Bassini L, Ragone-Figueroa C, Granato GL, Despali G, Giocoli C, Granata G, Moscardini L, Bergamini P, Rasia E, Valentini M, Borgani S, Calura F, Dolag K, Grillo C, Mercurio A, Murante G, Natarajan P, Rosati P, Taffoni G, Tornatore L, Tortorelli L (2022) Galaxies in the central regions of simulated galaxy clusters. Astron Astrophys 665:A16. https://doi.org/10.1051/0004-6361/202243651. arXiv:2204.09067 [astro-ph.CO]

Raghunathan S, Patil S, Baxter E et al (2019) Mass calibration of optically selected DES clusters using a measurement of CMB-cluster lensing with SPTpol data. Astrophys J 872(2):170. https://doi.org/10.3847/1538-4357/ab01ca. arXiv:1810.10998 [astro-ph.CO]

Randall SW, Markevitch M, Clowe D, Gonzalez AH, Bradač M (2008) Constraints on the self-interaction cross section of dark matter from numerical simulations of the merging galaxy cluster 1E 0657-56. Astrophys J 679(2):1173–1180. https://doi.org/10.1086/587859. arXiv:0704.0261 [astro-ph]

Raney CA, Keeton CR, Brennan S (2020a) Exploring effects on magnifications due to line-of-sight galaxies in the Hubble Frontier Fields. Mon Not R Astron Soc 492(1):503–527. https://doi.org/10.1093/mnras/stz3116. arXiv:1911.02101 [astro-ph.CO]

Raney CA, Keeton CR, Brennan S, Fan H (2020b) Systematic versus statistical uncertainties in masses and magnifications of the Hubble Frontier Fields. Mon Not R Astron Soc 494(4):4771–4793. https://doi.org/10.1093/mnras/staa921. arXiv:2004.05952 [astro-ph.CO]

Remolina González JD Sharon K, Mahler G (2018) An evaluation of 10 lensing models of the frontier fields cluster MACS J0416.1-2403. Astrophys J 863(1):60. https://doi.org/10.3847/1538-4357/aacf8e. arXiv:1807.03291 [astro-ph.CO]

Richard J, Smith GP, Kneib JP, Ellis RS, Sanderson AJR, Pei L, Targett TA, Sand DJ, Swinbank AM, Dannerbauer H, Mazzotta P, Limousin M, Egami E, Jullo E, Hamilton-Morris V, Moran SM (2010) LoCuSS: first results from strong-lensing analysis of 20 massive galaxy clusters at z = 0.2. Mon Not R Astron Soc 404(1):325–349. https://doi.org/10.1111/j.1365-2966.2009.16274.x. arXiv:0911.3302 [astro-ph.CO]

Richard J, Patricio V, Martinez J, Bacon R, Clement B, Weilbacher P, Soto K, Wisotzki L, Vernet J, Pello R, Schaye J, Turner M, Martinsson T (2015) MUSE observations of the lensing cluster SMACSJ2031.8-4036: new constraints on the mass distribution in the cluster core. Mon Not R Astron Soc 446:L16–L20. https://doi.org/10.1093/mnrasl/slu150. arXiv:1409.2488 [astro-ph.CO]

Rigby JR, Bayliss MB, Sharon K, Gladders MD, Chisholm J, Dahle H, Johnson T, Paterno-Mahler R, Wuyts E, Kelson DD (2018) The Magellan evolution of galaxies spectroscopic and ultraviolet reference atlas (MegaSaura). I. The sample and the spectra. Astron J 155(3):104. https://doi.org/10.3847/1538-3881/aaa2ff. arXiv:1710.07294 [astro-ph.GA]

Robertson A (2021) The galaxy-galaxy strong lensing cross-sections of simulated ΛCDM galaxy clusters. Mon Not R Astron Soc 504(1):L7–L11. https://doi.org/10.1093/mnrasl/slab028. arXiv:2101.12067 [astro-ph.GA]

Robertson A, Massey R, Eke V (2017) What does the Bullet Cluster tell us about self-interacting dark matter? Mon Not R Astron Soc 465(1):569–587. https://doi.org/10.1093/mnras/stw2670. arXiv:1605.04307 [astro-ph.CO]

Robertson A, Harvey D, Massey R, Eke V, McCarthy IG, Jauzac M, Li B, Schaye J (2019) Observable tests of self-interacting dark matter in galaxy clusters: cosmological simulations with SIDM and baryons. Mon Not R Astron Soc 488(3):3646–3662. https://doi.org/10.1093/mnras/stz1815. arXiv:1810.05649 [astro-ph.CO]

Robertson A, Smith GP, Massey R, Eke V, Jauzac M, Bianconi M, Ryczanowski D (2020) What does strong gravitational lensing? The mass and redshift distribution of high-magnification lenses. Mon Not R Astron Soc 495(4):3727–3739. https://doi.org/10.1093/mnras/staa1429. arXiv:2002.01479 [astro-ph.CO]

Rodney SA, Patel B, Scolnic D, Foley RJ, Molino A, Brammer G, Jauzac M, Bradač M, Broadhurst T, Coe D, Diego JM, Graur O, Hjorth J, Hoag A, Jha SW, Johnson TL, Kelly P, Lam D, McCully C, Medezinski E, Meneghetti M, Merten J, Richard J, Riess A, Sharon K, Strolger LG, Treu T, Wang X, Williams LLR, Zitrin A (2015) Illuminating a dark lens: a type Ia supernova magnified by the frontier fields galaxy cluster Abell 2744. Astrophys J 811(1):70. https://doi.org/10.1088/0004-637X/811/1/70. arXiv:1505.06211 [astro-ph.CO]

Rosati P, Balestra I, Grillo C, Mercurio A, Nonino M, Biviano A, Girardi M, Vanzella E, Clash-VLT Team (2014) CLASH-VLT: a VIMOS large programme to map the dark matter mass distribution in galaxy clusters and probe distant lensed galaxies. Messenger 158:48–53

Rossi G (2020) The sejong suite: cosmological hydrodynamical simulations with massive neutrinos, dark radiation, and warm dark matter. Astrophys J Suppl Ser 249(2):19. https://doi.org/10.3847/1538-4365/ab9d1e. arXiv:2007.15279 [astro-ph.CO]

Rykoff ES, Rozo E, Hollowood D, DES Collaboration et al (2016) The RedMaPPer galaxy cluster catalog from DES science verification data. Astrophys J Suppl Ser 224(1):1. https://doi.org/10.3847/0067-0049/224/1/1. arXiv:1601.00621 [astro-ph.CO]

Saha P, Read JI, Williams LLR (2006) Two strong-lensing clusters confront universal dark matter profiles. Astrophys J Lett 652(1):L5–L8. https://doi.org/10.1086/509782. arXiv:astro-ph/0610011 [astro-ph]

Sand DJ, Treu T, Ellis RS (2002) The dark matter density profile of the lensing cluster MS 2137-23: a test of the cold dark matter paradigm. Astrophys J Lett 574(2):L129–L133. https://doi.org/10.1086/342530. arXiv:astro-ph/0207048 [astro-ph]

Sand DJ, Treu T, Smith GP, Ellis RS (2004) The dark matter distribution in the central regions of galaxy clusters: implications for cold dark matter. Astrophys J 604(1):88–107. https://doi.org/10.1086/382146. arXiv:astro-ph/0309465 [astro-ph]

Sand DJ, Treu T, Ellis RS, Smith GP, Kneib JP (2008) Separating baryons and dark matter in cluster cores: a full two-dimensional lensing and dynamic analysis of Abell 383 and MS 2137-23. Astrophys J 674(2):711–727. https://doi.org/10.1086/524652. arXiv:0710.1069 [astro-ph]

Sartoris B, Biviano A, Rosati P, Borgani S, Umetsu K, Bartelmann M, Girardi M, Grillo C, Lemze D, Zitrin A, Balestra I, Mercurio A, Nonino M, Postman M, Czakon N, Bradley L, Broadhurst T, Coe D, Medezinski E, Melchior P, Meneghetti M, Merten J, Annunziatella M, Benitez N, Czoske O, Donahue M, Ettori S, Ford H, Fritz A, Kelson D, Koekemoer A, Kuchner U, Lombardi M, Maier C, Moustakas LA, Munari E, Presotto V, Scodeggio M, Seitz S, Tozzi P, Zheng W, Ziegler B (2014) CLASH-VLT: constraints on the dark matter equation of state from accurate measurements of galaxy cluster mass profiles. Astrophys J Lett 783(1):L11. https://doi.org/10.1088/2041-8205/783/1/L11. arXiv:1401.5800 [astro-ph.CO]

Sartoris B, Biviano A, Fedeli C, Bartlett JG, Borgani S, Costanzi M, Giocoli C, Moscardini L, Weller J, Ascaso B, Bardelli S, Maurogordato S, Viana PTP (2016) Next generation cosmology: constraints from the Euclid galaxy cluster survey. Mon Not R Astron Soc 459(2):1764–1780. https://doi.org/10.1093/mnras/stw630. arXiv:1505.02165 [astro-ph.CO]

Schäfer C, Fourestey G, Kneib JP (2020) Lenstool-HPC: a high performance computing based mass modelling tool for cluster-scale gravitational lenses. Astron Comput 30:100360. https://doi.org/10.1016/j.ascom.2019.100360. arXiv:2004.06352 [astro-ph.IM]

Schneider P (1984) The amplification caused by gravitational bending of light. Astron Astrophys 140(1):119–124

Schneider P (2014) Can one determine cosmological parameters from multi-plane strong lens systems? Astron Astrophys 568:L2. https://doi.org/10.1051/0004-6361/201424450. arXiv:1406.6152 [astro-ph.CO]

Schneider P, Seitz C (1995) Steps towards nonlinear cluster inversion through gravitational distortions. I. Basic considerations and circular clusters. Astron Astrophys 294:411–431. arXiv:astro-ph/9407032 [astro-ph]

Schombert JM (1986) The structure of brightest cluster members. I. Surface photometry. Astrophys J Suppl Ser 60:603. https://doi.org/10.1086/191100

Schrabback T, Bocquet S, Sommer M, Zohren H, van den Busch JL, Hernández-Martín B, Hoekstra H, Raihan SF, Schirmer M, Applegate D, Bayliss M, Benson BA, Bleem LE, Dietrich JP, Floyd B, Hilbert S, Hlavacek-Larrondo J, McDonald M, Saro A, Stark AA, Weissgerber N (2021) Mass calibration of distant SPT galaxy clusters through expanded weak-lensing follow-up observations with HST, VLT & Gemini-south. Mon Not R Astron Soc 505(3):3923–3943. https://doi.org/10.1093/mnras/stab1386. arXiv:2009.07591 [astro-ph.CO]

Schwinn J, Jauzac M, Baugh CM, Bartelmann M, Eckert D, Harvey D, Natarajan P, Massey R (2017) Abell 2744: too much substructure for ΛCDM?. Mon Not R Astron Soc 467(3):2913–2923. https://doi.org/10.1093/mnras/stx277. arXiv:1611.02790 [astro-ph.CO]

Schwinn J, Baugh CM, Jauzac M, Bartelmann M, Eckert D (2018) Uncovering substructure with wavelets: proof of concept using Abell 2744. Mon Not R Astron Soc 481(4):4300–4310. https://doi.org/10.1093/mnras/sty2566. arXiv:1804.07401 [astro-ph.CO]

Sebesta K, Williams LLR, Mohammed I, Saha P, Liesenborgs J (2016) Testing light-traces-mass in Hubble Frontier Fields cluster MACS-J0416 1-2403. Mon Not R Astron Soc 461(2):2126–2134. https://doi.org/10.1093/mnras/stw1433. arXiv:1507.08960 [astro-ph.CO]

Şengül A, Birrer S, Natarajan P, Dvorkin C (2023) Detecting low-mass perturbers in cluster lenses using curved arc bases. Mon Not R Astron Soc 526(2):2525–2541. https://doi.org/10.1093/mnras/stad2784. arXiv:2303.14786 [astro-ph.GA]

Sereno M, Covone G, Izzo L, Ettori S, Coupon J, Lieu M (2017) PSZ2LenS. Weak lensing analysis of the Planck clusters in the CFHTLenS and in the RCSLenS. Mon Not R Astron Soc 472(2):1946–1971. https://doi.org/10.1093/mnras/stx2085. arXiv:1703.06886 [astro-ph.CO]

Sharon K, Johnson TL (2015) Revised lens model for the multiply imaged lensed supernova, "SN refsdal" in MACS J1149+2223. Astrophys J Lett 800(2):L26. https://doi.org/10.1088/2041-8205/800/2/L26. arXiv:1411.6933 [astro-ph.CO]

Sharon K, Bayliss MB, Dahle H, Dunham SJ, Florian MK, Gladders MD, Johnson TL, Mahler G, Paterno-Mahler R, Rigby JR, Whitaker KE, Akhshik M, Koester BP, Murray K, Remolina González JD, Wuyts E (2020) Strong lens models for 37 clusters of galaxies from the SDSS giant arcs survey. Astrophys J Suppl Ser 247(1):12. https://doi.org/10.3847/1538-4365/ab5f13. arXiv:1904.05940 [astro-ph.GA]

Sharon K, Mahler G, Rivera-Thorsen TE, Dahle H, Gladders MD, Bayliss MB, Florian MK, Kim KJ, Khullar G, Mainali R, Napier KA, Navarre A, Rigby JR, Remolina González JD, Sharma S (2022a) The cosmic telescope that lenses the sunburst arc, PSZ1 G311.65-18.48: strong gravitational lensing model and source plane analysis. Astrophys J 941(2):203. https://doi.org/10.3847/1538-4357/ac927a. arXiv:2209.03417 [astro-ph.GA]

Sharon K, Mahler G, Rivera-Thorsen TE, Dahle H, Gladders MD, Bayliss MB, Florian MK, Kim KJ, Khullar G, Mainali R, Napier KA, Navarre A, Rigby JR, Remolina González JD Sharma S (2022b) The cosmic telescope that lenses the sunburst arc, PSZ1 G311.65-18.48: strong gravitational lensing model and source plane analysis. Astrophys J 941(2):203. https://doi.org/10.3847/1538-4357/ac927a. arXiv:2209.03417 [astro-ph.GA]

Smail I, Dickinson M (1995) Lensing by distant clusters: HST observations of weak shear in the field of 3C 324. Astrophys J Lett 455:L99. https://doi.org/10.1086/309842. arXiv:astro-ph/9510050 [astro-ph]

Soucail G, Fort B, Mellier Y, Picat JP (1987) A blue ring-like structure in the center of the A 370 cluster of galaxies. Astron Astrophys 172:L14–L16.

Soucail G, Mellier Y, Fort B, Cailloux M (1988) Spectroscopic observations of the distant cluster of galaxies Abell 370: a catalogue of 84 spectra. Astron Astrophys 73:471–514

Soucail G, Kneib JP, Golse G (2004) Multiple-images in the cluster lens Abell 2218: constraining the geometry of the Universe? Astron Astrophys 417:L33–L37. https://doi.org/10.1051/0004-6361:20040077. arXiv:astro-ph/0402658 [astro-ph]

Spergel DN, Steinhardt PJ (2000) Observational evidence for self-interacting cold dark matter. Phys Rev Lett 84(17):3760–3763. https://doi.org/10.1103/PhysRevLett.84.3760. arXiv:astro-ph/9909386 [astro-ph]

Springel V, Farrar GR (2007) The speed of the 'bullet' in the merging galaxy cluster 1E0657-56. Mon Not R Astron Soc 380(3):911–925. https://doi.org/10.1111/j.1365-2966.2007.12159.x. arXiv:astro-ph/0703232 [astro-ph]

Springel V, Wang J, Vogelsberger M, Ludlow A, Jenkins A, Helmi A, Navarro JF, Frenk CS, White SDM (2008) The aquarius project: the subhaloes of galactic haloes. Mon Not R Astron Soc 391(4):1685–1711. https://doi.org/10.1111/j.1365-2966.2008.14066.x. arXiv:0809.0898 [astro-ph]

Steinhardt CL, Jauzac M, Acebron A et al (2020) The BUFFALO HST survey. Astrophys J Suppl Ser 247(2):64. https://doi.org/10.3847/1538-4365/ab75ed. arXiv:2001.09999 [astro-ph.GA]

Strait V, Bradač M, Hoag A, Huang KH, Treu T, Wang X, Amorin R, Castellano M, Fontana A, Lemaux BC, Merlin E, Schmidt KB, Schrabback T, Tomczack A, Trenti M, Vulcani B (2018) Mass and light

of Abell 370: a strong and weak lensing analysis. Astrophys J 868:129. https://doi.org/10.3847/1538-4357/aae834. arXiv:1805.08789

Suyu SH, Halkola A (2010) The halos of satellite galaxies: the companion of the massive elliptical lens SL2S J08544-0121. Astron Astrophys 524:A94. https://doi.org/10.1051/0004-6361/201015481. arXiv:1007.4815 [astro-ph.CO]

Suyu SH, Hensel SW, McKean JP, Fassnacht CD, Treu T, Halkola A, Norbury M, Jackson N, Schneider P, Thompson D, Auger MW, Koopmans LVE, Matthews K (2012) Disentangling baryons and dark matter in the spiral gravitational lens B1933+503. Astrophys J 750(1):10. https://doi.org/10.1088/0004-637X/750/1/10. arXiv:1110.2536 [astro-ph.CO]

Torres-Ballesteros DA, Castañeda L (2023) RELENSING: reconstructing the mass profile of galaxy clusters from gravitational lensing. Mon Not R Astron Soc 518(3):4494–4516. https://doi.org/10.1093/mnras/stac3253. arXiv:2201.10076 [astro-ph.CO]

Treu T, Brammer G, Diego JM, Grillo C, Kelly PL, Oguri M, Rodney SA, Rosati P, Sharon K, Zitrin A, Balestra I, Bradač M, Broadhurst T, Caminha GB, Halkola A, Hoag A, Ishigaki M, Johnson TL, Karman W, Kawamata R, Mercurio A, Schmidt KB, Strolger LG, Suyu SH, Filippenko AV, Foley RJ, Jha SW, Patel B (2016) "Refsdal" meets popper: comparing predictions of the re-appearance of the multiply imaged supernova behind MACSJ1149.5+2223. Astrophys J 817(1):60. https://doi.org/10.3847/0004-637X/817/1/60. arXiv:1510.05750 [astro-ph.CO]

Tutusaus I, Martinelli M, Cardone VF, Camera S et al (2020) Euclid: the importance of galaxy clustering and weak lensing cross-correlations within the photometric Euclid survey. Astron Astrophys 643:A70. https://doi.org/10.1051/0004-6361/202038313. arXiv:2005.00055 [astro-ph.CO]

Tyson JA, Valdes F, Wenk RA (1990) Detection of systematic gravitational lens galaxy image alignments: mapping dark matter in galaxy clusters. Astrophys J Lett 349:L1. https://doi.org/10.1086/185636

Umetsu K (2020) Cluster-galaxy weak lensing. Astron Astrophys Rev 28(1):7. https://doi.org/10.1007/s00159-020-00129-w. arXiv:2007.00506 [astro-ph.CO]

Umetsu K, Medezinski E, Nonino M, Merten J, Zitrin A, Molino A, Grillo C, Carrasco M, Donahue M, Mahdavi A, Coe D, Postman M, Koekemoer A, Czakon N, Sayers J, Mroczkowski T, Golwala S, Koch PM, Lin KY, Molnar SM, Rosati P, Balestra I, Mercurio A, Scodeggio M, Biviano A, Anguita T, Infante L, Seidel G, Sendra I, Jouvel S, Host O, Lemze D, Broadhurst T, Meneghetti M, Moustakas L, Bartelmann M, Benítez N, Bouwens R, Bradley L, Ford H, Jiménez-Tej Y, Kelson D, Lahav O, Melchior P, Moustakas J, Ogaz S, Seitz S, Zheng W (2012) CLASH: mass distribution in and around MACS J1206.2-0847 from a full cluster lensing analysis. Astrophys J 755(1):56. https://doi.org/10.1088/0004-637X/755/1/56. arXiv:1204.3630 [astro-ph.CO]

Umetsu K, Medezinski E, Nonino M, Merten J, Postman M, Meneghetti M, Donahue M, Czakon N, Molino A, Seitz S, Gruen D, Lemze D, Balestra I, Benítez N, Biviano A, Broadhurst T, Ford H, Grillo C, Koekemoer A, Melchior P, Mercurio A, Moustakas J, Rosati P, Zitrin A (2014) CLASH: weak-lensing shear-and-magnification analysis of 20 galaxy clusters. Astrophys J 795(2):163. https://doi.org/10.1088/0004-637X/795/2/163. arXiv:1404.1375 [astro-ph.CO]

Umetsu K, Zitrin A, Gruen D, Merten J, Donahue M, Postman M (2016) CLASH: joint analysis of strong-lensing, weak-lensing shear, and magnification data for 20 galaxy clusters. Astrophys J 821(2):116. https://doi.org/10.3847/0004-637X/821/2/116. arXiv:1507.04385 [astro-ph.CO]

Umetsu K, Sereno M, Tam SI, Chiu IN, Fan Z, Ettori S, Gruen D, Okumura T, Medezinski E, Donahue M, Meneghetti M, Frye B, Koekemoer A, Broadhurst T, Zitrin A, Balestra I, Benítez N, Higuchi Y, Melchior P, Mercurio A, Merten J, Molino A, Nonino M, Postman M, Rosati P, Sayers J, Seitz S (2018) The projected dark and baryonic ellipsoidal structure of 20 CLASH galaxy clusters. Astrophys J 860(2):104. https://doi.org/10.3847/1538-4357/aac3d9. arXiv:1804.00664 [astro-ph.CO]

Uson JM, Boughn SP, Kuhn JR (1991) Diffuse light in dense clusters of galaxies. I. R-band observations of Abell 2029. Astrophys J 369:46. https://doi.org/10.1086/169737

van Weeren RJ, Ogrean GA, Jones C, Forman WR, Andrade-Santos F, Pearce CJJ, Bonafede A, Brüggen M, Bulbul E, Clarke TE, Churazov E, David L, Dawson WA, Donahue M, Goulding A, Kraft RP, Mason B, Merten J, Mroczkowski T, Nulsen PEJ, Rosati P, Roediger E, Randall SW, Sayers J, Umetsu K, Vikhlinin A, Zitrin A (2017) Chandra and JVLA observations of HST frontier fields cluster MACS J0717.5+3745. Astrophys J 835(2):197. https://doi.org/10.3847/1538-4357/835/2/197. arXiv:1701.04096 [astro-ph.CO]

Vega-Ferrero J, Diego JM, Miranda V, Bernstein GM (2018) The Hubble constant from SN refsdal. Astrophys J Lett 853(2):L31. https://doi.org/10.3847/2041-8213/aaa95f. arXiv:1712.05800 [astro-ph.CO]

Verdugo T, Motta V, Muñoz RP, Limousin M, Cabanac R, Richard J (2011) Gravitational lensing and dynamics in SL2S J02140-0535: probing the mass out to large radius. Astron Astrophys 527:A124. https://doi.org/10.1051/0004-6361/201014965. arXiv:1005.1566 [astro-ph.CO]

Verdugo T, Motta V, Foëx G, Forero-Romero JE, Muñoz RP, Pello R, Limousin M, More A, Cabanac R, Soucail G, Blakeslee JP, Mejía-Narváez AJ, Magris G, Fernández-Trincado JG (2014) Characterizing

SL2S galaxy groups using the Einstein radius. Astron Astrophys 571:A65. https://doi.org/10.1051/0004-6361/201423696. arXiv:1409.2900 [astro-ph.CO]
Wagner J (2019) A model-independent characterisation of strong gravitational lensing by observables. Universe 5(7):177. https://doi.org/10.3390/universe5070177. arXiv:1906.05285 [astro-ph.CO]
Wagner J (2020) Cosmic structures from a mathematical perspective 1: dark matter halo mass density profiles. Gen Relativ Gravit 52(6):61. https://doi.org/10.1007/s10714-020-02715-w. arXiv:2002.00960 [astro-ph.CO]
Wagner J (2022) Generalised model-independent characterisation of strong gravitational lenses - VII. Impact of source properties and higher-order lens properties on the local lens reconstruction. Astron Astrophys 663:A157. https://doi.org/10.1051/0004-6361/202243562
Wagner J, Tessore N (2018) Generalised model-independent characterisation of strong gravitational lenses. II. Transformation matrix between multiple images. Astron Astrophys 613:A6. https://doi.org/10.1051/0004-6361/201730947. arXiv:1704.01822 [astro-ph.CO]
Wagner J, Williams LLR (2020) Model-independent and model-based local lensing properties of B0128+437 from resolved quasar images. Astron Astrophys 635:A86. https://doi.org/10.1051/0004-6361/201936628. arXiv:1909.01349 [astro-ph.GA]
Wagner J, Liesenborgs J, Tessore N (2018) Model-independent and model-based local lensing properties of CL0024+1654 from multiply imaged galaxies. Astron Astrophys 612:A17. https://doi.org/10.1051/0004-6361/201731932. arXiv:1709.03531
Walsh D, Carswell RF, Weymann RJ (1979) 0957+561 A, B: twin quasistellar objects or gravitational lens?. Nature 279:381–384. https://doi.org/10.1038/279381a0
Wambsganss J, Bode P, Ostriker JP (2004) Giant arc statistics in Concord with a concordance lambda cold dark matter universe. Astrophys J Lett 606(2):L93–L96. https://doi.org/10.1086/421459. arXiv:astro-ph/0306088 [astro-ph]
Wang X, Hoag A, Huang KH, Treu T, Bradač M, Schmidt KB, Brammer GB, Vulcani B, Jones TA, Ryan RE, Amorín R, Castellano M, Fontana A, Merlin E, Trenti M (2015) The grism lens-amplified survey from space (GLASS). IV. Mass reconstruction of the lensing cluster abell 2744 from frontier field imaging and GLASS spectroscopy. Astrophys J 811:29. https://doi.org/10.1088/0004-637X/811/1/29. arXiv:1504.02405
Wang H, Cañameras R, Caminha GB, Suyu SH, Yıldırım A, Chirivì G, Christensen L, Grillo C, Schuldt S (2022) Constraining the multi-scale dark-matter distribution in CASSOWARY 31 with strong gravitational lensing and stellar dynamics. Astron Astrophys 668:A162. https://doi.org/10.1051/0004-6361/202243600. arXiv:2203.13759 [astro-ph.GA]
Wechsler RH, Bullock JS, Primack JR, Kravtsov AV, Dekel A (2002) Concentrations of dark halos from their assembly histories. Astrophys J 568(1):52–70. https://doi.org/10.1086/338765. arXiv:astro-ph/0108151 [astro-ph]
Williams LLR, Lewis GF (1998) Undistorted lensed images in galaxy clusters. Mon Not R Astron Soc 294:299–306. https://doi.org/10.1046/j.1365-8711.1998.01179.x. arXiv:astro-ph/9710042 [astro-ph]
Williams LLR, Liesenborgs J (2019) The role of multiple images and model priors in measuring H_0 from supernova Refsdal in galaxy cluster MACS J1149 5+2223. Mon Not R Astron Soc 482(4):5666–5677. https://doi.org/10.1093/mnras/sty3113. arXiv:1806.11113 [astro-ph.CO]
Williams LLR, Saha P (2004) Models of the Giant Quadruple Quasar SDSS J1004+4112. Astron J 128(6):2631–2641. https://doi.org/10.1086/426007. arXiv:astro-ph/0409418 [astro-ph]
Williams LLR, Navarro JF, Bartelmann M (1999) The core structure of galaxy clusters from gravitational lensing. Astrophys J 527(2):535–544. https://doi.org/10.1086/308127. arXiv:astro-ph/9905134 [astro-ph]
Williams LLR, Hjorth J, Wojtak R (2010) Statistical mechanics of collisionless orbits. III. Comparison with N-body simulations. Astrophys J 725(1):282–287. https://doi.org/10.1088/0004-637X/725/1/282. arXiv:1010.0267 [astro-ph.CO]
Williams LLR, Sebesta K, Liesenborgs J (2018) Evidence for the line-of-sight structure in the Hubble Frontier Field cluster MACSJ0717 5+3745. Mon Not R Astron Soc 480(3):3140–3151. https://doi.org/10.1093/mnras/sty2088. arXiv:1711.05265 [astro-ph.CO]
Windhorst RA, Cohen SH, Jansen RA, Summers J, Tompkins S, Conselice CJ, Driver SP, Yan H, Coe D, Frye B, Grogin N, Koekemoer A, Marshall MA, O'Brien R, Pirzkal N, Robotham A, Ryan RE, Willmer CNA, Carleton T, Diego JM, Keel WC, Porto P, Redshaw C, Scheller S, Wilkins SM, Willner SP, Zitrin A, Adams NJ, Austin D, Arendt RG, Beacom JF, Bhatawdekar RA, Bradley LD, Broadhurst T, Cheng C, Civano F, Dai L, Dole H, D'Silva JCJ, Duncan KJ, Fazio GG, Ferrami G, Ferreira L, Finkelstein SL, Furtak LJ, Gim HB, Griffiths A, Hammel HB, Harrington KC, Hathi NP, Holwerda BW, Honor R, Huang JS, Hyun M, Im M, Joshi BA, Kamieneski PS, Kelly P, Larson RL, Li J, Lim J, Ma Z, Maksym P, Manzoni G, Meena AK, Milam SN, Nonino M, Pascale M, Petric A, Pierel JDR, del Carmen Polletta M, Röttgering HJA, Rutkowski MJ, Smail I, Straughn AN, Strolger LG, Swirbul A, Trussler JAA, Wang L,

Welch B, Wyithe JS, Yun M, Zackrisson E, Zhang J, Zhao X (2023) JWST PEARLS. Prime extragalactic areas for reionization and lensing science: project overview and first results. Astron J 165(1):13. https://doi.org/10.3847/1538-3881/aca163. arXiv:2209.04119 [astro-ph.CO]

Wu HY, Weinberg DH, Salcedo AN, Wibking BD (2021) Cosmology with galaxy cluster weak lensing: statistical limits and experimental design. Astrophys J 910(1):28. https://doi.org/10.3847/1538-4357/abdc23

Yang D, Yu HB (2021) Self-interacting dark matter and small-scale gravitational lenses in galaxy clusters. Phys Rev D 104(10):103031. https://doi.org/10.1103/PhysRevD.104.103031. arXiv:2102.02375 [astro-ph.GA]

Young P, Gunn JE, Kristian J, Oke JB, Westphal JA (1980) The double quasar Q0957+561 A, B: a gravitational lens image formed by a galaxy at $z = 0.39$. Astrophys J 241:507–520. https://doi.org/10.1086/158365

Yue B, Castellano M, Ferrara A, Fontana A, Merlin E, Amorín R, Grazian A, Mármol-Queralto E, Michalowski MJ, Mortlock A, Paris D, Parsa S, Pilo S, Santini P, Criscienzo MD (2018) On the faint end of the galaxy luminosity function in the epoch of reionization: updated constraints from the hst frontier fields. Astrophys J 868(2):115. https://doi.org/10.3847/1538-4357/aae77f

Zhao DH, Mo HJ, Jing YP, Börner G (2003) The growth and structure of dark matter haloes. Mon Not R Astron Soc 339(1):12–24. https://doi.org/10.1046/j.1365-8711.2003.06135.x. arXiv:astro-ph/0204108 [astro-ph]

Zitrin A, Broadhurst T (2009) Discovery of the largest known lensed images formed by a critically convergent lensing cluster. Astrophys J Lett 703(2):L132–L136. https://doi.org/10.1088/0004-637X/703/2/L132. arXiv:0906.5079 [astro-ph.CO]

Zitrin A, Broadhurst T, Umetsu K, Coe D, Benítez N, Ascaso B, Bradley L, Ford H, Jee J, Medezinski E, Rephaeli Y, Zheng W (2009a) New multiply-lensed galaxies identified in ACS/NIC3 observations of Cl0024+1654 using an improved mass model. Mon Not R Astron Soc 396(4):1985–2002. https://doi.org/10.1111/j.1365-2966.2009.14899.x. arXiv:0902.3971 [astro-ph.CO]

Zitrin A, Broadhurst T, Umetsu K, Coe D, Benítez N, Ascaso B, Bradley L, Ford H, Jee J, Medezinski E, Rephaeli Y, Zheng W (2009b) New multiply-lensed galaxies identified in ACS/NIC3 observations of Cl0024+1654 using an improved mass model. Mon Not R Astron Soc 396(4):1985–2002. https://doi.org/10.1111/j.1365-2966.2009.14899.x. arXiv:0902.3971 [astro-ph.CO]

Zitrin A, Broadhurst T, Barkana R, Rephaeli Y, Benítez N (2011) Strong-lensing analysis of a complete sample of 12 MACS clusters at z > 0.5: mass models and Einstein radii. Mon Not R Astron Soc 410(3):1939–1956. https://doi.org/10.1111/j.1365-2966.2010.17574.x. arXiv:1002.0521 [astro-ph.CO]

Zitrin A, Rosati P, Nonino M, Grillo C, Postman M, Coe D, Seitz S, Eichner T, Broadhurst T, Jouvel S, Balestra I, Mercurio A, Scodeggio M, Benítez N, Bradley L, Ford H, Host O, Jimenez-Teja Y, Koekemoer A, Zheng W, Bartelmann M, Bouwens R, Czoske O, Donahue M, Graur O, Graves G, Infante L, Jha S, Kelson D, Lahav O, Lazkoz R, Lemze D, Lombardi M, Maoz D, McCully C, Medezinski E, Melchior P, Meneghetti M, Merten J, Molino A, Moustakas LA, Ogaz S, Patel B, Regoes E, Riess A, Rodney S, Umetsu K, der Van Wel A (2012b) CLASH: new multiple images constraining the inner mass profile of MACS J1206.2-0847. Astrophys J 749(2):97. https://doi.org/10.1088/0004-637X/749/2/97. arXiv:1107.2649 [astro-ph.CO]

Zitrin A, Menanteau F, Hughes JP, Coe D, Barrientos LF, Infante L, Mandelbaum R (2013) A highly elongated prominent lens at z = 0.87: first strong-lensing analysis of El Gordo. Astrophys J Lett 770(1):L15. https://doi.org/10.1088/2041-8205/770/1/L15. arXiv:1304.0455 [astro-ph.CO]

Zitrin A, Fabris A, Merten J, Melchior P, Meneghetti M, Koekemoer A, Coe D, Maturi M, Bartelmann M, Postman M, Umetsu K, Seidel G, Sendra I, Broadhurst T, Balestra I, Biviano A, Grillo C, Mercurio A, Nonino M, Rosati P, Bradley L, Carrasco M, Donahue M, Ford H, Frye BL, Moustakas J (2015a) Hubble space telescope combined strong and weak lensing analysis of the CLASH sample: mass and magnification models and systematic uncertainties. Astrophys J 801(1):44. https://doi.org/10.1088/0004-637X/801/1/44. arXiv:1411.1414 [astro-ph.CO]

Zitrin A, Fabris A, Merten J, Melchior P, Meneghetti M, Koekemoer A, Coe D, Maturi M, Bartelmann M, Postman M, Umetsu K, Seidel G, Sendra I, Broadhurst T, Balestra I, Biviano A, Grillo C, Mercurio A, Nonino M, Rosati P, Bradley L, Carrasco M, Donahue M, Ford H, Frye BL Moustakas J (2015b) Hubble space telescope combined strong and weak lensing analysis of the CLASH sample: mass and magnification models and systematic uncertainties. Astrophys J 801(1):44. https://doi.org/10.1088/0004-637X/801/1/44. arXiv:1411.1414 [astro-ph.CO]

Zwicky F (1937) On the masses of nebulae and of clusters of nebulae. Astrophys J 86:217. https://doi.org/10.1086/143864